Symposium Program

Te Whai Ao — Dodd Walls Centre Symposium

18 – 22 November 2024

Christchurch, Aotearoa New Zealand

Te Whai Ao
Dodd-Walls Centre
for Photonic and Quantum Technologies

HE MIHI NŌ TE KAIWHAKAHAERE — DIRECTOR'S WELCOME

Welcome to Our Symposium!

We are excited to have you join us as we come together to celebrate the research, achievements, and collaborations of Te Whai Ao, our Research Centre. This event offers a unique opportunity to connect with colleagues, exchange ideas, and envision the future of our Centre.

As you participate, take this time to:

- Get together: Meet new people, share insights, and explore potential new collaborations.
- Celebrate our successes: Learn about our Centre's most significant achievements and the innovations that have shaped our field.
- Engage in special sessions: Enjoy the exciting presentations and workshops organized by our teams, and invited speakers.
- Think about the future: As we celebrate our journey so far, let's look forward. Reflect on our path and imagine where we want to take our Centre.

In developing our strategy and preparing for the midterm review, we had two main objectives:

1. To position the Centre optimally for the rebid, and
2. To go further – imagining what the Centre could look like in 10-20 years (some of us may have retired by then 😉).

For this second goal, we encourage you to think big and envision the future of the Centre boldly as you engage with the Symposium activities.

Above all, enjoy yourself and immerse in the vibrant energy of this gathering. Together, we are shaping the future of Te Whai Ao!

ORGANISING COMMITTEE

Mike Reid

Keith Gordon

Vincent Ng

Michael Moull

Uli Zuelicke

Rowan Simmons

Jevon Longdell

WAIATA

As it is now a tradition, we encourage people to sing our waiata:

Tūtira mai ngā iwi,
Tātou tātou e
Tūtira mai ngā iwi,
Tātou tātou e
Whaia te māramatanga
Me te aroha – e ngā iwi
Kia tapatahi
Kiakotahi rā
Tātou tatou e!

(Repeat once more)

Tātou tatou e!
Hi aue hei

And to introduce yourself before your talk using the following mihi:

Ko (insert name) tōko ingoa.

Kei te (insert institution name) e mahi ana anau.

POLICY AND CODE OF CONDUCT

Te Whai Ao — Dodd-Walls Centre (DWC) is committed to fostering an environment that facilitates the free and robust exchange of scientific ideas. Such an environment requires all participants to be treated with equal consideration and respect. While we encourage vigorous debate, personal attacks can create an atmosphere in which individuals feel threatened or intimidated. Such conduct is not productive and does not contribute to the advancement of science. Therefore, all participants in DWC- managed events and activities are expected to conduct themselves in a professional and respectful manner.

The DWC strictly prohibits all forms of bullying, discrimination, and harassment, whether sexual or otherwise, in any of its events or activities. This policy applies to every individual at the event, including attendees, speakers, exhibitors, award recipients, staff, contractors, and others. Retaliation against an individual for reporting bullying, discrimination, or harassment, or intentionally filing a false report, also constitutes a violation of this policy.

Bullying, discrimination, and harassment by those in a position of power, prestige, or authority are particularly harmful, as those of lower status or rank may be reluctant to express their objections or discomfort out of fear of retaliation.

Upon thorough investigation, the DWC will take appropriate disciplinary action if it finds a violation has occurred.

Our policy aligns with Optica's policy which can be found here.

If you wish to report an incident of bullying, discrimination, or harassment that you have witnessed or experienced, you may do so by contacting any member of the DWC Executive or organising committee.

LOCATIONS AND TRANSPORT

Catering

Breakfast will be provided by Arcady Hall, with catered breaks at the Central Lecture Theatre foyer.

Accommodation

Accommodation for DWC members will be located on campus, at Arcady Hall. Click here for directions.

Events and Sessions

Events and sessions are primarily held at the Central Lecture Theatre on campus. Click here for directions.

The poster session on Tuesday will be held at Arcady Hall, from 5:30pm.

Dinner – International Antarctic Centre

Dinner on Wednesday night will be hosted by the International Antarctic Centre, from 5:30pm. Transport will be available from Arcady Hall from 5:15pm, and will return to the Hall at the end of the event.

Transport

Transport will be arranged from and to Christchurch Airport on Monday and Friday. If your travel falls outside these periods, you will need to arrange your own transport. For those whose flights depart before 6:00pm, please ensure you are at Arcady Hall for collection before your flight. This will mean leaving the QTA session early. Please email dwc@otago.ac.nz if you have any questions.

TIMETABLE

Talks and Presentations	Larger events and talks	Breaks	Leadership team meetings	Other events

Monday

TIME	SPEAKER	TITLE		LOCATION
11:00AM – 12:00PM	Awhina McGlinchy [Ngāi Tahu] Tokona te Raki	Opening Session		C2 Lecture Theatre
12:00PM – 1:14PM		Lunch	ISG Meeting (Rata 119 Engineering)	
1:45PM – 2:15PM		The One		C2 Lecture Theatre
2:15PM – 2:45PM		The Many		C2 Lecture Theatre
2:45PM – 3:15PM		The All		C2 Lecture Theatre
3:15PM – 3:45PM		Afternoon Tea		C2 Lecture Theatre
3:45PM – 4:45PM	Gwen Weerts	Introduction to Scholarly Publishing		C2 Lecture Theatre
4:45PM – 5:30PM	Prof. Keith Gordon	Science		C2 Lecture Theatre
5:30PM – 6:15PM	Jessa Barder/Andy Wang	Outreach		C2 Lecture Theatre
6:15PM	Stanley Tuang	Welcome Reception/BBQ		Arcady Hall

Tuesday

START TIME	SPEAKER	TITLE	LOCATION
9:00AM – 9:30AM	Clare Strachan	Applications of coherent Raman microscopy to advance pharmaceutical research and development	C2 Lecture Theatre
9:30AM – 10:00AM	Tim Bunning	US Airforce Representative	C2 Lecture Theatre
10:00AM – 10:30AM		Morning Tea	C2 Lecture Theatre
10:30AM – 11:15AM	Jessa Barder	Outreach 101: How to develop and deliver effective science engagement	C2 Lecture Theatre
11:15AM – 11:30AM	Matthew Mcnaughan	Spontaneous Soliton Emergence Under Pulsed-Pumping Conditions in a Driven Passive Kerr Resonator	C2 Lecture Theatre
11:30AM – 11:45AM	Fernando Fernandez	Optical fiber sensors for Tokamak fusion reactors	C2 Lecture Theatre
11:45AM – 12:00PM	Finnian Blaauw-Smith	Introducing the QO-LED	C2 Lecture Theatre
12:00PM – 1:00PM		Lunch	C2 Lecture Theatre
1:00PM – 2:00PM		Māori Rōpū Presentation	C2 Lecture Theatre
2:00PM – 2:15PM	Darvan Muralli Tharan	Cartilage degeneration assessement using compression-based depth-resolved polarisation-sensitive optical coherence tomography	C2 Lecture Theatre
2:15PM – 2:30PM	Nils Krause	Thermal Decay of Planar Jones-Roberts Solitons	C2 Lecture Theatre
2:30PM – 2:45PM	Elkhansa Elbashier	The investigation of the effect of bromine crosslinking in the photostability of PM6 donor polymer using Resonance Raman and DFT calculation study for Organic Solar Cells applications	C2 Lecture Theatre
2:45PM – 3:00PM	Freddy Lyzwa	THz dynamics of quantum materials studied at the Australian Synchrotron	C2 Lecture Theatre
3:00PM – 3:30PM		Afternoon Tea	C2 Lecture Theatre

3:30PM – 3:45PM	Jervee Punzalan	Application of Vibrational Spectroscopic Techniques in Sustainable Flaxseed Protein Extraction and Prediction	C2 Lecture Theatre
3:45PM – 4:15PM	Tim Bunning, Leslie Blaha, Geoff Andersen	US Government Funding Q&A	C2 Lecture Theatre
4:15PM – 4:30PM	Jacob Ngaha	Phase Resetting in the Yamada Model of a Q-Switching Laser	C2 Lecture Theatre
4:30PM – 4:45PM	Marie Graff	Seeing inside kiwifruit using imaging: from full0waveform inversion to uncertainty quantification	C2 Lecture Theatre
4:45PM – 5:00PM	Craig Steed	Deep learning from shallow data	C2 Lecture Theatre
5:15PM		Poster Sessions	Arcady Hall

Wednesday

START TIME	SPEAKER	TITLE	LOCATION
9:00AM – 9:30AM	Nir Navon	Quantum Many-body Physics with Fermions in an Optical Box	C2 Lecture Theatre
9:30AM – 9:45AM	Jodi Carter	Construction of an Upconversion Enabled Z-Scheme Heterojunction for Next-Generation Photovoltaic Devices	C2 Lecture Theatre
9:45AM – 10:00AM	Kyoung Lee	Phase Resetting in the Coupled Van der Pol Oscillator	C2 Lecture Theatre
10:00AM – 10:30AM		Morning Tea	C2 Lecture Theatre
10:30AM – 11:00AM	Rainer Blatt	Quantum Computation and Quantum Simulation with Strings of trapped Ca^{+}Ions	C2 Lecture Theatre
11:00AM – 11:15AM	Jessica Frederiksen	Development of fluorescent analogues of vitamin B12 and the cobinamide precursor for antibacterial applications	C2 Lecture Theatre
11:15AM – 11:30AM	Jordan Wise	Tunable Pump Wavelength-Displaced Solitons in Passive Kerr Resonators Mediated by Stimulated Raman Scattering	C2 Lecture Theatre
11:30AM – 11:45AM	Sara Miller	How does data augmentation alter classification performance of support vector machines and convoluted neural network models developed using transmission low frequency Raman spectra	C2 Lecture Theatre
11:45AM – 12:00PM	Peter Remoto	Evaluating the performance of non-destructive techniques for classifying and monitoring the aging of store-bought kiwifruit	C2 Lecture Theatre
12:00PM – 1:00PM		Lunch	C2 Lecture Theatre
1:00PM		Outreach Activities: Laser Maze at the Arts Centre / Governance Board Meeting (Rata Engineering 119)	
5:00PM	Cyndia Yu	Dinner	International Antarctic Centre

Thursday

START TIME	SPEAKER	TITLE	LOCATION
9:00AM – 9:30AM	Cindy Regal	Time-of-flight quantum tomography of an atom in an optical tweezer	C2 Lecture Theatre
9:30AM – 9:45AM	Rodrigues Bitha	Spontaneous symmetry breaking in a coupled photonic crystal dimer with periodic driving	C2 Lecture Theatre
9:45AM – 10:00AM	Alla Gisich	Quantitative measurement of extinction, scattering, and absorbtion spectra from metallic nanoparticles	C2 Lecture Theatre
10:00AM – 10:30AM		Morning Tea	C2 Lecture Theatre
10:30AM – 12:00PM	Gwen Weerts	GenAI's New Role in Scientific Discovery and Dissemination	C2 Lecture Theatre
12:00PM – 1:00PM		Lunch / Student Feedback Session	C2 Lecture Theatre
1:00PM – 1:15PM	Stefania Glukhova	Modelling Light Absorption by Core-satellite NanoStructures	C2 Lecture Theatre
1:15PM – 1:30PM	Nur Fadhillah binti Rahimi	The chicken or the egg? Coherence, entanglement, and superradiance	C2 Lecture Theatre
1:30PM – 1:45PM	Alex Elliott	Tailoring Nonclassical Light with Single-Atom Cavity QED	C2 Lecture Theatre
1:45PM – 2:00PM	Kane Hill	Ultra-thin Film Sensing with Whispering Gallery Mode Resonators at Terhertz Frequencies	C2 Lecture Theatre
2:00PM – 2:15PM	Wang Liao	The injection locking of breathing solitons in microresonators	C2 Lecture Theatre
2:15PM – 2:30PM	Michael Moull	Modelling Transition Intensities of the C3v(O2-) Centre in Eu3+ Doped CaF2 Crystals	C2 Lecture Theatre
2:30PM – 2:45PM		Afternoon Tea	C2 Lecture Theatre
2:45PM – 3:00PM	Liam Quinn	Experimental implimentation of an optical Ising maching using polarization symmetry breaking in a Kerr resonator	C2 Lecture Theatre
3:00PM – 3:15PM	Chengcai Tian	SHG in X-cut lithium tetraborate (LB4) whispering gallery mode resonators	C2 Lecture Theatre
3:15PM – 4:30PM	Jessa Barder	Outreach Challenge	C2 Lecture Theatre
4:30PM – 5:00PM	Fred Vanholsbeeck	Closing Remarks and Poster Prizegiving	C2 Lecture Theatre

Friday

START TIME	SPEAKER	TITLE	LOCATION
9:00AM – 9:40AM	Yasunobu Nakamura	High-fidelity control and readout of superconducting qubits	C2 Lecture Theatre
9:40AM – 10:00AM	Simon Granville	Superconducting Readout of a Compensated Memory Bit	C2 Lecture Theatre
10:00AM – 10:30AM		Morning Tea	C2 Lecture Theatre
10:30AM – 10:55AM	Luke Trainor	Storing single photons in a crystalline quantum memory	C2 Lecture Theatre
10:55AM – 11:25AM	Vahid Sandoghdar	TBC	C2 Lecture Theatre
11:25AM – 11:40AM	William Holmes-Hewett	Rare-earth Nitride Josephson Junctions and derivative products	C2 Lecture Theatre
11:40AM – 12:00PM	Waltraut Wustmann	Fast readout of superconducting qubits with fluxons	C2 Lecture Theatre
12:00PM – 12:15PM	Jevon Longdell	QTA Programme Update	C2 Lecture Theatre
12:15PM – 1:20PM		Lunch	C2 Lecture Theatre
1:20PM – 1:40PM	Miro Erkintalo	Quantum Optics of parametrically driven soliton microcombs	C2 Lecture Theatre
1:40PM – 1:55PM	Mathew Cloutman	Microwave Polarisation Spectroscopy of Rydeberg Atoms	C2 Lecture Theatre
1:55PM – 2:10PM	Ben Ripley	Progress towards a finite temperature c-field theory of supersolids	C2 Lecture Theatre
2:10PM – 2:25PM	Liam Dommett-Potts	Trapping Dysprosium in a Magnetic Optical Trap Directly from a Thermal Beam	C2 Lecture Theatre
2:25PM – 2:45PM	Nick Lambert	Optimising electro-optic resonators for efficient transduction	C2 Lecture Theatre
2:45PM – 3:15PM		Afternoon Tea	C2 Lecture Theatre
3:15PM – 3:35PM	Mikkel Andersen	Robust entanglement generation	C2 Lecture Theatre
3:35PM – 3:50PM	Danny Baillie	Self-bound droplets of dipolar molecules	C2 Lecture Theatre
3:50PM – 4:05PM	Matija Čufar	Rimu.jl: Random integrators for many-body quantum systems	C2 Lecture Theatre
11:25AM – 11:40AM	Jackson Miller	Advanced materials for quantum technologies	C2 Lecture Theatre

4:20PM – 4:40PM	Johan Grand	Ocean monitoring using optical interferometry in subsea cables	C2 Lecture Theatre
4:40PM – 5:00PM	Acting Science Lead/Fred Vanholsbeeck	Wrap Up	C2 Lecture Theatre

ABSTRACTS FOR INVITED TALKS

Gwen Weerts

Gwen Weerts is the SPIE Journals Manager and Editor in Chief of Photonics Focus, SPIE's award-winning bimonthly magazine. She has worked in scholarly publishing and science communication for sixteen years. Gwen is a member of the Society for Scholarly Publishing and the National Association of Science Writers

Intro to Scholarly Publishing

Scholarly publishing is an expected output of academic research, but it's not the part of science that most researchers signed up for. When it comes time to prepare a manuscript, you must navigate a whole new world of deadlines, acronyms, and jargon. If that's not enough, there are some serious pitfalls on the path to publication: ignore them at your peril. This interactive class will give you an introduction to scholarly publishing and teach you what to expect from the peer review process, how to steer clear of misconduct, and above all, how to successfully publish your research in a reputable peer-reviewed scholarly journal.

Applications of coherent Raman microscopy to advance pharmaceutical research and development

Clare Strachan

Drug Research Program, Faculty of Pharmacy, University of Helsinki, Finland

Coherent Raman microscopy offers rapid, non-destructive, label-free, chemically and structurally-specific imaging of samples with (sub)micron spatial resolution. While spectral resolution and range is generally still superior with the much slower spontaneous Raman mapping, spectral focusing, amongst other technologies, is increasingly allowing high quality coherent Raman spectra to be obtained at high imaging speeds. These qualities make the technique ideally suited to better understand diverse aspects of pharmaceutical behaviour, from crystallization, to formulation and drug delivery and finally, therapeutic action. Through the use of case studies, this talk will consider recent applications of coherent Raman microscopy, supported by complimentary non-linear optical imaging modalities, to advance pharmaceutical research and development. They include imaging of pharmaceutical crystallinity, drug release mechanisms from dosage forms, and phase behaviour in dissolution media. Overall, critically important insights into drug and dosage form behaviour, often inaccessible with established pharmaceutical characterization methods, can be obtained.

Time-of-flight quantum tomography of an atom in an optical tweezer

Cindy Regal

Single-atom trapping in optical tweezers has become an important capability in quantum systems of neutral atoms. I will present our efforts to broaden control of quantum motion in the versatile potential landscape of optical tweezer traps. In our experiments, we laser cool single 87Rb atoms to near their vibrational ground state in an optical tweezer, and prepare non-classical motion in the state space of a harmonic potential. I will discuss a demonstration of motional-state tomography that uses only time-of-flight combined with quadrature rotation through time evolution in the tweezer potential. I will also touch on recent efforts in our group to bring neutral atoms in optical tweezers to a cryogenic environment.

Quantum Computation and Quantum Simulation with Strings of Trapped Ca^+ Ions

Rainer Blatt

Institute for Experimental Physics, University of Innsbruck, Technikerstrasse 25, A-6020 Innsbruck, Austria
Rainer.Blatt@uibk.ac.at, www.quantumoptics.at
Institute for Quantum Optics and Quantum Information, Austrian Academy of Sciences, Otto-Hittmair-Platz 1, A-6020 Innsbruck, Austria
Rainer.Blatt@oeaw.ac.at, www.iqoqi.at

This talk reviews the advanced capabilities of the trapped-ion quantum computer at Innsbruck [1]. We provide an overview of the quantum toolbox available and discuss the scalability of our approach. With control over up to 50 ion qubits, we perform quantum simulations to explore quantum transport [2] and hydrodynamic properties [3]. Additionally, we utilize the quantum toolbox to optimize parameters for quantum metrology [4] and showcase quantum-enhanced sensing of an optical transition through collective quantum correlations [5]. To shield quantum computers from noise, we redundantly encode logical quantum information across multiple qubits using error-correcting codes. Following a fault-tolerant circuit design, we mitigate the spread of uncontrolled errors when manipulating logical quantum states with imperfect operations [6] and demonstrate a fault-tolerant universal set of gates on two logical qubits in the trapped-ion quantum computer [7].

[1] I. Pogorelov et al., PRX Quantum 2, 020343 (2021)
[2] C. Maier et al., Phys. Rev. Lett. 122, 050501 (2019)
[3] M. K. Joshi et al., Science 376, 720 (2022)
[4] C. D. Marciniak et al., Nature 603, 604 (2022)
[5] J. Franke et al., Nature 621, 740 (2023)
[6] L. Postler et al., PRX Quantum 5, 030326 (2024)
[7] L. Postler et al., Nature 605, 675 (2022)

Quantum Many-body Physics with Fermions in an Optical Box

Nir Navon

Yale University - Department of Physics

For the past two decades harmonically trapped ultracold atomic gases have been used with great success to study fundamental many-body physics in flexible experimental settings. However, the resulting gas density inhomogeneity in those traps makes it challenging to study paradigmatic uniform-system physics (such as critical behavior near phase transitions) or complex quantum dynamics.

The realization of homogeneous quantum gases trapped in optical boxes has marked a milestone in the quantum simulation program with ultracold atoms [1]. These textbook systems have proved to be a powerful playground by simplifying the interpretation of experimental measurements, by making more direct connections to theories of the many-body problem that generally rely on the translational symmetry of the system, and by altogether enabling previously inaccessible experiments.

I will present some of our recent studies of many-body physics with ultracold fermions trapped in a box of light [2-6]. This platform is particularly suitable to study problems of Fermi-system stability, of which I will discuss two cases: the spin-1/2 Fermi gas with repulsive contact interactions [2], and the three-component Fermi gas with spin-population imbalance [3]. Both studies lead to surprising results, highlighting how spatial homogeneity not only simplifies the connection between experiments and theory, but can also unveil unexpected outcomes. I will also present other recent works, including the first observation of the fermionic Joule-Thomson effect [4], the strongly driven Fermi polaron [5], and the emergence of sound in a Fermi gas with tunable interactions [6].

References

[1] N. Navon, R.P. Smith, Z. Hadzibabic, Nature Phys. 17, 1334 (2021)
[2] Y. Ji et al., Phys. Lev. Lett 129, 203402 (2022)
[3] G.L. Schumacher et al., arXiv:2301.02237
[4] Y. Ji et al., Phys. Lev. Lett 132, 153402 (2024)
[5] F.J. Vivanco , arXiv:2308.05746
[6] S. Huang, arXiv:2407.13769

High-fidelity control and readout of superconducting qubits

Yasunobu Nakamura

Quantum computing demands an unprecedentedly high level of precision in the control and readout of quantum states encoding quantum information in a large Hilbert space. Therefore, in parallel with the pursuit of scalability, persistent efforts are being made to improve the control and readout fidelities of qubits. We are developing two-dimensionally integrated superconducting qubit arrays for quantum computing. This talk will focus on new techniques for achieving high-fidelity readout [1] and entangling gates [2] based on circuit quantum electrodynamics.

References

[1] P. A. Spring et al., arXiv:2409.04967.
[2] R. Li et al., arXiv:2402.18926; to appear in PRX.

ABSTRACTS FOR CONTRIBUTED TALKS

Robust entanglement generation

Mikkel F. Andersen[1], Poramaporn Ruksasakchai[1], Lucile Sanchez[1], Marvin Weyland[1], and Scott Parkins[2]

[1]The Dodd-Walls Centre for Photonic and Quantum Technologies, Department of Physics, University of Otago, Dunedin 9016, New Zealand mikkel.andersen@otago.ac.nz
[2]The Dodd-Walls Centre for Photonic and Quantum Technologies, Department of Physics, University of Auckland, Auckland 1010, New Zealand

Quantum entanglement has undergone a remarkable journey since its inception. It initially led Einstein, Poldolsky, and Rosen to question the completeness of the quantum mechanical description of the physical reality [1]. Today it is an established scientific fact, and practical applications utilizing quantum entanglement are emerging [2]. Additionally, it is expected to play a revolutionizing role in the future technologies [3]. A significant challenge that impede widespread use of entanglement enhanced technologies lies within its fragility. In particular a coupling of a quantum system to a thermal environment often lead to rapid loss of entanglement. This normally necessitates the arduous task of careful shielding of the quantum system from any thermal degrees of freedom. However, a coupling to an environment drives evolution in a quantum system, and under certain conditions such dissipative dynamics can cause the quantum system to evolve into an entangled state [4, 5]. The prospect of utilizing dissipative dynamics to generate useful entanglement has spurred intense theoretical interest [6–16], with many schemes proposing to generate entanglement through couplings to thermal environments or baths [17–24]. However, to date experimental implementations has focused on disipative dynamics driven by coupling to an effectively zero temperature environment [25–30]. The robustness of entanglement generated through interaction with a thermal environment makes it of considerable interest.

In this talk we go through our experiments in which coupling of spin-states of a pair of atoms to thermal motion dissipatively drive the spin-states from an un-entangled state into an entangled one. The dominant energy scale in the two-atom system is kB T where kB is Boltzmann's constant and T the temperature associated with the atoms' motional degree's of freedom. It is significantly larger than both the energy level separation associated with the atoms' motion in the trap and energy differences between different atomic spin-states part- taking in the dynamics. In this regime the atomic motion is usually considered classical.

Furthermore, we demonstrate that the entanglement generated is technologically useful and can enhance the sensitivity of magnetic field measurements beyond the standard quantum limit. Finally, we will discuss the prospect of seperating the atoms to generate spacially distributed entanglement, of potential use in magnetic field gradiometry or quantum information processing.

References

[1] B. P. A. Einstein and N. Rosen, Phys. Rev. 47, 777 (1935).
[2] J. A. et al, Nature Photonics 7, 613619 (2013).
[3] D. J. P. and M. G. J., Phil. Trans. R. Soc. A. 361, 16551674 (2003).
[4] D. Braun, Phys. Rev. Lett. 89, 277901 (2002).
[5] M. S. Kim, J. Lee, D. Ahn, and P. L. Knight, Phys. Rev. A 65, 040101 (2002).

[6] E. S. A. S. Parkins and J. I. Cirac, Phys. Rev. Lett. 053602, 053602 (2006).
[7] S. Pielawa, G. Morigi, D. Vitali, and L. Davidovich, Phys. Rev. Lett. 98, 240401 (2007).
[8] S. Diehl, A. Micheli, A. Kantian, B. Kraus, H. P. Büchler, and P. Zoller, Nat. Phys. 4, 878883 (2008).
[9] M. J. Kastoryano, F. Reiter, and A. S. Sørensen, Phys. Rev. Lett. 106, 090502 (2011).
[10] M. Foss-Feig, A. J. Daley, J. K. Thompson, and A. M. Rey, Phys. Rev. Lett. 109, 230501 (2012).
[11] A. W. Carr and M. Saffman, Phys. Rev. Lett. 111, 033607 (2013).
[12] F. Reiter, L. Tornberg, G. Johansson, and A. S. Sørensen, Phys. Rev. A 88, 032317 (2013).
[13] L. C. . L. X. Chen, RX., Sci Rep 7, 14497 (2017).
[14] S. He, D. Liu, and M.-H. Li, Chinese Physics B 28, 080303 (2019).
[15] Z.-Q. Liu, C.-S. Hu, Y.-K. Jiang, W.-J. Su, H. Wu, Y. Li, and S.-B. Zheng, Phys. Rev. A 103, 023525 (2021).
[16] F. Wang, K. Shen, and J. Xu, New Journal of Physics 24, 123044 (2023).
[17] T. Zell, F. Queisser, and R. Klesse, Phys. Rev. Lett. 102, 160501 (2009).
[18] D. P. S. McCutcheon, A. Nazir, S. Bose, and A. J. Fisher, Phys. Rev. A 80, 022337 (2009).
[19] A. A. Valido, D. Alonso, and S. Kohler, Phys. Rev. A 88, 042303 (2013).
[20] B. Bellomo and M. Antezza, Europhysics Letters 104, 10006 (2013).
[21] C. Eltschka, D. Braun, and J. Siewert, Phys. Rev. A 89, 062307 (2014).
[22] F. Tacchino, A. Auffèves, M. F. Santos, and D. Gerace, Phys. Rev. Lett. 120, 063604 (2018).
[23] K. Ullah, E. Köse, R. Yagan, M. C. Onbaşl ı, and O. E. Müstecaplıoğlu, Phys. Rev. Res. 4, 023221 (2022).
[24] M. T. Naseem and zgr E Mstecaplolu, Quantum Science and Technology 7, 045012 (2022).
[25] H. Krauter, C. A. Muschik, K. Jensen, W. Wasilewski, J. M. Petersen, J. I. Cirac, and E. S. Polzik, Phys. Rev. Lett. 107, 080503 (2011).
[26] J. T. Barreiro, M. Mller, P. Schindler, D. Nigg, T. Monz, M. Chwalla, M. Hennrich, C. F. Roos, P. Zoller, and R. Blatt, Nature 470, 486491 (2011).
[27] Y. Lin, J. P. Gaebler, F. Reiter, T. R. Tan, R. Bowler, A. S. Sørensen, D. Leibfried, and D. J. Wineland, Nature 504, 415 (2013).
[28] S. Shankar, M. Hatridge, Z. Leghtas, K. M. Sliwa, A. Narla, U. Vool, S. M. Girvin, M. M. L. Frunzio, and M. H. Devoret, Nature 504, 419422 (2013).
[29] M. H. M. Passos, W. F. Balthazar, A. Z. Khoury, M. Hor-Meyll, L. Davidovich, and J. A. O. Huguenin, Phys. Rev. A 97, 022321 (2018).
[30] X. Wang, H. Zhang, W. Zhang, X. Ouyang, X. Huang, Y. Yu, Y. Liu, X. Chang, D.-l. Deng, and L. Duan, Phys. Rev. A 102, 032615 (2020).

Self-bound droplets of dipolar molecules

D. Baillie

Department of Physics, University of Otago
Dodd-Walls Centre for Photonic and Quantum Technologies
danny.baillie@otago.ac.nz

Droplets of dipolar atomic gases were predicted [1] and subsequently realised [2] in 2016. Bose–Einstein condensation of dipolar molecules has just been reported (published July 2024) [3]. Molecules significantly enrich dipolar physics, with much stronger dipolar interactions; the ability to change the sign of the dipolar interaction; and dependence of the interaction on the azimuthal angle between atoms, as well as the usual polar angle.

We develop the theoretical and numerical tools to study this system including a variational ansatz, cutoff interaction potentials, quantum fluctuation energies, and an extended Gross-Pitaevskii equation (GPE). We use these tools to map out the phase diagram for self-bound droplets in this system, see Fig. 1.

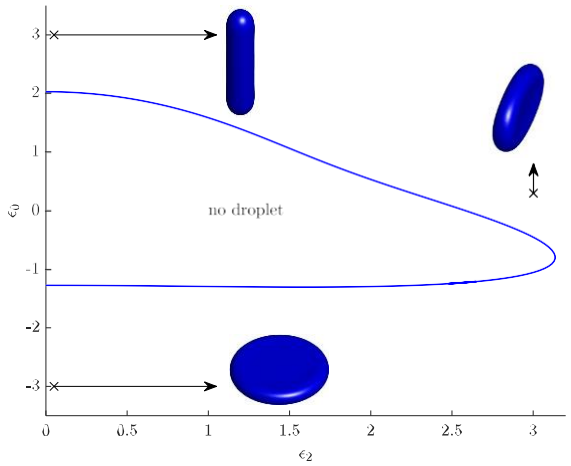

Figure 1: Phase diagram for droplets with N = 1000 dipolar molecules, depending on the relative dipole strengths ϵ0 and ϵ2 for the Y20(θ, ϕ) and Y22(θ, ϕ)+Y2−2(θ, ϕ) spherical harmonics, respectively. Isosurfaces are for GPE solutions at the indicated parameters.

References

[31] D. Baillie, R. M. Wilson, R. N. Bisset, and P. B. Blakie, “Self-bound dipolar droplet: a localized matter wave in free space”, Phys. Rev. A 94, 021602(R) (2016).

[32] M. Schmitt, M. Wenzel, F. Böttcher, I. Ferrier-Barbut, and T. Pfau, “Self-bound droplets of a dilute magnetic quantum liquid”, Nature **539**, 259 (2016).

[33] N. Bigagli, W. Yuan, S. Zhang, B. Bulatovic, T. Karman, I. Stevenson, and S. Will, “Observation of Bose–Einstein condensation of dipolar molecules”, Nature **631**, 289 (2024).

Spontaneous symmetry breaking in a coupled photonic crystal dimer with periodic driving

Rodrigues Dikande Bitha*, Kevin Stitely, Bernd Krauskopf, Neil G. R. Broderick

Dodd-Walls Centre for Photonic and Quantum Technologies, University of Auckland, Auckland, New Zealand
*rodrigues.bitha@auckland.ac.nz

In this presentation, we explore the interactions between two optical modes in a periodically driven photonic crystal dimer. We discover that the system exhibits spontaneous symmetry and investigate its impact on the generation of subharmonic frequency combs.

Spontaneous symmetry breaking in optical cavities is the process by which, two optical modes with apparent symmetry break down spontaneously into two non-identical states. Recently, this phenomenon was reported in different configurations of optical resonators with two interacting modes coupled either linearly or nonlinearly. In this work, we study the dynamics of two modes in a photonic crystal dimer, where the configuration of the system favors linear and nonlinear coupling of the two modes, as well as a four-wave mixing-induced nonlinearity. We show that, under these conditions, the system can still exhibit a wide range of interesting dynamics, including spontaneous symmetry breaking of different types of solutions.

Recently, Goldman *et al*. [1] described a method by which the interactions between two optical modes induce an effective four-wave-mixing nonlinearity in different optical systems. Here, we consider the case of two coupled photonic crystal nanocavities: by periodically driving these two resonators, an exchange of energy is induced, leading to the creation of new frequencies and exotic states of light. This photonic-based coupled system simulates the interactions of continuously driven two-component Bose-Einstein condensates, that are described in the quantum many-body interaction by a two-axis countertwisting Hamiltonian. In the semiclassical approximation, the rate equations of the light fields in each cavity are

$$\frac{dE_a}{dt} = -iz_1|E_a|^2E_a - 2iz_1|E_b|^2E_a + z_2E_a^*E_b^2 + i\Omega E_b - E_a + i\Delta_0 E_a + \sqrt{F},$$
$$\frac{dE_b}{dt} = -iz_1|E_b|^2E_b - 2iz_1|E_a|^2E_b + z_2E_b^*E_a^2 + i\Omega E_a - E_b + i\Delta_0 E_b + \sqrt{F},$$

where E_a and E_b are the field amplitudes of the two modes, z_1 is the strength of the nonlinear response of the cavity due to the nonlinear Kerr effect, z_2 is the induced four-wave-mixing nonlinearity, Ω is the linear coupling strength, Δ_0 is the detuning from the nearest cavity resonance, F is the driving strength, and t is time. Here z_1 and z_2 depend on a tunable parameter α, which encodes the pulse timings of the periodic drive. Note that exchanging E_a and E_b leaves the system invariant.

We use a dynamical system approach, to study different behaviors the system under study can display by describing its bifurcations. To achieve this, we utilize numerical continuation techniques~\cite{auto} implemented in the software package AUTO07P. We also study a quantum mechanical model which retrieves the semiclassical equations of motion described above.

References

[1] N. Goldman, O. K. Diessel, L. Barbiero, M. Pruufer, M. Di Liberto, and L. Peralta Gavensky, “Floquet-Engineered Nonlinearities and Controllable Pair-Hopping Processes: From Optical Kerr Cavities to Correlated Quantum Matter,” Phys. Rev. X 4, 040327(2023).
[2] B. Krauskopf, H. M. Osinga and J. Galan-Vioque, Numerical Continuation Methods for Dynamical Systems: Path following and boundary value problems, eds. (Springer-Verlag 2007).

Regimes of steady turbulence of a quantum gas in a shaken box trap

Ashton Bradley

The University of Otago

A variety of turbulent regimes have been observed in quantum fluids, some analogous to classical fluids and others uniquely quantum in nature. Optical box-traps for atomic condensates have enabled creation of bulk phases of forced turbulence, free from strong inhomogeneity of harmonic confinement. Recent works have reported signatures for weak-wave turbulence in otherwise uniform systems with hard-wall confinement, observing slightly different power-laws and suggesting different underlying mechanisms for the turbulence. Here we numerically create and analyse quasi-steady state turbulence in a three dimensional Gross-Pitaevskii fluid confined by an anisotropic box potential. We simulate large scale forcing starting from the ground state, and observe the development of isotropic turbulence from anisotropic forcing for a wide range of forcing amplitudes. Analysis of the momentum distribution reveals a wide regime of $k^{-3.5}$ scaling for weak forcing consistent with experimental data, and a wide regime of $k^{-2.4}$ scaling for strong forcing. Further decomposing the momentum distribution we find $k^{-3.5}$ involves a simultaneous cascade of compressible kinetic energy and quantum pressure, while the bulk superfluid remains vortex free. The $k^{-2.4}$ regime for strong forcing is consistent with an inverse particle cascade driven by small-scale vortex annihilation.

Construction of an Upconversion Enabled Z-Scheme Heterojunction for Next-Generation Photovoltaic Devices

Jodi G. Carter, Nathaniel J. L. K. Davis

Solar panel technology can be used to combat climate change, however are only able to harvest a small fraction of the solar spectrum. There are many different processes that have been studied to harvest more of the solar spectrum, such as multiple exciton generation, singlet fission and triplet-triplet annihilation upconversion.1-3 Here we report the proposal for the construction and characterization of a Z-Scheme heterojunction using two inorganic semiconductors for upconversion in solar cells. Upconversion will occur where the two semiconductors each absorb a low energy photon, where the electron-hole recombination can occur. This allows the remaining free charges to be extracted, obtaining an 'upconverted energy' (Figure 1).

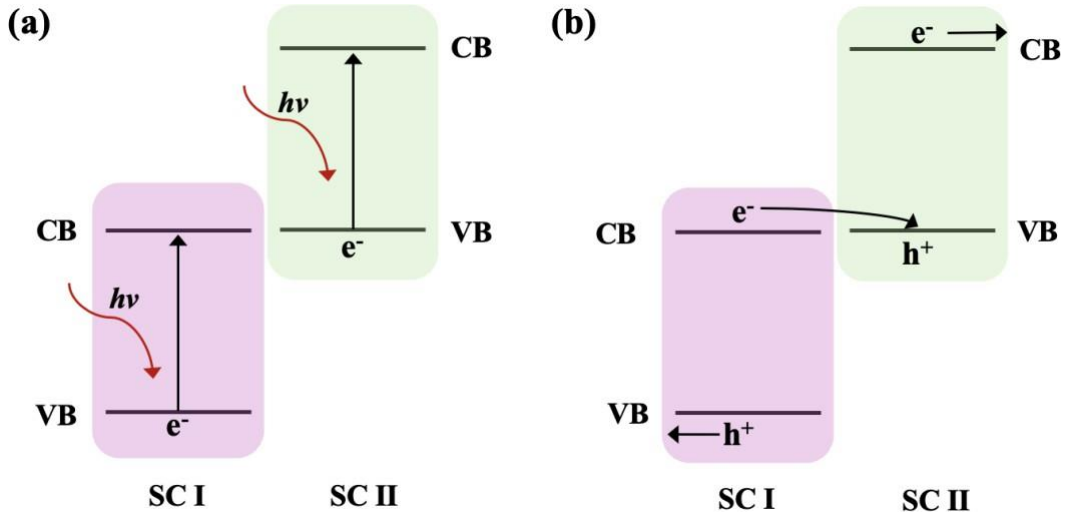

Figure 1: (a) Semiconductors (SC) I and II absorb low energy light, exciting an electron into the conduction band (CB) and leaving a hole in the valence band (VB). (b) The electron on SC I can recombine with hole on SC II, leaving the remaining charges to be harvested to obtain upconverted energy.

References

[1] Beard, M. C.; Luther, J. M.; Semonin, O. E.; Nozik, A. J. Acc. Chem. Res. **2013**, 46 (6), 1252–1260. DOI: 10.1021/ar3001958.

[2] Baldacchino, A. J.; Collins, M. I.; Nielsen, M. P.; Schmidt, T. W.; McCamey, D. R.; Tayebjee, M. J. Y. Chem. Phys. Rev. **2022**, 3 (2), 021304. DOI: 10.1063/5.0080250.

[3] Feng, J.; Alves, J.; de Clercq, D. M.; Schmidt, T. W. Annu. Rev. Phys. Chem. **2023**, 74 (1). DOI: 10.1146/annurev-physchem-092722-104952.

Microwave Polarisation Spectroscopy of Rydberg Atoms

Matthew Cloutman[1], Matthew Chilcott[1], J. Susanne Otto[1], Alexander Elliott[2], Niels Kjærgaard[1]

[1]Department of Physics, QSO—Quantum Science Otago, and Dodd-Walls Centre for Photonic and Quantum Technologies, University of Otago
[2]Department of Physics and Dodd-Walls Centre for Photonic and Quantum Technologies, University of Auckland

Rydberg atoms are alkali atoms that have been electronically excited into a high n quan- tum state. Rydberg atoms have exaggerated properties such as their lifetimes, atomic radii, and polarisabilities, which have garnered a great deal of interest in recent decades. Additionally, transitions between Rydberg states have extremely large electronic transition dipole moments, and range in frequency from the RF into the terahertz domain. This makes Rydberg atoms a promising candidate for field sensing applications. When optically addressed using electromagnetically induced transparency (EIT), Rydberg atoms allow an all-optical readout of the field amplitude. [1].

Here we explore some of the intricacies involved with Rydberg atom based electrometry, including how the choice of atomic states involved alters the characteristics and polarisation-dependence of the optical EIT measurement. We experimentally perform polarisation spectroscopy of several different atomic transitions, showing that some transitions can be chosen for their polarisation independence, while other sets of transitions can display complementary polarisation-dependent characteristics.

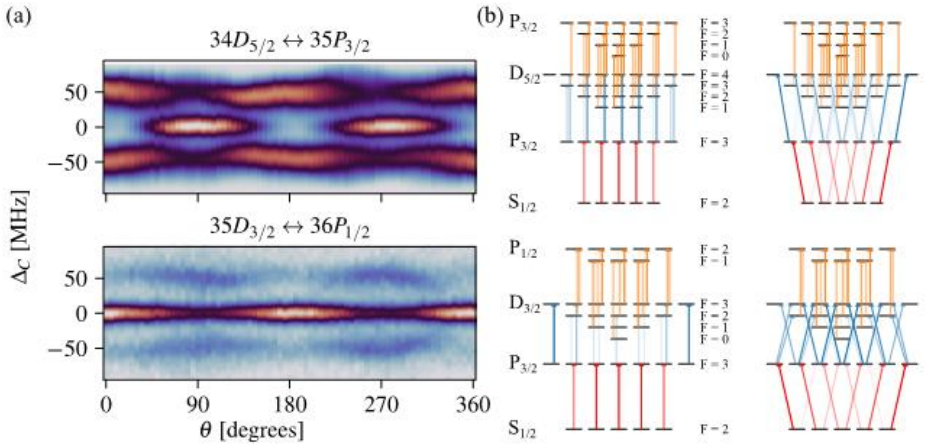

Figure 1: (a) Polarisation spectra of D5/2 ↔ P3/2 and D3/2 ↔ P1/2 transitions showing the complementary behaviour of the EIT spectrum as a linearly polarised THz emitter is rotated. (b) Hyperfine level diagrams showing all the fields and states involved for both transitions, for 0◦ and 90◦ polarisations.

References

[1] Jonathon Sedlacek, Arne Schwettmann, Harald Kübler, Robert Löw, Tilman Pfau, and James Shaffer. Microwave electrometry with Rydberg atoms in a vapour cell using bright atomic resonances. *Nat. Phys.*, 8:819–824, 2012.

Rimu.jl: Random integrators for many-body quantum systems

Matija Čufar[1], Mingrui Yang[1,2], Chris Bradly[3], Elke Pahl[4], Joachim Brand[1]

[1]Dodd-Walls Centre for Photonic and Quantum Technologies, Institute for Advanced Study and Centre for Theoretical Chemistry and Physics, Massey University, Auckland 0632, New Zealand
[2]Department of Chemistry, Washington University in St. Louis, St. Louis, Missouri, MO 63130, USA
[3]School of Mathematics & Statistics, The University of Melbourne, Victoria 3010, Australia [4]MacDiarmid Institute for Advanced Materials and Nanotechnology, Department of Physics, University of Auckland, Auckland 1010, New Zealand

Solving the time-independent Schrödinger equation for a quantum many-body system is equivalent to finding the lowest eigenpair of a large matrix. The dimension of this matrix grows exponentially with the size of the underlying quantum system, which makes finding the ground state with exact methods computationally intractable even for modestly-sized problems. Full Configuration Interaction Quantum Monte Carlo (FCIQMC) [1] is a stochastic computational method used to sample the ground state wave functions of quantum many-body systems. By employing stochastic sampling and compression, it can be applied to systems much larger than would be possible with standard, exact methods.

In this presentation, we will present our pure Julia implementation of FCIQMC, Rimu [2, 3, 4]. We will discuss how the package works, its various features, and how we have applied it to researching the physics of ultra-cold atoms.

References

[1] George H Booth, Alex JW Thom, and Ali Alavi. Fermion Monte Carlo without fixed nodes: A game of life, death, and annihilation in slater determinant space. The Journal of Chemical Physics, 131(5):054106, 2009.
[2] Matija Čufar, Mingrui Yang, Chris Bradly, Elke Pahl, and Joachim Brand. Rimu.jl. In preparation, 2024.
[3] Mingrui Yang, Elke Pahl, and Joachim Brand. Improved walker population control for full configuration interaction quantum Monte Carlo. The Journal of Chemical Physics, 153(17):174103, 2020.
[4] Joachim Brand, Mingrui Yang, and Elke Pahl. Stochastic differential equation approach to understanding the population control bias in full configuration interaction quantum monte carlo. Physical Review B, 105(23):235144, 2022.

Trapping Dysprosium in a Magnetic Optical Trap Directly from a Thermal Beam

Liam Domett-Potts[12], Lucile Sanchez[12], Marvin Weyland[12] Chris Hayton[12], Mikkel F. Andersen[12]

[1] The University of Otago
[2]The Dodd-Walls Centre for Photonic and Quantum Technologies domli388@student.otago.ac.nz

Dysprosium is the most magnetic element on the periodic table, which gives it the potential to display exotic physics. To study magnetic interacting atoms, we plan to capture single atoms of Dysprosium in optical tweezers, similarly to [1]. The first step is a 3-D magneto-optical trap (MOT), which combines the optical molasses technique [2] and spatial-dependent Zeeman splitting [3] to trap a cloud of Dysprosium atoms. The MOT is inside an ultra-high vacuum (UHV) chamber and an effusion cell produces a hot beam of Dysprosium atoms, from which it loads. An amplified external cavity diode laser, locked to an optical reference cavity, generates the 421nm light that forms the optical molasses. Water-cooled coils in an anti-Helmholtz configuration generate the magnetic fields. Our experiment is the first to load the MOT directly in the hot beam, prioritising simplicity over a large MOT population by going without a 2-D MOT or Zeeman slower, used in [4] and [5]. This talk presents our design and implementation of a simpler Dysprosium MOT, shown in Fig. 1. We also show the characteristics of the MOT and atomic source. We have greatly simplified the Dysprosium MOT by going without frequency doubling setups to generate the laser light [5], [6] and pre-cooling stages [5], [7]. Simplifying this process allows more laboratories worldwide to implement Dysprosium trapping and further our understanding of its exotic physics.

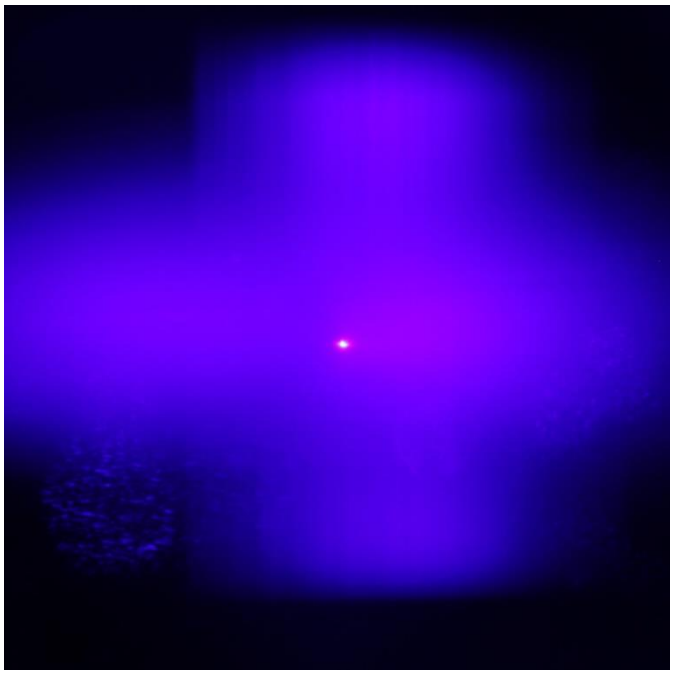

Figure 1: The first Dysprosium MOT, trapped directly from the hot atomic source, with fast-moving Dys- prosium atoms fluorescing in the background.

References

[1] Matthew McGovern. *Isolating and manipulating single atoms*. PhD thesis, The University of Otago, 2012.
[2] Harold J. Metcalf and Peter. Van der Straten. *Laser cooling and trapping*. Graduate texts in contemporary physics. Springer, New York, 1999.
[3] B. H. Bransden and C. J. (Charles Jean) Joachain. *Physics of atoms and molecules*. Prentice Hall/Pearson Education, Harlow, 2nd ed. edition, 2003.
[4] Jianshun Gao. *A First Two-Dimensional Optical Trap For Dysprosium*. PhD thesis, University of Heidelberg, 2022.
[5] Mingwu Lu. Quantum bose and Fermi gases of dysprosium [electronic resource]: production and initial study. PhD thesis, Stanford University, 2014.
[6] Leonardo Del Bino. Development of an experimental apparatus for the realization of dipolar quantum gases of Dysprosium atoms. PhD thesis, University of Florence, 2015.
[7] Davide Dreon. Designing and building an ultracold Dysprosium experiment: a new framework for light-spin interaction. Theses, Universite´ Paris sciences et lettres, July 2017.

The investigation of the effect of bromine crosslinking in the photostability of PM6 donor polymer using Resonance Raman and DFT calculation study for Organic Solar Cells applications

Elkhansa Elbashier[1,*], Hye Won Cho[2], Minhun Jee[3], Jae Hyeong Kim[2], Jin A Roe[2], Jeong Min Son[2], Yeon Jeong Lee[2], Dong Chan Lee[4], Shinuk Cho[4], Keith C. Gordon[1,*], Han Young Woo[3], Jin Young Kim[2,5]

[1]The Dodd-Walls Centre for Photonic and Quantum Technologies, Department of Chemistry, University of Otago, P.O. Box 56, Dunedin 9001, New Zealand
[*]Elbel670@student.otagoac.nz, keith.gordon@otago.ac.nz
[2]School of Energy and Chemical Engineering, Ulsan National Institute of Science and Technology (UNIST), Ulsan 44919, Republic of Korea
[3]Department of Chemistry, Korea University, Seoul 136-713, Republic of Korea
[4]Department of Physics and Energy Harvest Storage Research Center, University of Ulsan, Ulsan 44610, Republic of Korea
[5]Graduate School of Carbon Neutrality, Ulsan National Institute of Science and Technology (UNIST), Ulsan 44919, Republic of Korea

Organic solar cells (OSCs) are nearing commercial viability, but their long-term stability remains a challenge. The PM6 polymer, known for good performance, suffers from low stability after light exposure in air. This study explores photo cross-linking of PM6 to enhance its light stability, both as a pristine film and in a blend with the Y6-HU acceptor. Resonance Raman spectroscopy was used to assess photo-oxidation and the effectiveness of cross- linking in both pristine and blend films. Density Functional Theory (DFT) calculations simulated the Raman spectra of oxidized PM6 species (hydroxides and sulfoxides) and compared them to aged film spectra. Results showed that aged PM6 films resembled oxidized and twisted PM6, while cross-linked PM6 exhibited less degradation and fewer similarities to these species. These findings suggest that cross-linking can slow down the degradation and photo-oxidation rate by reducing molecular twisting and the formation of oxidized species. DFT simulations were conducted to compare the band gap, molecular orbitals, electronic transitions, and geometrical structures of the PM6 polymer and its oxidized species. The results indicated that the main electronic transition in the hydroxide species becomes a π-π* in nature with a narrower band gap, suggesting reduced charge transfer efficiency and potentially reducing OSC performance. The sulfoxide species exhibited significant twisting, distinct FMO orbitals, extended charge transfer but with lower oscillation strength, and more electronic transitions in the blue region, which could lead to higher formation of trap states or polaron pairs, further lowering OSC performance. Overall, cross-linking PM6 improves its stability and could enhance the long-term performance of OSCs.

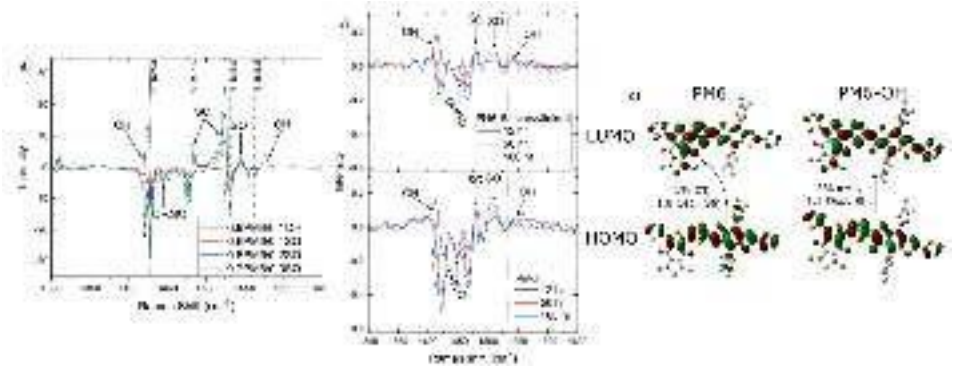

Figure 1: a) simulated diff. Raman spectra of PM6-oxidised species, b) experimental Resonance Raman spectra of the studied PM6 films, and c) the FMO orbitals of PM6 and its hydroxide species.

Tailoring Nonclassical Light with Single-Atom Cavity QED

Alex Elliott[1,2] and Scott Parkins[1,2]

[1] Department of Physics, Waipapa Taumata Rau The University of Auckland
[2] Te Whai Ao Dodd-Walls Centre For Photonic and Quantum Technologies
alexander.elliott@auckland.ac.nz

Cavity QED experiments probe controllable atom-light interactions at the scale of single quanta, which can cause emitted light to exhibit nonclassical characteristics. The production of nonclassical states of light is an essential component in the advancement of quantum information and quantum communication technologies. This theoretical investigation, guided by the modern experimental capabilities, proposes viable and novel configurations for generating nonclassical light from single-atom cavity QED systems.

An atom in the vicinity of a high-quality cavity will couple to near-resonant modes of the electromagnetic field (Fig. 1). If the spatial volume of a mode is sufficiently small, the per-photon electric field becomes correspondingly large. Absorption and emission of photons, through electric dipole transitions in the atom, can therefore heavily alter the state of the cavity field.

We explore cavity QED systems which utilise single Rubidium or Caesium atoms. A set of Auxiliary lasers with Rabi frequencies Ω_i are used to manipulate the internal state of the atom within the hyperfine Zeeman sublevels. The principles of conservation of energy and angular momentum are leveraged to control properties of light coupled into the cavity. Managing the frequencies and polarisations of the coupling fields give a means to control the light emitted from the cavity. This offers new avenues for the generation of light which exhibits nonclassical features such as negativity of the Wigner distribution, quadrature squeezing, and Fock states.

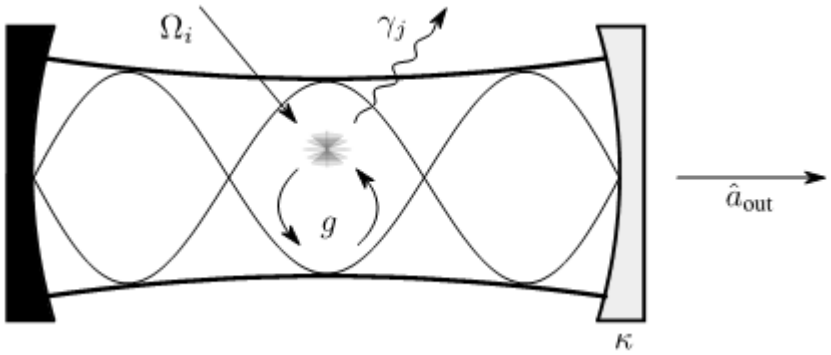

Figure 1: Single atom in a cavity, with excited-state linewidths γj, and an atom-cavity coupling strength g. The cavity is designed to be one-sided, where the "bad" mirror has a decay rate of κ. The atom is driven by classical laser fields with Rabi frequencies Ω_i. Light escapes from the cavity into the output field $\hat{\alpha}_{out}$.

The systems are described by a Lindblad master equation, where the atomic excited states have linewidths γ_j, and the cavity has a photonic decay rate κ. The output field is calculated through the input-output relation $\hat{\alpha}_{\text{out}} = \sqrt{2\kappa\hat{\alpha}} + \hat{\alpha}_{in}$, in terms of the cavity field mode annihilation operator $\hat{\alpha}$.

Quantum optics of parametrically driven soliton microcombs

Sophie Shamailov[1,2] and Miro Erkintalo[1,2]

[1]Department of Physics, University of Auckland, Auckland 1010, New Zealand
[2]The Dodd-Walls Centre for Photonic and Quantum Technologies, New Zealand

Coherent microresonator frequency combs corresponding to dissipative Kerr cavity solitons (CSs) have attracted significant attention over the past decade, enabling groundbreaking advances in applications from telecommunications to sensing. Beyond classical photonics applications, there has recently been increasing recognition of the potential of such combs as a multimode resource for quantum technologies, allowing e.g. for the realization of complex high- dimensional entangled states and squeezing [1, 2].

Microresonator CSs studied to date are underpinned by direct additive driving of the resonator with a monochromatic laser. In this case, the solitons spectrally form around the driving laser frequency, which becomes part of the ensuing frequency comb. Recently, a new type of dissipative soliton frequency comb has been discovered, where the solitons are driven through the parametric interaction of two monochromatic lasers with different frequencies. The resultant parametrically driven cavity solitons (PDCSs) form spectrally in between the two driving fields, and display unique characteristics compared to the conventional additively driven CSs. However, these PDCSs have hitherto only been studied in the classical regime, and their quantum optical properties (and how such properties compare with conventional CSs) is wholly unexplored.

In this work, we report on a comprehensive theoretical study of the quantum optical properties of bichromatically-driven PDCSs. Following [3], we derive a linearized model that describes the quantum dynamics of the system, examining and comparing the predicted properties of the PDCS system with that of conventional CSs. Salient properties under study include spontaneous emission spectra, the second-order correlation function $g2(\tau)$, and quadrature squeezing spectra. Our calculations suggest that PDCSs are associated with stronger squeezing and entanglement compared to their conventional CS counterparts.

References

[1] Z. Yang et al., Nature Communications **12**, 4781 (2021)
[2] M. A. Guidry et al., Nature Photonics **16**, 52-58 (2022)
[3] Y. K. Chembo, Physical Review A **93**, 033820 (2016)

Optical fiber sensors for Tokamak fusion reactors

F. Solis Fernandez, B. M. Ludbrook, S. M. Haneef, M. Davies, X. Huang, D. A. Moseley, J. Schuyt, R. A. Badcock

Nuclear fusion energy is almost a reality now but there are still some challenges we need to overcome before it becomes a reliable and sustainable source of energy. Toakamak reactors are subjected to extreme conditions: temperatures as hot as the sun are reached inside the reactor but the superconducting magnets that confine the plasma need operate at temperatures as low as 20 K. Furthermore, extremely high levels of electromagnetic radiation and ionizing radiation are present in this environment. All of these factors make the use of traditional voltage-based sensors non viable and an alternative is necessary. Optical fiber sensors seem to be a great potential since they are inmune to electromagnetic noise and can withstand very low temperatures without problem. However, their implementation still poses some difficulties. Ionizing radiation can cause a large increase in the attenuation of the fibers called Radiation-Induced Attenuation (RIA) that can deem them unusable. This phenomenon has been studied for the last 20-30 years [1], but RIA is very complex and depends o numerous factors. So, there are still many gaps in the literature regarding this topic, specially in the temperatures we are intrested. It is known that RIA gets aggravated at low temperatures [2] but very little has been devoted to studying RIA at 77 K and below. Radiation-induced attenuation can be mitigated through thermal [3–5] or optical annealing [6, 7] (the latter is also known as photobleaching). In both cases, some energy is supplied to the fibers (either in the form of heat or light) which anneals the defects created by the radiation and restores the transmission levels close to before irradiation. But very few works have been devoted to study this effect at the temperatures we are interested. In this work, we explore the relation between the power of the photobleaching light and its effectiveness in mitigating the radiation-induced attenuation by X-rays and neutrons. We investigate the region of cryogenic temperatures (77 K and below) to help characterize the phenomenon of photobleaching and obtain a better understanding of the dynamics of RIA.

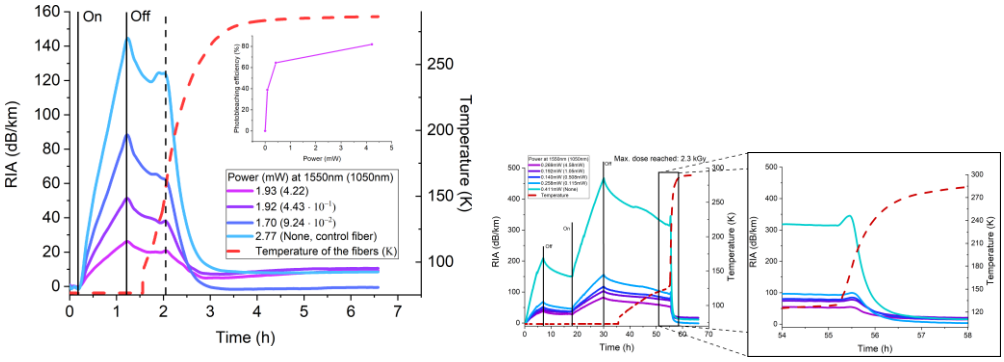

References

[1] Sylvain Girard et al. “Overview of radiation induced point defects in silica-based optical fibers”. In: *Reviews in Physics* 4 (Nov. 2019). issn: 24054283. doi: 10.1016/j.revip.2019.100032.

[2] A. Morana et al. “Temperature Dependence of Low-Dose Radiation-Induced Attenuation of Germanium- Doped Optical Fiber at Infrared Wavelengths”. In: *IEEE Transactions on Nuclear Science* 69 (3 Mar. 2022), pp. 512–517. issn: 15581578. doi: 10.1109/TNS.2021.3133421.

[3] B.W. Morgan et al. “Optical Absorption of Fused Silica and Sapphire Exposed to Neutron and Gamma Radiation with Simultaneous Thermal Annealing”. In: *Journal of Nuclear Materials* 570 (Nov. 2022), p. 153945.

issn: 00223115. doi: 10 . 1016 / j . jnucmat . 2022 . 153945. url: https : / / linkinghub . elsevier.com/retrieve/pii/S0022311522004317.

[4] P. Martin et al. “Thermal stability of gamma irradiation induced defects for different fused silica”. In: *Journal of Nuclear Materials* 417 (1-3 Oct. 2011), pp. 818–821. issn: 0022-3115. doi: 10.1016/J.JNUCMAT.2010.12.171.

[5] S. V. Solov’ev, I. I. Milman, and A. I. Syurdo. “Thermal- and photo-induced transformations of lumi- nescence centers in αd-Al 2O 3 anion-defective crystals”. In: *Physics of the Solid State* 54 (4 Apr. 2012), pp. 726–734. issn: 10637834. doi: 10.1134/S1063783412040270.

[6] E.M. Dianov et al. Reversible optical bleaching of the induced absorption in fiber-optic waveguides. 1979.

[7] E J Friebele and M E Gingerich. Photobleaching effects in optical fiber waveguides. 1981.

Development of fluorescent analogues of vitamin B_{12} and the cobinamide precursor for antibacterial applications

Jessica Fredericksen[1], Julia Robertson[1], Yan Li[1], Ji He[1], Scott Ferguson[2], Brent Seale[1] and Nicola E. Brasch[1]

[1]School of Science, Auckland University of Technology Jessica.fredericksen@aut.ac.nz
[2]Department of Microbiology and Immunology, University of Otago

The increase in antibiotic resistance is a major health concern that is rapidly spreading across the globe.[1] Novel drugs and technologies urgently need to be developed to combat this issue. Our research proposes to hijack the native vitamin B_{12} uptake pathway, essential to bacteria, for the delivery of drugs into bacterial cells. By utilizing the vitamin B_{12} precursor, cobinamide (Cbi), selective treatment of bacteria over mammalian cells may be afforded. It is well established in the literature that Cbi is not utilised by human cells (except for hepatocytes[2]) whereas most bacterial species have uptake mechanisms to scavenge Cbi.[3,4] In a proof-of-concept study, fluorescent conjugates of B_{12} and Cbi have been synthesised utilising commercial fluorophores as imaging agents. Fluorescence experiments identified substantial quenching of the conjugates where spectral overlap occurred between the absorbance of the B_{12}/Cbi moiety and the fluorophore emission, likely to occur via FRET. The quenching phenomenon was overcome by either inclusion of a chemically cleavable linker or the use of near-infrared emitting fluorophores. These conjugates have been used as tools to assess the uptake of Cbi and B_{12} into the gram-negative bacterium, *Escherichia coli,* visualised using fluorescence microscopy. These studies demonstrated successful uptake of both the B_{12} and Cbi conjugates into *E. coli*. Furthermore, preliminary data has supported the selectivity for B_{12} over Cbi conjugates within mammalian kidney and intestinal cells. Current studies are underway where the fluorescent moiety has been substituted for an established antimicrobial drug and the antimicrobial properties of these compounds investigated in wild type and antimicrobial resistant bacteria.

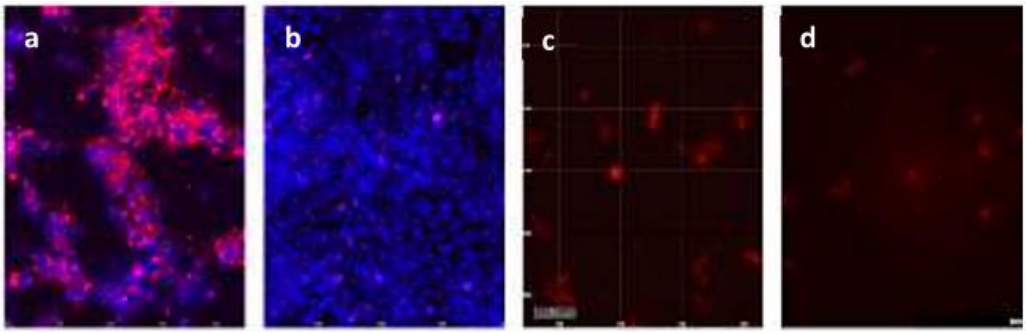

Figure 1: Fluorescence microscopy images of; mammalian HEK293 (kidney) cells incubated with B_{12}-PEG-Cy7 (a) and Cbi-PEG-Cy7 (b) and Escherichia coli cells incubated with B_{12}- PEG-Cy7 (c) and Cbi-PEG-Cy7 (d).

References

[1] Thomas, M. G.; Smith, A. J.; Tilyard, M. The New Zealand Medical Journal 2014, 127, 72–84.
[2] Sokolovskaya, O. M.; Plessl, T.; Bailey, H.; Mackinnon, S.; Baumgartner, M. R.; Yue, W. W.; Froese, D. S.; Taga, M. E. Biochimie 2021, 183, 35–43.
[3] Woodson, J. D.; Zayas, C. L.; Escalante-Semerena, J. C. Journal of Bacteriology 2003, 185 (24), 7193–7201.

[4] Rodionov, D. A.; Vitreschak, A. G.; Mironov, A. A.; Gelfand, M. S. Journal of Biological Chemistry 2003, 278 (42), 41148–41159.

Quantitative measurement of extinction, scattering, and absorption spectra from metallic nanoparticles

Alla Gisich[1,2,3], Baptiste Auguié[1,2,3] and Eric C. Le Ru[1,2]

[1]School of Chemical and Physical Sciences, Victoria University of Wellington, Wellington, 6012
alla.gisich@vuw.ac.nz
[2]The MacDiarmid Institute for Advanced Materials and Nanotechnology Wellington, 6012
[3]The Dodd-Walls Centre for Photonic and Quantum Technologies, University of Otago, Dunedin 9054

Metallic nanoparticles are used in many applications, relying on either scattering or absorption of light. Unfortunately, their optical characterisation using traditional UV–vis spectroscopy cannot distinguish between absorption and scattering contributions to extinction. Recent progress has been made with an integrating sphere technique [1,2] enabling the collection of pure absorption spectra to complement standard extinction measurements. While pure absorption can be accurately measured using an integrating sphere, determining scattering from such measurements is indirect, as it involves subtracting absorption from extinction [1,2]. This approach faces challenges when dealing with weakly scattering samples, as extinction closely resembles absorption, resulting in noisy and unreliable scattering signals. Scattering measurements can alternatively be performed directly using a 90-degree configuration. However, the measurement is non-trivial, and a careful correction function that describes the spectral modification of the incident light due to extinction in the incident beam's path length is necessary to interpret the data accurately.

In this study, we apply these three techniques to characterise solutions of Au nanospheres with diameters in the range of 20–100 nm and check the consistency of extinction as the sum of absorption and scattering. Our analysis will demonstrate that the representation of the correction function in previous studies [3] as an only extinction-depended function is an approximation with limited applicability, and we propose an alternative method to obtain this factor experimentally with a reference measurement. We used the Cloudspec [1,2] spectrophotometer for combined extinction/absorption measurements while scattering was measured using a 90-degree configuration [4].

Experimental access to all three types of spectra, rather than only extinction as in standard UV–vis spectroscopy, provides a much richer characterisation tool and offers therefore a more stringent test of the parameters used in a theoretical fit. Notably, good agreement with Mie theory could only be obtained by considering the size polydispersity of the colloids and choosing the correct, non-trivial correction function and dielectric function for the metal [1].

These findings are crucial to improve measurement reliability using UV–vis and integrating sphere techniques, across their broad range of applications. Direct measurement of scattering is also advantageous for the smaller particle sizes, where subtraction between extinction and absorption is unreliable. Conducting experiments with a broader range of nanoparticle types and concentrations can provide a more robust understanding of the correction methods' applicability. This approach can help identify specific conditions under which each model excels or fails.

References

[1] Djorović A, Oldenburg SJ, Grand J, Le Ru EC. Extinction-to-Absorption Ratio for Sensitive Determination of the Size and Dielectric Function of Gold Nanoparticles. ACS Nano. 2020;14(12):17597-17605. doi:10.1021/acsnano.0c08431.

[2] Grand J, Auguié B, Le Ru EC. Combined Extinction and Absorption UV–Visible Spectroscopy as a Method for Revealing Shape Imperfections of Metallic Nanoparticles. Anal Chem. 2019;91(22):14639-14648. doi:10.1021/acs.analchem.9b03798.

[3] Norberto Micali et al. Separation of Scattering and Absorption Contributions in UV/Visible Spectra of Resonant Systems". In: Anal Chem. 73.20 (Oct. 2001): 4958–4963. ISSN: 0003-2700. doi: 10.1021/ac010379n.

[4] Liu BJ, Lin KQ, Hu S, et al. Extraction of Absorption and Scattering Contribution of Metallic Nanoparticles Toward Rational Synthesis and Application. Anal Chem. 2015;87(2):1058-1065. doi:10.1021/ac503612b.

Modelling light absorption by core-satellite nanostructures

Stefania Glukhova[1*], Eric C. Le Ru[1,2] and Baptiste Auguié[1,2,3]

[1]School of Chemical and Physical Sciences, Victoria University of Wellington, PO Box 600, Wellington, New Zealand
[2]The MacDiarmid Institute for Advanced Materials and Nanotechnology, New Zealand
[3]The Dodd-Walls Centre for Photonic and Quantum Technologies, New Zealand

Background and aims

Metallic core-satellite nanostructures composed of a plasmonic core particle surrounded by smaller satellite nanoparticles have recently been proposed for photocatalytic applications [1]. Computer simulations of the absorbance by such structures can prove challenging, even with state-of-the-art numerical methods, due to the large difference in size between core and satellite particles. We have developed a theoretical framework that enables efficient computations of light absorption by such nanostructures with a large number of satellites.

Methods

We introduce a generalised couple-dipole model to describe the electromagnetic interactions between particles, where the small satellites are represented as point dipoles surrounding a spherical core particle, treated with Mie theory. A further extension of this couple-dipole approximation treats the collection of satellites as a shell with an anisotropic effective dielectric function [2]. Both models were tested against rigorous solutions of Maxwell's equations based on the T-matrix method [3]. The particle configurations were chosen to match experimentally relevant parameters, with a ~60nm Au core surrounded by ~5nm Pd satellites. Ag satellites were also studied, allowing a more direct interpretation of the spectral resonances corresponding to the core and satellite particles.

Results

Both models offer excellent computational performance, allowing rapid simulations of core-satellite nanostructures with coverage reaching hundreds of satellites. Our benchmarks delineate the regime of validity of the coupled-dipole and effective-medium approximations, in terms of satellite radius, coresatellite spacing, and minimum inter-satellite distance.

Conclusion

The proposed models allow efficient calculation of the optical response by core-satellite nanostructures with a large number of satellites. These approaches can facilitate the design of catalytic nanoparticles.

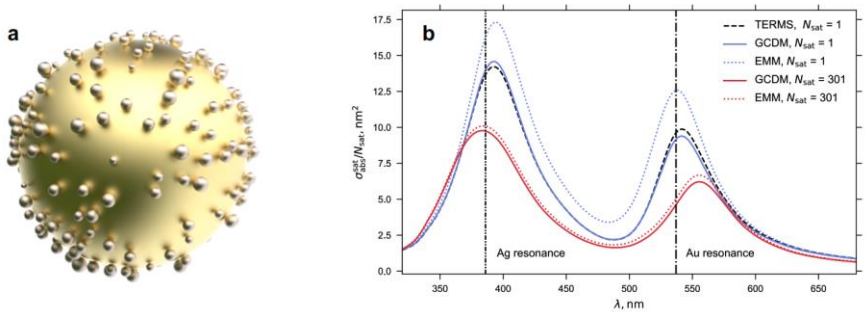

Figure 1. a) 3D representation of a core-satellite nanoparticle. b) Partial absorbance spectra of Ag satellites on the Au core for a different number of satellites N_{sat} calculated with the generalised couple-dipole model (GCDM) and the effective medium model (EMM) in comparison to the rigorous T-matrix method implemented in the TERMS programme.

References

[1] M. Herran, A. Sousa-Castillo, C. Fan, S. Lee, W. Xie, M. Döblinger, B. Auguié, and E. Cortés, Tailoring Plasmonic Bimetallic Nanocatalysts Toward Sunlight-Driven H2 Production, Adv. Funct. Mater. 32, 2203418 (2022).

[2] C. Tang, B. Auguié, and E. C. Le Ru, Refined Effective-Medium Model for the Optical Properties of Nanoparticles Coated with Anisotropic Molecules, Phys. Rev. B 103, 085436 (2021).

[3] D. Schebarchov, A. Fazel-Najafabadi, E. C. Le Ru, and B. Auguié, Multiple Scattering of Light in Nanoparticle Assemblies: User Guide for the Terms Program, J. Quant. Spectrosc. Radiat. Transf. 284, 108131 (2022).

Seeing inside kiwifruit using imaging: from full-waveform inversion to uncertainty quantification

Marie Graff[1]

[1]Department of Mathematcs, The University of Auckland
marie.graf@auckland.ac.nz

Inverse scattering and imaging go hand in hand and have multiple applications: medical imaging, geophysical prospecting or non-destructive testing. More recently, imaging, in the context of quality control in primary industry, has been used to understand the interior of other organic bodies: fruits [1,2] or trees. There is still a huge demand from industrials to come up with a technology that allows to know the level of ripeness, sweetness, disease or any suitable properties of a product without cutting it open.

The fundamental task in imaging is indeed to infer the characteristics of a medium from indirect measurements. Full waveform inversion is commonly used to tackle this imaging problem [3]. This technique requires a comprehensive knowledge of the model, including the source term, as the forward problem needs to be solved multiple times during the iterative process. However, in many applications, the source term may not be available, which calls for novel methods to take into account this lack of information [4].

In this presentation, we will propose an upgraded version of full-waveform inversion using Bayesian inference [5] to account for uncertainty in the source term.

References

[1] K. van Wijk, S. Hitchman (2017) Apple seismology. Physics Today 70 (10): 94–95. https://doi.org/10.1063/PT.3.3740
[2] L.A. Cobus, K. van Wijk (2023) Non-contact acoustc method to measure depth-dependent elastc propertes of a kiwifruit. Wave Moton 119: 103126. https://doi.org/10.1016/j.wavemot.2023.103126
[3] L. Cobden et al. (2024) Full-waveform tomography reveals iron spin crossover in Earth's lower mantle. Nature Communicaton 15: 1961. https://doi.org/10.1038/s41467-024-46040-1
[4] M. Graf, M.J. Grote, F. Nataf, F. Assous (2019) How to solve inverse scatering problems without knowing the source term: a three-step strategy. Inverse Problems 35(10): 104001. https://doi.org/10.1088/1361-6420/ab2d5f
[5] A.M. Stuart (2010) Inverse problems: A Bayesian perspectve. Acta Numerica. 19:451-559. https://doi.org/10.1017/S0962492910000061

Ocean monitoring using optical interferometry in subsea cables

Johan Grand[1], Giuseppe Marra[2], Max Tamussino[2]

[1]Measurement Standards Laboratory, Wellington, NZ
[2]National Physical Laboratory, Teddington, UK
johan.grand@measurement.govt.nz

In recent years, significant advances have been made in Earth observation technology, particularly using optical fibre-based sensing to monitor environmental changes. We discuss here an interferometric technique that utilizes existing submarine communication cables to detect environmental signals such as earthquakes and ocean currents. Unlike previous methods that measured cumulative changes over entire cable lengths, this approach enables the detection of environmentally induced optical phase changes on individual spans between repeaters of a submarine cable.

By converting each repeater-to-repeater section of the cable into an independent sensor, we aim at creating a distributed array of real-time environmental sensors across the ocean floor. The spatial resolution is significantly improved compared to cumulative methods, which had limitations in noise floor levels and location triangulation. This method is scalable, leveraging existing infrastructure without requiring modifications, thus presenting an affordable and efficient method for expanding global Earth monitoring capabilities.

This technique could transform environmental monitoring across the largely unexplored ocean floor, providing unprecedented insight into Earth's dynamic processes and advancing research in earthquake detection, ocean circulation, and climate change impacts.

Ultra-thin Film Sensing with Whispering Gallery Mode Resonators at Terahertz Frequencies

Kane H. J. Hill[1,2] and Dominik W. Vogt[1,2,*]

[1] The Dodd-Walls Centre for Photonic and Quantum Technologies, New Zealand
[2] Department of Physics, The University of Auckland, Auckland 1010, New Zealand
*d.vogt@auckland.ac.nz

We conduct ultra-thin film sensing at terahertz (THz) frequencies [1], through the implementation of an advanced sub-wavelength thin disc whispering gallery mode resonator (WGMR) [2]. The incredibly low losses and vast evanescent fields brought forth at resonance provide an efficient platform for ultra-thin film sensing. Films of poly(methyl methacrylate) form a compelling proof-of-concept of the thin disc WGMR's sensing capabilities. We deposit a range of films from 45–210 nm atop the thin disc WGMR [3], $9 - 45 \cdot 10^{-5}/\lambda$. Each film induces discernable effects to the disc WGMR resonance characteristics, measurable with a standard continuous-wave THz system. The addition of a spherical resonator [4], provided an invaluable reduction in the inherent absolute frequency uncertainty of the THz spectrometer, in figure 1.

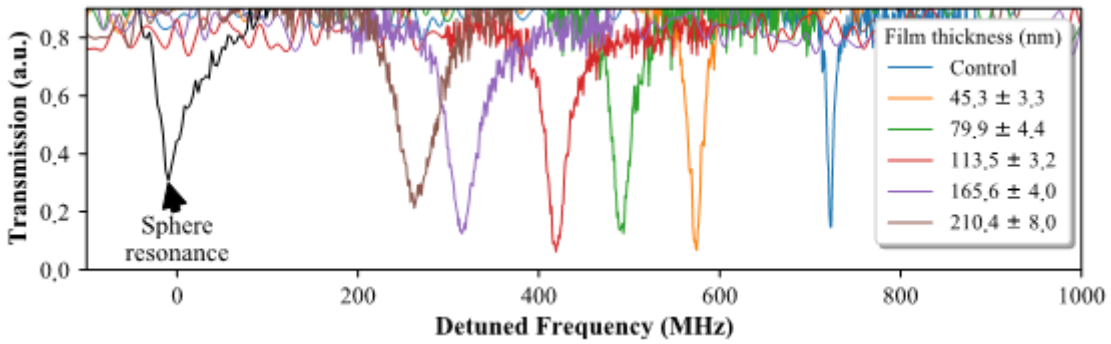

Figure 1: Detuned resonances demonstrating redshifting and broadening with film addition.

We observe coherent trends to resonance characteristics with increasing film thickness: A reduction in intrinsic Quality factor (Q-factor) and strong redshifting to the resonance frequency (in figure 2). Rigorous numerical analysis is used to guide device fabrication and provides further

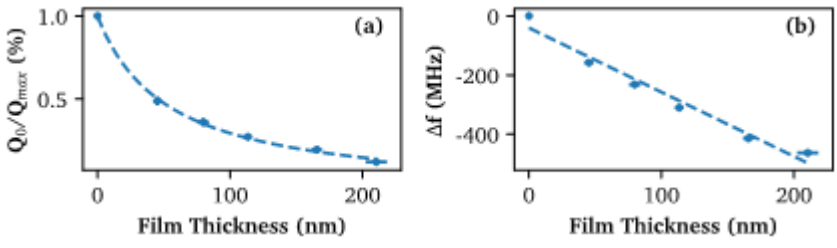

Figure 2: (a) Drop in Q-factor, and (b) redshift with film addition.

insight into the experimental findings. The experimental results establish the efficacy of thin disc WGMRs for precise sensing of ultra-thin films.

References

[1] P. Rodr´ıguez-Ulibarri and M. Beruete, Fiber Optic Sensors: Current Status and Future Possibilities, 301-327 (2017)
[2] D. W. Vogt, et al., Sensors, 20(10), 3005 (2020)
[3] T. Tippo, et al., Thin Solid Films, 546 180-184 (2013)
[4] R. Ghandi, et al., EEE Transactions on Terahertz Science and Technology, 12(1), 70–74 (2021)

QTA: Advanced materials for quantum technologies

W. F. Holmes-Hewett[1,3], J. D. Miller[1], S. Granville[1,3], H. J. Trodahl[2], and B. J. Ruck[2,3]

[1]Robinson Research Institute, Victoria University of Wellington, P.O. Box 33436, Petone 5046, New Zealand
[2]School of Chemical and Physical Sciences, Victoria University of Wellington, P.O. Box 600, Wellington 6140, New Zealand
[3]MacDiarmid Institute for Advanced Materials and Nanotechnology, P.O. Box 600, Wellington 6140, New Zealand

Superconducting memory systems and other advanced components are required to facilitate the scale up of quantum- and superconducting-computing [1,2]. The designs for these systems exist [3- 5], but the materials to realise these designs at scale do not [6]. Here we describe the results of a computational study on rare-earth nitrides in the context of engineering materials appropriate for application in high characteristic voltage magnetic Josephson junctions.

Conventional superconducting electronics are based on the mature and remarkably success Nb/AlO_x Josephson junction. These structures have enabled the formation of incredibly efficient logic systems with clock speeds on the order of 10 GHz [7,8]. With the ever increasing need for computational speed and efficiency and the continued transition to centralised large scale facilities with incredible economies of scale the future for superconducting computing is bright, and the future for hyper-scale computing is cold. However, the large-scale development of these systems will ultimately be impeded by issues relating to density if new technology is not developed [1,2,6].

AlO_x is chosen as the barrier layer in existing systems as the large (normal state) resistance results in the fast-switching times and related clock speeds. However, the superconducting circuits formed from these structures face physical limits on their minimum size [2]. There are significant advantages, particularly relating to the density of memory systems, found using ferromagnetic materials as the barrier layer in a Josephson junction [6]. Metallic ferromagnetic materials have been used to form proof of concept devices, however these devices function at speeds orders of magnitude lower (MHz) than the AlO_x based logic devices [9]. The conventional magnetic materials used so far lack the careful control of the electronic and magnetic properties required for integration with existing logic devices. What is required are insulating ferromagnetic materials compatible with thin film growth. In this regard GdN has seen significant interest in various magnetic Josephson junction structures, however the complete spin polarisation of the conduction band places limits on its effectiveness.

Here we present a computational study of $(Gd_x,Lu_{1-x})N$ where we show the large exchange splitting of GdN can be reduced by cation substitution to engineer an insulating weak-ferromagnetic material appropriate for the formation of high speed magnetic Josephson junctions.

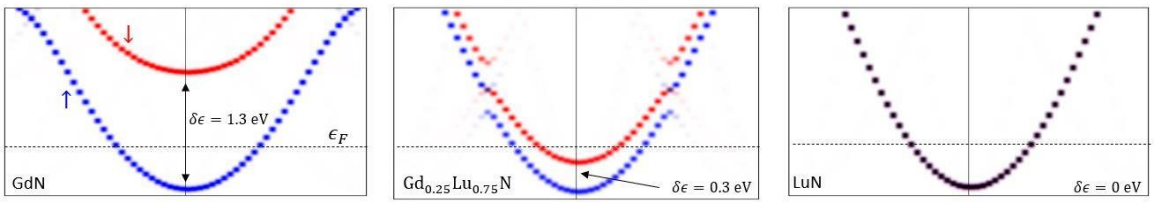

Figure 1: Calculated band structure of (Gd_xLu_{1-x})N for x = [1, 0.25, 0] showing the reduction of exchange splitting with cation substitution.

References

[1] D. S. Holmes and E. P. DeBenedictis, 'Superconductor Electronics and the International Roadmap for Devices and Systems', 2017 16th International Superconductive Electronics Conference (ISEC), Naples, Italy (2017).

[2] Igor I. Soloviev, Nikolay V. Klenov, Sergey V. Bakurskiy, Mikhail Yu. Kupriyanov, Alexan- der L. Gudkov and Anatoli S. Sidorenko, 'Beyond Moore's technologies: operation principles of a superconductor alternative', Beilstein Journal of Nanotechnology, vol. 8 (2017).

[3] Ya. M. Blanter and F. W. J. Hekking 'Supercurrent in long SFFS junctions with antiparallel domain configuration', Phys. Rev. B. 69, 024525 (2004).

[4] Gingrich, E., Niedzielski, B., Glick, J. et al. 'Controllable 0–π Josephson junctions contain- ing a ferromagnetic spin valve'. Nature Phys 12, 564–567 (2016).

[5] Baek, B., Rippard, W., Benz, S. et al. 'Hybrid superconducting-magnetic memory device using competing order parameters'. Nat Commun 5, 3888 (2014).

[6] Alam, S., Hossain, M.S., Srinivasa, S.R. et al. 'Cryogenic memory technologies', Nat Elec- tron 6, 185–198 (2023).

[7] K. K. Likharev and V. K. Semenov 'RSFQ Logic/Memory Family: A new josephson junction technology for sub THz clock frequency digital systems' IEEE Trans. Appl. Supercon. 1, 1, (1991).

[8] N. K. Katam, J. Kawa and M. Pedram, "Challenges and the status of superconducting sin- gle flux quantum technology," 2019 Design, Automation & Test in Europe Conference & Exhibition (DATE), Florence, Italy, (2019).

[9] Igor V. Vernik, Vitaly V. Bol'ginov, Sergey V. Bakurskiy, Alexander A. Golubov, Mikhail Yu. Kupriyanov, Valery V. Ryazanov and Oleg A. Mukhanov 'Magnetic Josephson Junctions with Su- perconducting Interlayer for Cryogenic Memory' IEEE Transactions on Applied Superconductivity· June (2013)

Thermal Decay of Planar Jones-Roberts Solitons

Nils Krause[1,2], Ashton Bradley[1,2]

[1]University of Otago
Krani857@student.otago.ac.nz
[2]Dodd-Walls Centre

Homogeneous planar superfluids support a variety of low-energy excitations that also feature in highly excited states such as superfluid turbulence. In dilute gas Bose-Einstein condensates the family of excitations collectively known as Jones-Roberts solitons include vortex dipoles and rarefaction pulses in the low and high velocity regimes respectively. As stable nonlinear eigenstates in a translating frame of reference these excitations carry both energy and linear momentum, making their decay characteristics of fundamental interest for superfluid dynamics. In this work we develop the theory of planar soliton decay due to thermal effects arising in the stochastic projected Gross-Pitaevskii theory of reservoir interactions. We analyse the two distinct damping terms arising in the theory: number damping, involving particle transfer between the condensate and the non-condensate reservoir, and energy damping, arising from number-conserving interactions between condensate and non-condensate. We develop analytical treatment in the low and high velocity regimes, and identify conditions for the dominance of either mechanism, finding that energy damping is dominant at high phase space density. Our results are supported by numerical studies spanning the full velocity range from vortex dipole to rarefaction pulse. The interaction energy is used to characterise rarefaction pulses, analogous to the distance between vortices for vortex dipoles, providing an experimentally accessible test for finite temperature theory of Bose-Einstein condensates.

Optimising electro-optic resonators for efficient transduction

Nicholas J. Lambert[1,2,*], Florian Sedlmeir[1,2], Pablo C. Paulson[1,2], Mallika I. Suresh[1,2], Harald G. L. Schwefel[1,2]

[1] Department of Physics, University of Otago, Dunedin, New Zealand
[2] The Dodd-Walls Centre for Photonic and Quantum Technologies, Dunedin, New Zealand
*nicholas.lambert@otago.ac.nz

Many nascent quantum technologies operate in a sub-kelvin environment – often a dilution fridge, with limited cooling power of order 100 μW at 100 mK – and with characteristic frequencies in the microwave range. This creates two problems. i) Communication over long distances with other nodes of a quantum network cannot be done over room temperature microwave links, as the thermal population of the communication channel will degrade the fidelity of the transferred quantum state. ii) Microwave cabling between room temperature and the millikelvin environment can quickly result in unacceptable heat loads on the cold stages of the dilution refrigerator as the complexity of the system grows. One solution to both of these problems is to use telecoms frequency channels to transfer both quantum information, and control and readout signals, to and from the quantum platform. Optical fibres are exceptionally low loss channels, with losses below 0.2 dB km^{-1} at telecom wavelengths, comparing very favourably to typical attenuation in low-loss microwave cables of above 1 dB m^{-1} at 10 GHz.

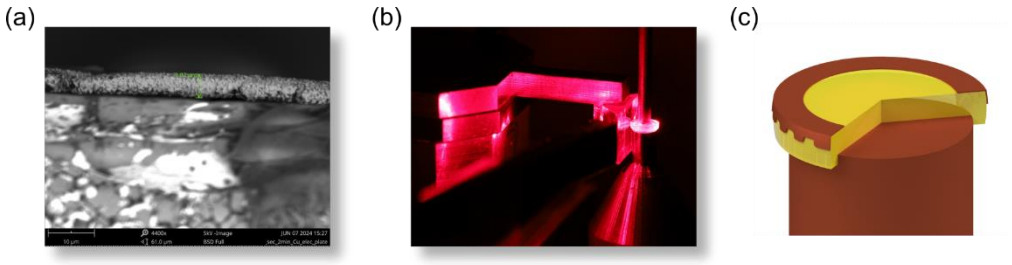

Fig. 1. ***Steps towards fabrication.*** *(a) Metal trilayer structure deposited on glass using thermal evaporation and electroplating. (b) A toroidal WGM resonator with red light coupled into modes. (c) Cartoon of proposed device.*

Coherent transduction between microwave and optical frequencies is therefore a crucial technology [1,2]. In this talk, I will describe our proposal to tackle this problem with an optimised triple resonant electro-optic transducer [3, 4]. We will fabricate a lithium tantalate [5] whispering gallery mode (WGM) optical resonator, with a thin-film metal microwave resonator (Fig. 1) structured directly on to its surface. An advantage of this approach is the exploitation of the off-diagonal components of the electro-optic tensor, which allow the conversion of an optical pump in one polarisation to a signal in the orthogonal polarisation. This will enable straightforward separation of the weak signal from the pump. Phase matching requirements will be met by periodic structuring of the microwave electrode, with the low birefringence of lithium tantalate helping to minimise fabrication challenges.

As well as providing a key component of quantum networks, such a device will allow optical control and readout of quantum systems housed in a cryogenic environment, decreasing the cooling power and space requirements due to microwave cabling.

References

[1] N. J. Lambert et al., Coherent Conversion Between Microwave and Optical Photons—An Overview of Physical Implementations, Advanced Quantum Technologies **3**, 1900077 (2020)

[2] X. Han et al, Microwave-optical quantum frequency conversion, Optica B, 1050 (2021)

[3] A. Rueda et al, Efficient microwave to optical photon conversion: An electro-optical realization, Optica **3**, 597 (2016)

[4] L. Fan et al, Superconducting cavity electro-optics: A platform for coherent photon conversion between superconducting and photonic circuits, Science Advances **4**, eaar4994 (2018)

[5] C. Wang et al, Lithium tantalate photonic integrated circuits for volume manufacturing, Nature **629**, 784 (2024)

Phase Resetting in the Coupled Van der Pol Oscillator

Kyoung Hyun Lee[1,2], Neil Broderick[1,3], Bernd Krauskopf[1,2], Hinke Osinga[1,2]

[1]Dodd-Walls Centre for Photonic and Quantum Technologies, New Zealand
[2]Department of Mathematics, University of Auckland, New Zealand
[3]Department of Physics, University of Auckland, New Zealand
kyoung.hyun.lee@Auckland.ac.nz

Coupled nonlinear oscillators are found in many application contexts; specific examples in photonics are coupled optical cavities and ring resonators. Synchronisation properties of such systems can be probed by studying the response to external perturbations: after relaxation back to the stable oscillation, there is generally a phase shift. Important information can be gained by studying such phase resets as a function of when the perturbation is applied during the oscillation.

We present a case study of a prototypical example: two coupled 1:1 phase-locked Van der Pol oscillators. In contrast to single oscillators, this system has a phase space of dimension four. In particular, the basin of attraction of the stable synchronised oscillation has a complicated boundary, and we show how this affects the observed phase resetting in unexpected ways.

The injection locking of breathing solitons in microresonators

Wang Liao[1,2,†], Stéphane Coen[1,2], Stuart Murdoch[1,2], Gregory Moille[3,4], Kartik Srinivasan[3,4], Miro Erkintalo[1,2]

[1] Department of Physics, University of Auckland, New Zealand
[2] The Dodd-Walls Centre for Photonics and Quantum technologies, New Zealand
[3] Joint Quantum Institute, NIST/University of Maryland, College Park, MD, USA
[4] Microsystems and Nanotechnology Division, NIST, Gaithersburg, MD, USA
[†] wang.liao@auckland.ac.nz

Recent research shows that the repetition rate of a stable dissipative Kerr cavity soliton generated in an optical microresonator can be synchronized to an external reference frequency by injecting a secondary laser into the cavity [1]. However, a stable soliton is not the only thing that possesses synchronization properties, e.g., synchronization of the breathing frequency of a breather soliton by cavity pump field modulation has also been demonstrated [2]. Here we experimentally show that the breather soliton's breathing frequency can also be synchronized to an external reference laser, unveiling the high frequency synchronization dynamics. Our experiments are performed on a Si_3N_4 microring resonator with an FSR of 1 THz, driven at 1550 nm. Figure 1(**a**) shows the spectrogram measured when sweeping the injected laser across the breather's first harmonic component. As can be seen, when sufficiently close to the breather's natural oscillation frequency of 160 MHz, the harmonic component is entrained into the injected laser (emphasized by the red dashed line). We also experimentally investigated the dependence of the locking range on the injected laser power, and found that the locking range increases linearly with the square root of the injected laser power (i.e., the "injected amplitude"). Figure 1(**b**) shows the linear trend between the injected laser amplitude and the breather injection locking range. Our research reveals a potential alternative to stable soliton synchronization.

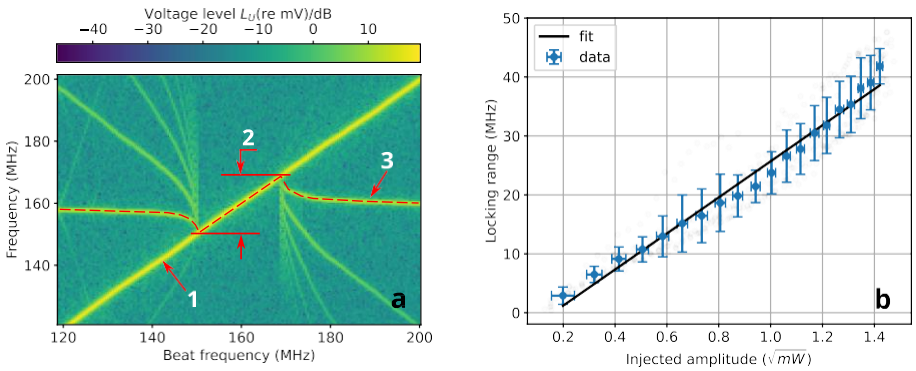

Figure 1: Data from the experiment on the injection locking of breathing solitons. a A spectrogram shows the first harmonic component of the soliton breather locked to the beat between the injected laser and the driving laser: 1 — Beat signal between the driving laser and the injected laser; 2 — The locking range; 3 — Breather's breathing first harmonic signal. b Locking range dependence on injected laser amplitude (the square root of the power).

References

[1] G. Moille, J. Stone, M. Chojnacky, R. Shrestha, U. A. Javid, C. Menyuk, and K. Srinivasan, "Kerr-induced synchronization of a cavity soliton to an optical reference", Nature 624, 267–274 (2023).

[2] S. Wan, R. Niu, Z.-Y. Wang, J.-L. Peng, M. Li, J. Li, G.-C. Guo, C.-L. Zou, and C.-H. Dong, "Frequency stabilization and tuning of breathing solitons in Si3N4 microresonators", Photonics Research 8, 1342–1349 (2020).

THz dynamics of quantum materials studied at the Australian Synchrotron

Freddy Lyzwa[1,2], Neil Broderick[1,2], Dom Appadoo[3]

[1]Department of Physics, The University of Auckland, New Zealand
[2]Te Whai Ao — Dodd-Walls Centre for Photonic and Quantum Technologies, New Zealand
[3]ANSTO, Australian Synchrotron, Melbourne, Australia

A prerequisite for the design of next-generation electronic devices, or so-called 'quantum' devices', is a detailed knowledge of the materials' ground state dynamics. There are several experimental approaches how to derive a better understanding of the underlying mechanisms that define the macroscopic properties of a material system. For instance, THz & Far-Infrared spectroscopy is a suitable method to investigate the low-energy dynamics of structural (phonons), magnetic and electronic origin, as well as their potential coupling to each other. In addition, this approach is compatible with cryogenic conditions – the Australian Synchrotron offers this possibility of having a) a bright and broadband light source down to the THz range (ca. 10 cm^{-1}), and b) cryogenic conditions (temperatures of ca. 4K).

In this talk, I will present our past and current research at the Australian Synchrotron in Melbourne, Australia, together with its state-of-the-art capabilities. We are investigating the THz & Infrared spectroscopic response for a series of semiconducting materials as a function of doping and tuning the sample temperature from room-to-cryogenic environment. The findings are discussed in comparison with complementary techniques such as X-ray diffraction and magnetometry, and a perspective for future research in this field is given.

Spontaneous Soliton Emergence Under Pulsed-Pumping Conditions in a Driven Passive Kerr Resonator

Matthew Macnaughtan,[1,2,*] Zongda Li,[1,2] Yiqing Xu,[1,2] Xiaoming Wei,[3] Zhongmin Yang,[3] Ste´phane Coen,[1,2] Miro Erkintalo,[1,2] and Stuart Murdoch [1,2]

[1]Department of Physics, University of Auckland, Auckland, New Zealand [2]The Dodd-Walls Centre for Photonic and Quantum Technologies, Auckland, New Zealand
[3]School of Physics and Optoelectronics, South China University of Technology, Guangzhou 510640, People's Republic of China
[*]*mmac848@aucklanduni.ac.nz*

Dissipative temporal cavity solitons (CSs), first observed in a fiber ring cavity in 2010 [1], are ultra-short localized pulses of light that can circulate indefinitely within an optical cavity without distortion. They have attracted particular attention in the context of optical microresonators, where they enable the realisation of coherent broadband optical frequency combs. Driven by the many potential applications of such frequency combs — from real-time spectroscopy [2] to ultra-fast ranging [3] — the applied potential of CSs is now beginning to be realised. Therefore, it is no surprise that over the past few years there has been a push towards tackling more practical issues, chief among these being the reliable and robust generation of CSs. For many cavity architectures, CS generation typically required the intracavity field to be either externally seeded [1] or subject to a parameter ramp that forces the field to undergo a substantial state change from modulation instability (MI) to a CS state [4]. Although such methods are known to work, they often require a prohibitive suite of equipment, as well as being susceptible to environmental perturbations or generating a random pattern of CSs at each realisation. More recently, efforts have been made towards injection-locking systems in which CSs can be generated through the use of Rayleigh scattering as a feedback mechanism [5]. Although such systems show promise in tiny microresonator setups, in macroscopic systems, Brillouin scattering may prove to be a compromising factor. In this contribution, we experimentally and numerically explore a pulse-driven passive Kerr resonator, identifying a new parameter regime where CSs can spontaneously emerge, thus eliminating the need for external seeding or parameter ramping through MI. Furthermore, we show that, in addition to single isolated soliton states, deterministic generation of complex CS bound states (molecules) can also be realised thanks to higher-order dispersion.

In our experiments, we use a 0.29-m-long dispersion-shifted fiber enclosed in a Fabry-Pérot (FP) system of two dielectric-coated fiber tips (yielding a free spectral range of 350 MHz and a finesse of 180). We drive our cavity with a train of picosecond pulses obtained from an electro-optic (EO) comb. The pump repetition rate, f_p, can be readily controlled by adjusting the clock frequency, allowing us to systematically control the desynchronisation, ΔT, between the pump repetition rate and the cavity roundtrip time. We actively stabilise our pump detuning, δ, via a Pound-Drever-hall technique. To numerically model our system, we make use of the Lugiato-Lefever equation (LLE) with higher-order dispersion and Raman scattering terms included [6]. For the measurements discussed below, we set the central wavelength of our pump to 1565 nm, putting us into the anomalous group-velocity dispersion (GVD) regime (the zero dispersion wavelength of our fiber is located at 1553 nm, and significant third- and fourth-order dispersive terms are also present).

In our first experiment, we demonstrate the spontaneous emergence of CSs. Specifically, we first ramp the cavity detuning (while maintaining the desynchronisation) through MI to values for which CSs exist, illustrating the conventional method for CS generation, then gradually increase the detuning till the intracavity field can no longer sustain a CS and collapses to the lower homogeneous steady-state (HSS). We then re-tune the detuning back to its initial value, observing the spontaneous generation of CSs in the absence of any external perturbation or MI. The experimentally measured spectral evolution is compiled into a pseudo-coloured map and displayed in Fig. 1(a), with Fig. 1(b) showing the simulated temporal evolution of the region outlined by the dashed white box in Fig. 1(a). Finally, Fig. 1(c) shows both an experimental (blue) and simulated (red) spectrum of the intracavity field taken from Fig. 1(a) at a detuning of 0.055 rad. Both Figs. 1(a) and (b) illustrate how, in the appropriate parameter region, a CS can spontaneously form out of the intracavity field under pulsed-pumping conditions. The physical mechanism that underpins the observed CS self-generation can be explained in terms of switching wave dynamics. Specifically, because the pump is inhomogeneous, each position along the intracavity field sees different driving conditions. This opens up the possibility for spontaneous up-switching to occur at localised points along the intracavity pulse, effectively self-seeding CSs.

For our second experiment, we show how under this particular pulsed-pumping scheme, both singular and bound CS states can be reliably selected. To achieve this, we first tune into the fundamental CS state, then gradually change the pump desynchronisation, ΔT, until a bound state is achieved. Once such a state forms, we then reverse the desynchronisation until once again we generate the fundamental CS state. Figure 1(e) shows an experimentally acquired pseudo-coloured map of this process, with Fig. 1(d) showing the numerically simulated temporal result when using the same parameters as in (e). We can clearly observe deterministic switching between the fundamental CS state (with smooth spectral envelope) and bound states (that exhibit spectral interference).

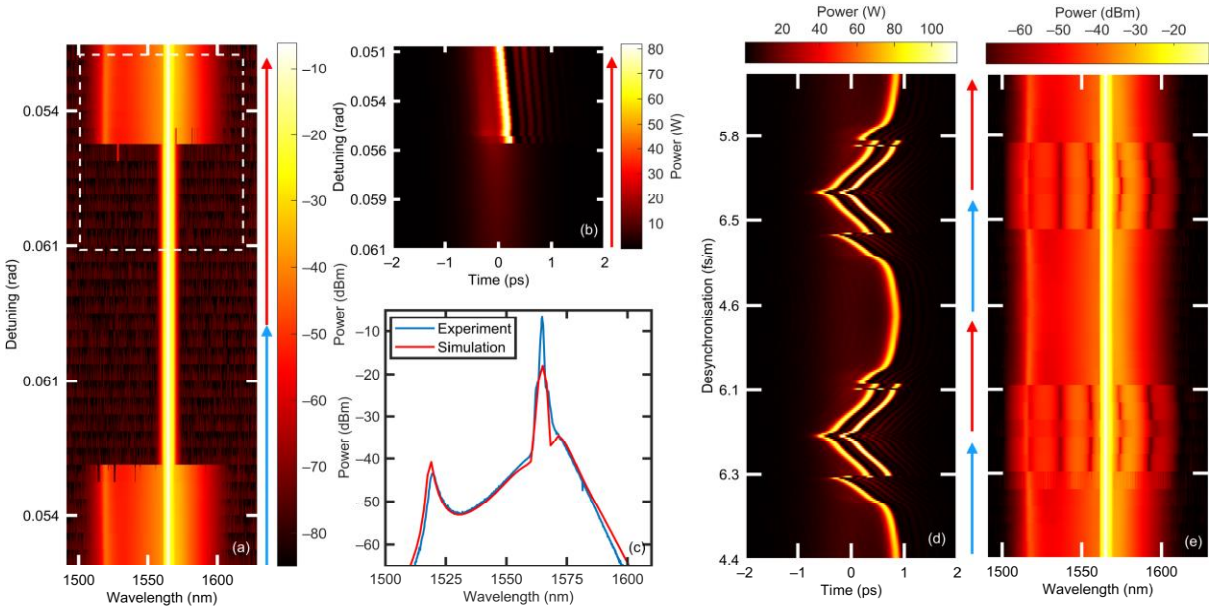

Fig. 1: (a) Experimentally measured spectra of spontaneous CS formation after the cavity is forced into the lower HSS via a detuning scan when driving with a picosecond driving pulse at a peak power of 2.3 W with ΔT = 4.4 fs/m. (b) Numerically simulated temporal trace of the region outlined

by the dashed white box in (a) under the same driving conditions. (c) Experimentally measured spectrum (blue) taken from (a) at a detuning δ = 0.055 rad overlapped with a numerically simulated one (red). (e) Experimentally measured spectral map of bound and singular CS formation when changing the pump desynchronisation with δ = 0.068 rad at a peak driving power of 3.2 W. (d) shows, using the same parameters in (e), the numerically simulated temporal evolution of the intracavity field when subjected to the same change in desynchronisation seen in (e). The red (blue) arrows beside the pseudo-coloured maps indicate when their respective parameters are decreasing (increasing).

In conclusion, by utilising a passive fiber based Fabry-Pérot setup, we have investigated through experimental and numerical methods both cavity soliton self-generation and deterministic bound state formation under coherent pulsed driving conditions. This work provides further insight into cavity soliton formation under pulsed driving, and hopes to further the push into efficient, robust, and reliable cavity architectures for future applications.

References

[1] Leo, F., Coen, S., Kockaert, P., Gorza, S.P., Emplit, P., and Haelterman, M. (2010) “Temporal cavity solitons in one-dimensional Kerr media as bits in an all-optical buffer,” Nature Photon., 4 (7), 471–476.

[2] Lucas, E., Lihachev, G., Bouchand, R., Pavlov, N.G., Raja, A.S., Karpov, M., Gorodetsky, M.L and Kippenberg, T.J. (2018) “Spatial multiplexing of soliton microcombs,” Nature Photon., 12, 699–705.

[3] Trocha, P., Karpov, M., Ganin, D., Pfeiffer, M.H.P., Kordts, A., Wolf, S., Krockenberger, J., Marin-Palomo, P., Weimann, C., Randel, S., Freude, W., Kippenberg, T.J. and Koos, C. (2018) “Ultrafast optical ranging using microresonator soliton frequency combs,” Science., 359, 887–891.

[4] Herr, T., Brasch, V., Jost, J. D., Wang, C. Y., Kondratiev, N. M., Gorodetsky, M. L. and Kippenberg, T.J. (2018) “Temporal solitons in optical microresonators,” Nature Photon., 8, 145–152.

[5] Lihachev, G., Weng, W., Liu, Chang, L., Guo, J., He, J., Wang, R.N., Anderson, M.H., Liu, Y., Bowers, J.E. and Kippenberg, T.J. (2022) “ Platicon microcomb generation using laser self-injection locking,” Nat Commun., 13, 1771.

[6] Wang, Y., Anderson, M., Coen, S., Murdoch, S.G. and Erkintalo, M. (2018) “Stimulated Raman Scattering Imposes Fundamental Limits to the Duration and Bandwidth of Temporal Cavity Solitons,” Phys. Rev. Lett., 120, 053902.

Rare-earth Nitride Josephson Junctions and derivative products.

J. D. Miller[1], W. F. Holmes-Hewett[1,3], S. Granville[1,3], and B. J. Ruck[2,3]

[1]Robinson Research Institute, Victoria University of Wellington, P.O. Box 33436, Petone 5046, New Zealand
[2]School of Chemical and Physical Sciences, Victoria University of Wellington, P.O. Box 600, Wellington 6140, New Zealand
[3]MacDiarmid Institute for Advanced Materials and Nanotechnology, P.O. Box 600, Wellington 6140, New Zealand

Using ferromagnetic materials to form the barrier layer of a Josephson junction offers additional functionality to low-temperature electronics, as the superconducting phase must behave differently passing through a magnetised barrier layer [1]. Metallic ferromagnetic materials have been used to form proof of concept devices, however these devices function at speeds orders of magnitude lower (MHz) than the AlOx based logic devices, due to their low normal- state resistances [2]. For this reason, the tendency of materials to be either magnetic or insulating, but not both, has to date impeded efforts to use magnetic Josephson junctions in high-speed applications.

The rare-earth nitrides (RN, with R a lanthanide) offer a series of magnetic materials in which in conductivity can be controlled. By implementing an RN barrier, the switching speed of magnetic Josephson junctions can, in principle, be improved. Moreover, the wide range of magnetic behaviours of the rare-earth nitrides and the ability to tune these magnetic behaviours through a host of interactions offers greater scope to explore the fundamental physics of magnetic Josephson junctions than previous studies using traditional transition metal-based barriers.

We present preliminary experimental results from a collaboration with researchers in Nagoya, in which the rare-earth nitrides barrier MJJs are fabricated and characterised both as unshunted junctions and as part of larger superconducting devices, such as DC SQUIDs.

References

[1] Birge, Norman O., and Nathan Satchell. "Ferromagnetic materials for Josephson π junctions." APL Materials 12.4 (2024).
[2] Alam, Shamiul, et al. "Cryogenic memory technologies." Nature Electronics 6.3 (2023): 185-198.

Superconducting Readout of a Compensated Memory Bit

Jackson Miller[1], William Holmes-Hewett[1,2], Simon Granville[1,2], Joe Trodahl[3], Ben Ruck[2,3]

[1]Paihau-Robinson Research Institute, 5010, Lower Hutt, New Zealand
[2] MacDiarmid Institute of Advanced Materials and Nanotechnology, 6012, Wellington, New Zealand
[3] School of Chemical and Physical Sciences, Victoria University of Wellington, 6012, Wellington, New Zealand

Future computing, both classical and quantum, will be performed using superconducting electronics at low temperature. The most recent single flux quantum based logic systems have demonstrated clock-speeds of 10s of GHz [1], and switching energies as low as eJ [2], while companies such as Google and IBM are continuing to increase their logical qubit count, with the aggressive scaling so far meeting projections [3]. However, for the promised advances of these technologies to be realised a dense, cryogenic memory must be developed [4].

Here, we present our work forming such a prototype superconducting memory device comprising ferromagnetic rare-earth nitrides [5] and conventional Josephson junctions. The combination and competition of spin and unquenched orbital angular momentum on the tri-valent lanthanide ions allow the tuning of various magnetic properties, to a much greater degree than in transition-metal based ferromagnets. Using combinations of (GdSm)N we demonstrate independent control of the net-magnetisation and coercive field [6,7]. We show the incorporation of these layers into tri-layer structures and the formation micron-scale switchable magnetic dots [8]. The fringe field of these dots is determined by the relative orientation of the ferromagnetic layers. The dots can affect the superconducting state of a nearby Josephson junction, which is used for electrical readout of the memory state, forming a micron-scale superconducting memory device.

References

[1] O. A. Mukhanov, IEEE Transactions on Applied Superconductivity, 21, (2011).
[2] Igor I. Soloviev, Nikolay V. Klenov, Sergey V. Bakurskiy, Mikhail Yu. Kupriyanov, Alexander L. Gudkov and Anatoli S. Sidorenko, Beilstein Journal of Nanotechnology, 8, (2017).
[3] International Roadmap For Devices And Systems™ 2022 Edition, Cryogenic Electronics And Quantum Information Processing, IEEE, 2022.
[4] Alam, S., Hossain, M.S., Srinivasa, S.R. et al., Nature Electronics, 6, 185–198, (2023).
[5] F. Natali, B.J. Ruck, N.O.V. Plank, H.J. Trodahl, S. Granville, C. Meyer, and W.R.L. Lambrecht, Progress in Materials Science, 58, 8, (2013).
[6] J. D. Miller, H. J. Trodahl, M. Al Khalfioui, S. Vézian, and B. J. Ruck;. Appl. Phys. Lett.,122, 9 (2023).
[7] J. D. Miller, J. F. McNulty, B. J. Ruck, M. Al Khalfioui, S. Vézian, M. Suzuki, H. Osawa, N. Kawamura, and H. J. Trodahl, Phys. Rev. B, 106, 174432, (2022).
[8] C. Pot, W. F. Holmes-Hewett, E.-M. Anton, J. D. Miller, B. J. Ruck and H. J. Trodahl, Appl. Phys. Lett., 123, 202401, (2023).

How does data augmentation alter classification performance of support vector machines and convoluted neural network models developed using transmission low frequency Raman spectra?

Sara J. Miller[1], Mitchell Chalmers[2], Brendan McCane[3] and Keith C. Gordon[2].

[1]College of Science and Engineering, Flinders University, Bedford Park, SA, Australia.
sara.miller@flinders.edu.au
[2]Te Whai Ao – Dodd-Walls centre, Department of Chemistry, University of Otago, Dunedin, New Zealand.
[3]Te Whai Ao – Dodd-Walls centre, School of Compu1ng, University of Otago, Dunedin, New Zealand.

Deep Raman spectroscopic techniques have been highlighted as a potential avenue for disease diagnosis and characterizing disease states. Transmission Raman spectroscopy has been explored in the literature for applications such as breast cancer detection as a non-invasive, non-ionising and chemically specific characterization method to target detection of breast microcalcification composition.[1, 2] However the sensitivity has not yet reached levels for uptake in clinic. The use of the low wavenumber[3] analogue to transmission Raman (transmission low frequency Raman) provides additional information on the order of solid microcalcifications which is proposed to add information to increase the sensitivity of the approach. In addition, the multivariate classification methods (e.g. convolutional neural networks[4] and support vector machines[5]) used for diagnosis need to be further optimised. The stability of two machine learning techniques were probed by intentionally introducing spectral artefacts to the transmission low frequency Raman spectroscopic data collected from calcifications (calcium oxalate, crystalline, intermediate and amorphous hydroxyapatite) buried in chicken breast. SVM yielded a slightly better model with an AUC of 0.989 compared to 0.979 for the CNN. However, in general SVM were found to be more susceptible to spectral artefacts than CNN. Additionally, the performance of the CNNs and SVMs was not dependent on the magnitude of the shifts and stretches in the augmented data. An example is the linear- stretching of the data where the AUC remained at 0.977 and 0.969 for both 2 cm^{-1} and 5 cm^{-1} shifts for CNN and SVM, respectively.

References

[1] Matousek, P.; Stone, N. Chemical Society Reviews 2016, 45 (7), 1794-1802.
[2] Nicolson, F.; Kircher, M. F.; Stone, N.; Matousek, P. Chemical Society Reviews 2021, 50 (1), 556-568.
[3] Kirkham, J.; Korter, T. M.; Berzins, K.; McGoverin, C. M.; Gordon, K. C.; Fraser-Miller, S. J. Crystal Growth & Design 2023, 23 (8), 5748-5761.
[4] LeCun, Y.; Bengio, Y.; Hinton, G. nature 2015, 521 (7553), 436-444.
[5] Cortes, C.; Vapnik, V. Machine learning 1995, 20, 273-297.

Phase Resetting in the Yamada Model of a Q-Switching Laser

J. Ngaha[1,2*], N. G. R. Broderick[2,3], and B. Krauskopf[1,2]

[1] Department of Mathematics, The University of Auckland, Private Bag 92019, Auckland, New Zealand
[2] The Dodd-Walls Centre for Photonic and Quantum Technologies, New Zealand
[3] Department of Physics, The University of Auckland, Private Bag 92019, Auckland, New Zealand
*j.ngaha@auckland.ac.nz

In this work we investigate the phase resetting of a self pulsing laser, also known as a *Q-switching* laser, with a saturable absorber, consisting of a gain and an absorber section. We study a specific model, due to Yamada [1, 2], consisting of a set of three coupled ordinary differential equations for the gain G, the absorption Q, and the intensity I.

We take a dynamical systems approach and employ recently developed methods [3] to address how the regular self-pulsating behaviour of a Q-switching laser is affected by external perturbations. In Fig. 1 we consider an intensity perturbation, given by $\vec{d}_p$ = (0, 0, 1) and amplitude $A_p > 0$. Figure 1a depicts the time-series of the intensity of an unperturbed periodic orbit, along with an example of a perturbed orbit. The perturbation is applied at $t = 0$, initially advancing the oscillations compared to the unperturbed orbit. The perturbed orbit eventually returns to the same pulsing behaviour at $t \sim 300$, though with a slight delay of $\Delta t \approx 4.5$.

Figure 1(b) depicts phase transition curves (PTCs) for four different perturbation amplitudes. This represents the relationship between the phase of the periodic orbit where the perturbation is applied, θ_{old}, and the shifted phase, θ_{new}, where each phase specifies a point on the periodic orbit. If no perturbation is applied, the two phases are the same and thus the PTC is the identity (dashed line in Fig. 1b). For weaker perturbations, we see qualitatively similar behaviour to the unperturbed case, as the new phase θ_{new} changes over 2π (as does θ_{old}). For much larger perturbations, we see completely different behaviour. As the perturbation is applied along the original periodic orbit, there is no longer an increase of 2π in θ_{new}, as shown for $A_p = 25$ and 30 in Fig. 1b.

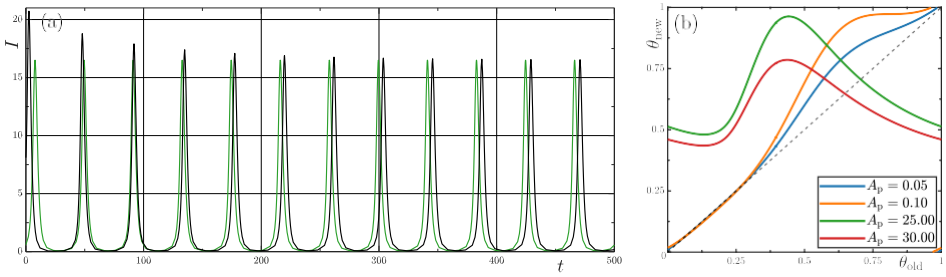

Figure 1: (a) Time series of the unperturbed pulsations (green). The perturbed response (black) returns back to the original pulsations at t ∼ 300, with a delay. The perturbation is applied in the positive I-direction, $\vec{d}$ = (0, 0, 1), with amplitude A_p = 7.5 at t = 0. (b) PTCs for four different perturbation amplitudes as shown. The PTCs for the two weaker perturbations are close to the identity (black, dashed), while those for the two larger perturbations, are qualitatively different.

References

[1] M. Yamada. “A theoretical analysis of self-sustained pulsation phenomena in narrow-stripe semiconductor lasers”. IEEE J. Quantum Electron 29, 1330 (1993).
[2] J. L. A. Dubbeldam and B. Krauskopf. “Self-pulsations of lasers with saturable absorbers: Dynamics and bifurcations”. Opt. Commun., 159, 325 (1999).
[3] P. Langfield, B. Krauskopf, and H. M. Osinga. “A continuation approach to computing phase resetting curves” in Advances in Dynamics, Optimization and Computation”, Vol. 304 of SSDC (Springer International Publishing, 2020), pp.3-30.

Application of Vibrational Spectroscopic Techniques in Sustainable Flaxseed Protein Extraction and Prediction

Jervee M. Punzalan[1-4], Peter Hartono[2,3,5], Sara J. Fraser-Miller[6], Sze Ying Leong[2,5], Kevin Sutton[2,3], Gert-Jan Moggre[2,3], Indrawati Oey[2,5], and Keith C. Gordon[1,2]

[1]Dodd-Walls Centre for Photonic and Quantum Technologies and Department of Chemistry, University of Otago, Dunedin 9016, New Zealand
[2]Riddet Institute, Private Bag 11 222, Palmerston North 4442, New Zealand
[3]The New Zealand Institute for Plant and Food Research Limited, Private Bag 4704, Christchurch Mail Centre, Christchurch 8140, New Zealand
[4]Department of Physical Sciences and Mathematics, College of Arts and Sciences, University of the Philippines, Manila, 1000, Philippines
[5]Department of Food Science, University of Otago, PO BOX 56, Dunedin 9054, New Zealand [6]College of Science and Engineering, Flinders University, Adelaide 5042, South Australia

This study explores the structural properties of semi-refined flaxseed protein extract (SFE) using Raman spectroscopy and a rapid method for quantifying protein levels in aqueous extracted samples using near-infrared (NIR) spectroscopy coupled with chemometrics. The research focuses on developing a sustainable approach for extracting SFE using pulsed electric field (PEF) treatment prior to aqueous extraction. The resulting extracts were centrifuged, freeze-dried, and analyzed using MicroNIR 1700 ES and the Dumas method was used as the reference. Spectral preprocessing and partial least square regression were applied, with the second derivative method showing superior fit and predictability. PEF-assisted extraction up to 363 kJ/kg enhances protein content without the use of high pH or solvents.

This research provides valuable insights into the structural changes induced by PEF treatment in flaxseed protein extracts, demonstrating the potential of vibrational spectroscopy coupled with chemometrics in characterizing complex biomolecular systems.

References

[1] Boussetta, N., et al., Valorization of oilseed residues: Extraction of polyphenols from flaxseed hulls by pulsed electric fields. Industrial crops and products, 2014. 52: p. 347- 353.

Experimental implementation of an optical Ising machine using polarization symmetry breaking in a Kerr resonator

Liam Quinn[1,2], Yiqing Xu[1,2], Julien Fatome[3], Stuart Murdoch[1,2], Miro Erkintalo[1,2], and Stéphane Coen[1,2]

[1] Physics Department, The University of Auckland, Auckland 1142, New Zealand
[2] The Dodd-Walls Centre for Photonic and Quantum Technologies, Auckland, New Zealand
[3] ICB, UMR 6303 CNRS, Universit Bourgogne-Franche-Comt, Dijon, France

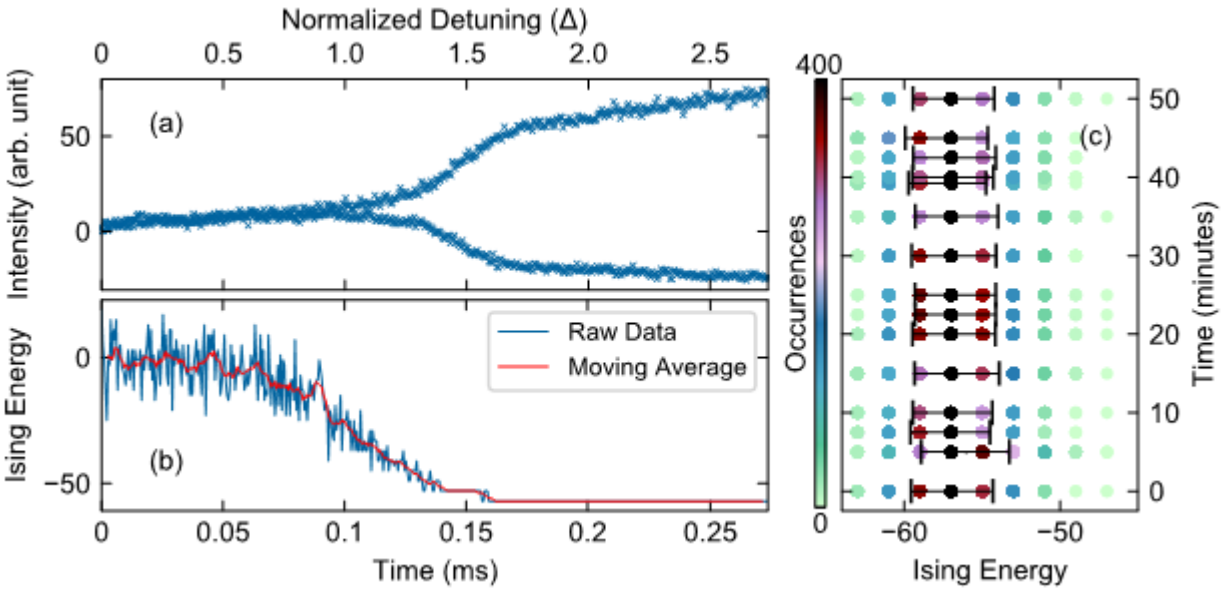

*Figure 1: Experimental results of the polarization Ising machine. (**a**) Amplitude evolution of the polarization states in the resonator as the frequency detuning of the driving laser is increased. (**b**) Evolution of the Ising energy corresponding to 64 pulses coupled in a nearest-neighbour configuration as the detuning is increased. (**c**) Long time experimental measurements of the statistical distribution of Ising energies. Each row shows statistics over 1500 experimental trials.*

Coherent Ising machines (CIMs) are a cutting-edge approach to solving complex optimization problems, with a wide array of applications [1,2]. They are composed of networks of degenerate optical parametric oscillators (DOPOs) that leverage the bistable output phase of each oscillator to emulate artificial spin states. By coupling the oscillators together, CIMs simulate the dynamics of an Ising model, enabling the efficient calculation of the minimum energy state of a given Ising Hamiltonian. In this study, we present proof-of-concept experiments for a novel Ising machine based on polarization spontaneous symmetry-breaking (SSB) in a Kerr resonator driven by picosecond pulses. As the frequency detuning between the driving laser and a cavity resonance increases, each of the pulses circulating the resonator undergoes spontaneous polarization symmetry breaking, yielding independent spin-like states [Fig. 1(a)]. By measuring the polarization state of each spin and feeding these measurements to a phase modulator acting on the driving field, we create a network of spins that evolve towards a low energy solution of a given Ising Hamiltonian (Fig. 1b). Operating in a novel period-2 regime, where the polarization modes of the resonator switch with each round trip, shields the SSB dynamics from asymmetries [3, 4]. This innovation leads to a highly robust system capable of performing

consistent Ising calculations for up to an hour [Fig. 1(c)]. Additionally, spin states are measured through intensity measurements, eliminating the need for complex stabilization practices typically associated with direct phase measurements, which are required for existing CIM architectures.

References

[1] McMahon, P., Marandi, A., Haribara, Y., Hamerly, R., Langrock, C., Tamate, S., Inagaki, T., et al. "A fully programmable 100-spin coherent Ising machine with all-to-all connections." Science **354**, 614-617 (2016).

[2] Inagaki, T., Haribara, Y., Igarashi, K., Sonobe, T., Tamate, S., Honjo, T., Marandi, A., et al. "A coherent Ising machine for 2000-node optimization problems." Science **354**, 603-606 (2016).

[3] Coen, S., Garbin, B., Xu, G., Quinn, L., Goldman, N., Oppo, G.-L., Erkintalo, M., et al. "Nonlinear topological symmetry protection in a dissipative system." Nat. Commun. **15**, (2024).

[4] Quinn, L., Xu, G., Xu, Y., Li, Z., Fatome, J., Murdoch, S. G., Coen, S., Erkintalo, M. "Random Number Generation Using Spontaneous Symmetry Breaking in a Kerr Resonator." Opt. Lett. **48**, 16 (2024).

The chicken or the egg? Coherence, entanglement, and superradiance

Nur Fadhillah binti Rahimi[1,2,*], Daniel Schumayer[1,2], David A.W. Hutchinson[1,2,3]

[1]Dodd-Walls Centre for Photonics and Quantum Technology
[2]Department of Physics, University of Otago, Dunedin, New Zealand
[3]Centre for Quantum Technologies, National University of Singapore, Singapore
*rahnu978@student.otago.ac.nz

In 1954 Robert Dicke proposed a novel description of spontaneous light emission in a system of particles coupled to an electromagnetic field [1]. Prior to this, the concept of light emission had been described as radiation of photons emitted by independent particles. This approach is indeed justified if the typical distance between emitters is larger than the wavelength of emitted light waves. However, if the close proximity of emitters cannot be neglected, as Dicke argued, spontaneous light emission is better described as a collective phenomenon of particles, which are correlated with one another since they are influenced by each other's radiation field.

Since the emitters are initially prepared in their excited state, they would eventually decay into ground state at a certain rate as the system evolves. If the emitters evolve independently, then the decay rate is proportional to the number of emitters, N. In contrast, Dicke's picture deduces that the collective behavior of the emitters leads to their decay to scale at a rate of N 2, resulting in 'superradiance', a term introduced to characterise the sudden burst of emitted light.

Building upon our previous work [2] we investigate the correlations of spin- 1 emitters coupled to a single bosonic mode whose time-evolution is governed by Tavis-Cummings hamiltonian [3]

$$\mathrm{H} = h_{\mathrm{emitters}} + h_{\mathrm{interaction}} + h_{photons} = \sum_{i=1}^{N} ½wq\sigma_i^Z + g\sum_{i=1}^{N}(\sigma_i^+\sigma + \sigma_i^-\sigma^\dagger) + w_c\alpha^\dagger\alpha,$$

where ω_q is the resonance frequency of a two-level emitter, g is the coupling strength, while ω_c is the angular frequency of the emitted photon. We treat this as an open quantum system subject to decay, photon loss and pure dephasing at rates γ, κ and γ_ϕ, respectively. We solve the Lindblad quantum master equation to evolve the system in time, and measure correlation through an entanglement witness, W, relative coherence, C_{rel} and the von Neumann entropy, S. We investigate whether Dicke's picture on superradiance is valid., i.e., does the correlation of emitters enhance spontaneous light emission?

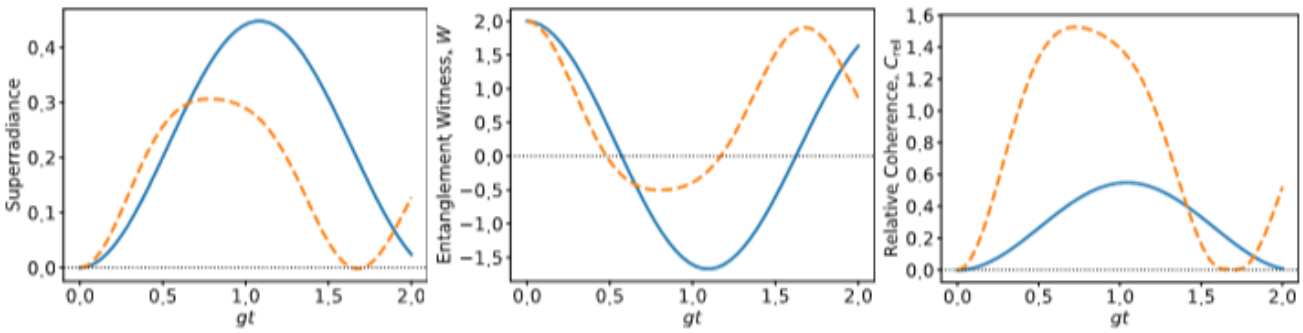

Figure 1: (left) The superradiance $\langle\sigma_i^+\sigma_j^-\rangle$ is shown as a function of time. (middle) The time evolution of entanglement witness, W is depicted. (right) The relative coherence, C_{rel} is plotted for the same duration as in the left and middle graphs. Blue solid lines correspond to N = 2, while the

dashed orange lines represent N = 4. The other common parameters are: $g = 1, \frac{\gamma}{g} = 0.0, \frac{k}{g} = 0.1$*, and* $\frac{\gamma\phi}{g} = 0.0225$.

References

[1] R. H. Dicke, Coherence in spontaneous radiation processes, Phys. Rev. 93, 99 (1954)

[2] F. Lohof, D. Schumayer, D. A. W. Hutchinson, and C. Gies, Signatures of Superradiance as a Witness to Multipartite Entanglement, Phys. Rev. Lett. 131, 063601 (2023)

[3] M. Tavis, F. W. Cummings, Exact solution for an n-molecule – Radiation-field Hamiltonian, Phys. Rev. 170, 379 (1968)

Evaluating the performance of non-destructive techniques for classifying and monitoring the aging of store-bought kiwifruit

Peter III J.G. Remoto[1], Darven Murali Tharan[2], Frédérique Vanholsbeeck[2], Cushla McGoverin[2], Keith C. Gordon[1], Sara J. Fraser-Miller[3]*

[1]The Dodd-Walls Centre for Photonic and Quantum Technologies, University of Otago, Dunedin, New Zealand
rempe782@student.otago.ac.nz
[2] The Dodd-Walls Centre for Photonic and Quantum Technologies, University of Auckland, Auckland, New Zealand
[3]University of Flinders University, Adelaide, Australia

Kiwifruit can ripen after being harvested despite reaching physiological maturity. The most common indices of fruit maturity and ripeness are soluble solids content (SSC), titratable acidity (TA) of fruit juices, fruit firmness (FF), dry matter (DM) weight, and colour. Analytical instruments such as the penetrometer and refractometer reliably record FF and SSC data, respectively. These methods are destructive approaches that render the examined fruit unsuitable for sale after testing.1

Vibrational spectroscopy techniques, such as near-infrared (NIR), mid-infrared (MIR), and Raman spectroscopy as well as optical coherent tomography (OCT), are powerful, fast, non-destructive approaches that require little to no sample preparation. In this study, we evaluated the qualitative performances of various non-destructive analytical tools for classifying kiwifruit samples and monitoring kiwifruit aging. These tools include two custom-made multi-spectroscopic probes (Probe A and Probe B), a hand-held near-infrared sensor and an optical coherence tomography instrument. Principal component analysis (PCA) was used to assess the capabilities of these tools. Additionally, classification models were developed using support vector machines (SVM), principal component analysis-linear discriminant analysis (PCA-LDA), and partial least-squares discriminant analysis (PLS-DA) to compare performance. Low-level and mid-level data fusion approaches were also explored and found to generally improve kiwifruit type classification and more effectively predict the day of their measurements.

References

[1] Huang, W.; Wang, Z.; Zhang, Q.; Feng, S.; Burdon, J.; Zhong, C. Horticulturae, 2022, 8, 852.

Progress towards a finite temperature c-field theory of supersolids

B. T. E. Ripley

Department of Physics, Centre for Quantum Science, and Dodd-Walls Centre for Photonic and Quantum Technologies, University of Otago, Dunedin 9016, New Zealand
ripbe022@student.otago.ac.nz

The supersolid is a novel state of matter in which the properties of both solids and fluids are combined: the particles form a spatially ordered crystal, and yet simultaneously flow without friction. This seemingly contradictory behaviour is a manifestation of quantum effects on a macroscopic scale, and is part of what makes the supersolid a system of great interest in the field of condensed matter physics.

Dipolar supersolids were first produced experimentally by three separate groups in 2019 [1–3]. The typical process conducted by these experiments involves cooling a normal (i.e. thermal) dipolar gas through the superfluid transition, before slowly reducing the short-ranged interaction until the magnetic dipole interactions dominate and a supersolid develops.

An alternative pathway into the supersolid is by evaporatively cooling from the normal gas directly into the supersolid state [2]. For this pathway, we develop a finite-temperature stochastic Gross-Pitaevskii equation (SGPE) theory [4] for dipolar supersolids. The SGPE is a description of the low energy modes of the system, and couples them to a reservoir that introduces both noise and damping to the usual GPE. This is represented schematically in Fig. 1, where the coherent region contains only modes with significant occupation and thus can be well described classically; the incoherent regime then acts as the thermal reservoir. Our interest is in both canonical and grand canonical forms of the theory, in that a canonical (energy-exchange only) form overcomes the chemical instability of dipolar gases in the dipole dominant regime where it is favourable for the droplets to continue taking particles from the reservoir.

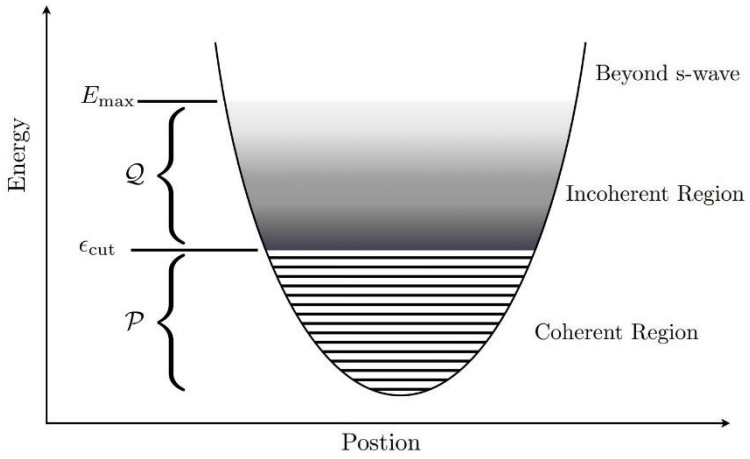

Figure 1: Schematic showing the division of modes into the coherent and incoherent regions [5].

References

[1] F. Böttcher et al., Phys. Rev. X 9, 011051 (2019).

[2] L. Chomaz et al., Phys. Rev. X 9, 021012 (2019).
[3] L. Tanzi et al., Phys. Rev. Lett. 122, 130405 (2019).
[4] P. B. Blakie et al., Adv. Phys. 57, 363 (2008).
[5] S. J. Rooney, PhD thesis (University of Otago, 2015).

Introducing the QO-LED

Finnian J. Blaauw-Smith[1,2,3], Justin M. Hodgkiss[1,3], Nathaniel J. L. K. Davis[1,2,3]

[1]School of Chemical and Physical Sciences, Victoria University of Wellington, Wellington
smithfi@staff.ac.nz
[2]The Dodd-Walls Centre for Photonic and Quantum Technologies, Dunedin
[3]The Alan MacDiarmid Institute for Advanced Materials and Nanotechnology, Wellington

As technology continues to progress, the load on the current electrical infrastructure increases, calling for research toward more efficient devices.

One promising device architecture is the quantum dot-based LED (Q-LED), which offers higher efficiency and wavelength tunability compared to its conventional counterparts[1]. Though the QLED is not fully developed, surface ligands have shown to affect the efficiency and stability of the device.

We present a new hybrid device by way of ligand exchange with an organic chromophore. This new device, the quantum organic LED (QOLED), shows a modest increase in external quantum efficiency (EQE). We also thoroughly investigate the device morphology and kinetics to determine the electron recombination path.

References

[1] Jang E, Jang H. Review: Quantum Dot Light-Emitting Diodes. Chem Rev. 2023;123(8):4663-4692. doi:10.1021/acs.chemrev.2c00695

Figure 1 QO LED lighting up

Deep learning from shallow data

Craig Steed[1,2], Katerina Taškova[3], Julia Robertson[2,4], Simon Swift[2,4], Frédérique Vanholsbeeck[1,2], Cushla McGoverin[1,2]

[1]Department of Physics, University of Auckland, [2]The Dodd-Walls Centre for Photonic and Quantum Technologies, [3]Department of Computer Science, University of Auckland, [4]Department of Molecular Medicine and Pathology, University of Auckland

Rapid quantification of bacterial viability will benefit food safety and healthcare. Fluorescence spectroscopy is a promising method for quantifying bacterial viability. Previously, the UoA Biophotonics group developed a portable fibre-based fluorometer (the optrode) for the measurement of fluorescence. Bacterial viability was quantified through a differential fluorescence spectroscopic method, and machine learning (ML) from the whole spectrum yielded the best predictive performance.

Experiments to determine bacterial viability are typically run on a number of biological replicates, and the experimental effort precludes large numbers of samples. This means the spectral data from optrode experiments is “wide”, with a small number of observations (e.g. 40) and a relatively large number of features (e.g. 800). This shape of data and paucity of observations can work with classical ML models based on mathematical algorithms (e.g. support vector machines, random forest), but not with Deep Learning (DL) models, which typically require data where the number of observations significantly exceeds the number of features, and the number of observations is relatively large (e.g. >10000).

To explore the efficacy of DL for this case, simple data augmentation was applied, adding synthetic data to real data spectral data in the training data set, and the predictive performance of DL models was assessed on data external to the training data, against the degree of data augmentation and model parameters. Surprisingly, a simple DL model exhibited good predictive performance when the ratio of synthetic data to real data exceeded 99%, and when the synthetic data was either simple noise mimicking the distribution of the real data, or even duplicates of the real data. For this case classical ML models failed, while the DL model predicted qualitative trends and quantitative values for bacterial viability that aligned with results from plate culture.

This approach may have utility for modelling spectral data where a limited amount of supervised data is available to train a model, and classical ML models have poor predictive performance.

SHG in *x*-cut lithium tetraborate (LB4) whispering gallery mode resonators

C. Tian[1,2,3], F. Sedlmeir[1,2], P. Becker[4], L. Bohatý [4], R. Blaikie[1,2,3] and H. G. L. Schwefel[1,2,*]

[1]The Dodd-Walls Centre for Photonic and Quantum Technologies, New Zealand

[2]Department of Physics, University of Otago, Dunedin 9016, New Zealand

[3]The MacDiarmid Institute for Advanced Materials and Nanotechnology, Wellington 6012, New Zealand

[4]Institute of Geology and Mineralogy, Sect. Crystallography, Zülpicher Str. 49 b, 50674 Köln, Germany

[*]harald.schwefel@otago.ac.nz

Lithium tetraborate (LB4) is a popular nonlinear crystal and has very low material loss in the visible and ultraviolet (UV) range. Here, we report broadband second-harmonic generation (SHG) at 258 nm 397 nm, and 780 nm in x-cut LB4 whispering gallery mode resonators (WGMRs). In an x-cut WGMR made from uniaxial crystals with its optic axis lying within the plane of the equator, cyclic phase matching takes advantage of oscillating refractive index of the transverse-magnetic (TM) mode [1, 2]. This spatial refractive index modulation in an x-cut WGMR allows negative uniaxial crystals, such as BBO [3] and here LB4, to achieve broad- band phase matching within the transparency window of the nonlinear materials [3]. Our x-cut LB4 WGMRs are manufactured via single-point diamond cutting, with quality (Q) factors in the order of 107 at all pump wavelength. In z-cut LB4 WGMRs, Q factors of 2×10^9 can be achieved. Exploiting a cubic z-cut LB4 prism as a second outcoupling prism, selective outcoupling of SHG is achieved [4], which improves the SHG conversion efficiency by a factor of two, and detect SHG signals at 780 nm, 397 nm and 258 nm. Table1 summarizes the Q factors and conversion efficiency of SHG in our LB4 WGMRs.

Table 1: Summary of second harmonic (SH) generation for three different pump wavelengths: maximum incident pump power (P_p^{max}), maximum second harmonic (SH) power (P_{SH}^{max}), the Q factor of the pump mode, and conversion efficiency (P_{SH}/P_p^2) per mW incident pump power[a]

wavelength (nm)	Q factor ($\times 10^7$)	P_p^{max} (mW)	P_{SH}^{max} (μW)	SH wavelength (nm)	P_{SH}/P_p^2 (%/mW)[b]
1560	4.8	1.05	0.19	**780**	0.016
795	2.0	7.83 [c]	10.51	**397**	0.021
517	6.7	10.49	133.60	**258**	0.129

[a]*The shown results are measured using selective coupling;*

[b]*The conversion efficiency is obtained from quadratic fitting of power scaling measurements, not from the maximum pump and SH signal;*

[c]*The maximum pump power for 800 nm is subtracted by an offset of 6.20 mW due to back scattering from the quadratic fitting.*

References

[1] J. Fürst, B. Sturman, K. Buse, I. Breunig, Optics Express 2016, 24, 18 20143.

[2] L. S. Trainor, Ph.D. thesis, University of Otago, 2021.
[3] G. Lin, J. U. Fürst, D. V. Strekalov, N. Yu, Applied Physics Letters 2013, 103, 18.
[4] F. Sedlmeir, M. R. Foreman, U. Vogl, R. Zeltner, G. Schunk, D. V. Strekalov, C. Marquardt, G. Leuchs, H. G. Schwefel, Physical Review Applied 2017, 7, 2 024029.

Cartilage degeneration assessment using compression-based depth-resolved polarisation-sensitive optical coherence tomography

Darven Murali Tharan[1,2], Marco Bonesi[1,2], Daniel Everett[2,4], Matthew Goodwin[1,2], Cushla McGoverin[1,2], Sue McGlashan[3], Ashvin Thambyah[4], Frédérique Vanholsbeeck[1,2]

[1]Department of Physics, [2]The Dodd-Walls Centre for Photonic and Quantum Technologies, [3] Department of Anatomy and Medical Imaging, [4] Department of Chemical and Materials Engineering, The University of Auckland, New Zealand

Osteoarthritis (OA) affects millions worldwide, costing billions in healthcare and productivity in Aotearoa New Zealand alone. The early onset of OA manifests as a disruption of the articular cartilage (AC) collagen network, altering its mechanical integrity and leading to changes in tissue birefringence. To address the pressing need for early OA detection, we employ polarisation-sensitive optical coherence tomography (PS-OCT) to detect micro-scale collagen network disruptions associated with early-stage damages. Our investigation studies AC during compression to better assess its response to mechanical stimuli. When subjected to compression, collagen fibrils in healthy AC form a characteristic chevron boundary to dissipate forces effectively[1]. Loss or deformation of this boundary is a clear indicator of AC degeneration.

We present, for the first time to our knowledge,a dynamic depth-resolved PS-OCT approach that enables mechanical testing of biological tissues under creep loading using a custom-built PS-OCT system and compression imaging head. We use the compression head to apply a fixed load on cartilage and simultaneously acquire a time sequence of high-resolution PS-OCT data to observe the deformation of cartilage under creep loading. Our experimental configuration allows depth-resolved quantification of the optical axis (OpAx) and birefringence, correcting for erroneous effects that appear in cumulative PS-OCT imaging. The birefringence is related to the organisation of fibrillar structures while the OpAx proxies the orientation of these fibrils, which are then visualised using tractography. We have developed a novel tractography algorithm called density encoded line integral convolution (DELIC) to enhance the visualization of the cartilage OpAx. This method builds upon the traditional line integral convolution technique by incorporating sample birefringence into the tractography density. DELIC operates by using a sparse texture composed of points whose density is determined by the sample's birefringence. These points are then convolved based on the OpAx vector field. Conceptually, this process is akin to placing ink droplets on a plane at varying densities and smearing them to reveal the underlying OpAx vector field. To achieve a point density that accurately represents the birefringence, we employ weighted Centroidal Voronoi Tessellation(CVT)[2].

Our results reveal compression based PS-OCT allows nondestructive observation of the chevron pattern and how it changes during creep loading. The location and shape of the chevron was validated using differential interference contrast microscopy. In summary, this study demonstrates a pioneering approach to biomechanical testing using depth-resolved PS-OCT, providing a powerful tool to study the early onset of OA. Understanding these early changes is crucial for developing effective early diagnostic strategies and therapeutic interventions.

References

[1] A. Thambyah and N. Broom, “Micro-anatomical response of cartilage-on-bone to com- pression: mechanisms of deformation within and beyond the directly loaded matrix,” Journal of anatomy 209(5), 611–622 (2006).
[2] Q. Du, M. Gunzburger and L. Ju, “Advances in studies and applications of centroidal Voronoi tessellations,” Numerical Mathematics: Theory, Methods and Applications 3(2), 119- 142 (2010).

QTA: Storing single photons in a crystalline quantum memory

Luke S. Trainor[1,2], Helen M. Chrzanowski[3], Xavier Barcons Planas[3,4,5], Janik Wolters[3,4], and Jevon J. Longdell[1,2]

[1]The Dodd Walls Centre for Quantum and Photonic Technologies
[2]Department of Physics, University of Otago, Dunedin
[3]Institute of Optical Sensor Systems, German Aerospace Center (DLR), Berlin, Germany [4]Institut für Optik und Atomare Physik, Technische Universität Berlin, Berlin, Germany [5]Institut für Physik, Humboldt-Universität zu Berlin, Berlin, Germany

The storage of single photons is an ongoing technological challenge. Storage in an on-demand quantum memory would enable new technologies such as quantum repeaters, which would allow creation of a quantum network over longer distances than currently possible. Hosting part of the network on satellites could allow even better distance scaling, beating the current exponential loss seen in optical fibres.

Rare-earth doped crystals are a promising platform for quantum memories, in particular due to their long coherence times. A coherence time of over a second has been observed in the hyperfine levels of erbium-167 doped yttrium orthosilicate [1]. A bonus feature is erbium's optical transition in the telecom C-band.

We share our progress with storing single photons in an erbium quantum memory. The coherent properties of our erbium-doped crystal are measured with photon echo techniques. The long hyperfine lifetime, see Fig. 1, allows us to tailor the absorption spectrum of the erbium. By burning a comb structure into the absorption spectrum, an optical quantum memory is created.

The photons we will store are generated by a monolithic photon pair source, which generates pairs of photons by spontaneous parametric down conversion from a pump laser. To improve the conversion efficiency and reduce the photon bandwidth, the crystal is shaped into a Fabry-Perot cavity and its end faces are coated with mirror coatings. The detection of a photon at one frequency heralds the generation of a photon in the other frequency, which will trigger storage in a memory. The source generates over ten million photon pairs per milliwatt of pump power. The arm efficiencies are 26.7 % at 1536 nm and 9.7 % at 580 nm. The difference in the two is due to asymmetric detector efficiencies.

[1] M. Rančić, M. P. Hedges, R. L. Ahlefeldt, and M. J. Sellars, "Coherence time of over a second in a telecom-compatible quantum memory storage material," Nature Physics, vol. 14, pp. 50–54, Jan. 2018.

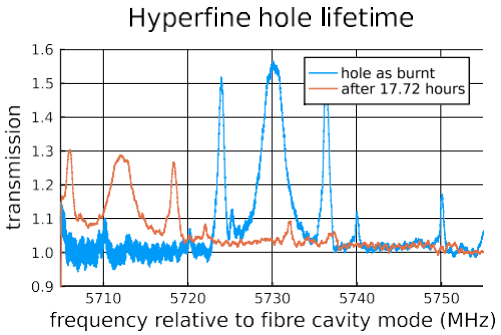

Figure 1: The hyperfine lifetime of 167Er at 40 mK. A strong telecom laser pulse is absorbed by erbium ions with transitions at that frequency. They are moved into adjacent hyperfine levels by spontaneous emission. This

results in a central hole and two side holes caused by coupling to nearby yttrium nuclei. The hole is measured by absorption spectroscopy. After more than 17 hours the same hole is measured again, showing the hyperfine lifetime is hours.

Tunable Pump Wavelength-Displaced Solitons in Passive Kerr Resonators Mediated by Stimulated Raman Scattering

Jordan J. Wise[1,2,†], Zongda Li[1,2], Yiqing Xu[1,2], Miro Erkintalo[1,2], Stéphane Coen[1,2], Stuart G. Murdoch[1,2]

[1]Department of Physics, University of Auckland, New Zealand
[2]Dodd-Walls Centre for Photonic and Quantum Technologies, New Zealand
[†]jordan.wise@auckland.ac.nz

Stimulated Raman scattering in passive optical fibre resonators has recently been demonstrated as a means of generating ultrashort pump wavelength-displaced dissipative solitons which are locked in phase to cavity-desynchronised driving pulses [1]. Relaxing the phase-matching condition and leveraging group velocity dispersion, we demonstrate a new regime for soliton generation in which the centre frequencies of the solitons produced is tunable over a small range.

External driving of passive optical resonators is a well-established method for generating ultrashort solitons. Driving with a pulsed pump synchronised to the roundtrip time of the cavity allows us to control where within a resonator a soliton will form. Changing the repetition rate of our driving pulses thus changes the repetition rate, and therefore velocity, of our solitons. Group velocity dispersion means that pulses traveling at different velocities must necessarily have different centre wavelengths. While solitons formed in passive resonators typically have the same centre frequency as the driving field, Raman scattering can be used to provide optical gain across a wide range of frequencies. Scanning the repetition rate of our input pulses (and therefore the desynchronisation between the pump pulse period and the roundtrip time at the pump frequency) we find that for certain negative desynchronisation values, solitons form spontaneously more than 15 THz below the centre frequency of the pump (see Figures 1a and 1c).

The solitons that form in this regime have the same repetition rate as the pump pulse. Therefore the corresponding pump and soliton frequency combs have the same spacing. However, they have different carrier envelope offset frequencies and so beat against each other. In the time domain this manifests as a time-varying pattern of amplitude modulation across the soliton (see Figure 1b).

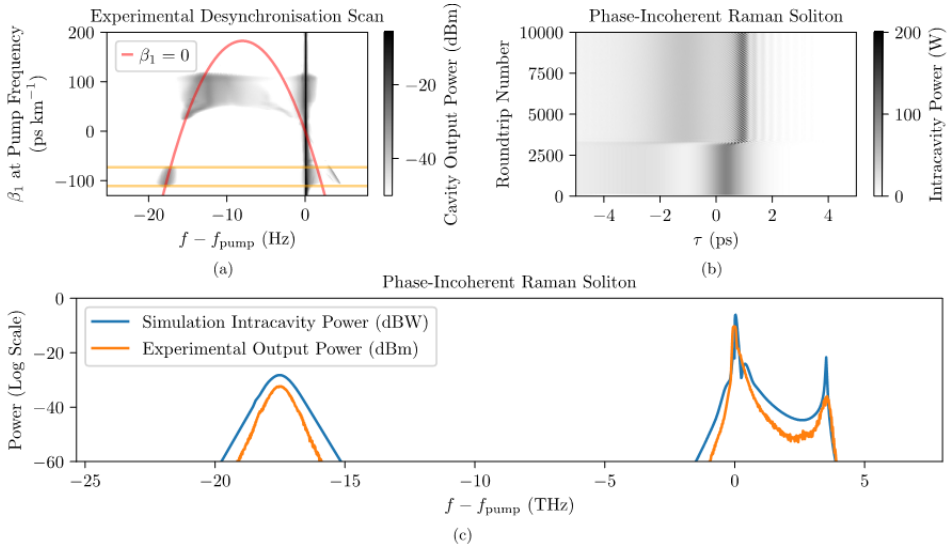

Figure 1: Tunable phase-incoherent Raman solitons. (a) Output spectra of a passive fibre resonator driven with pulses of different repetition rates. The red line indicates the optical frequencies at which the repetition rate of the input pulse is matched to the roundtrip time of the cavity and the orange lines indicate the desynchronisation values for which phase-incoherent Raman solitons exist. (b) Simulated temporal evolution of a phase-incoherent Raman soliton. (c) Simulated and experimental optical spectra of an phase-incoherent Raman soliton.

Reference

[1] Z. Li, Y. Xu, S. S. Shamailov, X. Wen, W. Wang, X. Wei, Z. Yang, S. Coen, S. G. Murdoch, and M. Erkintalo, "Ultrashort dissipative Raman solitons in Kerr resonators driven with phase-coherent optical pulses," Nature Photonics, vol. 18, pp. 46–53, 2022.

QTA: Fast readout of superconducting qubits with fluxons

W. Wustmann & K.D. Osborn

Superconducting circuits are a leading platform for quantum information technology, with qubits based on Josephson junctions. The established techniques for control and readout of superconducting qubits relies on their strong and coherent coupling to microwave photons in high-quality resonators. Here we describe a theoretical study of a different approach, employing fluxons for the fast readout of a superconducting flux-based qubit, such as a fluxonium qubit. The qubit is galvanically connected to a circuit interface connecting long Josephson junctions (LJJs). Such LJJs can host topological solitons, so-called fluxons, which are spatially extended single-flux quanta.

To read out the qubit state, a ballistically traveling fluxon is launched into one of the LJJs and scatters at the interface. Depending on the qubit state, the fluxon can undergo different types of resonant elastic scattering, with or without inversion of its flux-polarity. In this study we concentrate on qubits with macroscopically distinguishable flux states, which affect the classical dynamics of the (highly classical) fluxons. To study the feedback on the qubit evolution, we employ a model that reduces the many circuit degrees of freedom to only a few collective coordinates, allowing to treat the quantum dynamics of the coupled fluxon-qubit system in adiabatic approximation.

ABSTRACTS FOR POSTER PRESENTATIONS

Nonlinear Dynamics of the Spin-1 Dicke Model

Ofri Adiv[1], Scott Parkins[1], and Bernd Krauskopf[2]

[1]Department of Physics, University of Auckland, Auckland 1010, New Zealand
[2]Department of Mathematics, University of Auckland, Auckland 1010, New Zealand

Interactions between many-body atomic systems and light have received much attention, both recently and in the past, due in part to advances in quantum technologies. More specifically, the Dicke model has long been a focus of research for its applicability to a range of physical systems, and for the quantum phase transitions it exhibits. Originally proposed in Ref. [1], it describes the collective interaction between an ensemble of two-level atoms and a single mode of radiation in an optical cavity. At a critical value of the light-matter coupling it displays a quantum phase transition to superradiance [2], where the atoms emit coherently and the cavity is populated in steady-state.

Continuing that line of research, in this work we investigate a spin-1 variant of the traditional two-level Dicke model, where three energy levels are now accessible to each atom. We focus on the semiclassical (mean field) dynamics described by a system of nonlinear differential equations, which we analyse by means of dynamical systems methods. The system's behaviours are characterized systematically, and include a variety of hitherto unreported dynamics; examples include oscillatory and quasiperiodic phases, chaos, and structurally stable homoclinic orbits. Finding phase boundaries between these behaviours additionally reveals several multistable regions, where more than one stable phase may be found. Lastly, we investigate the ubiquity of these behaviours when the energy level structure is varied.

References

[1] Dicke, R. H. Coherence in Spontaneous Radiation Processes. Physical Review 93, 99–110 (1954).
[2] Hepp, K. & Lieb, E. H. On the Superradiant Phase Transition for Molecules in a Quantized Radiation Field: the Dicke Maser Model. Annals of Physics 76, 360–404 (1973).

Exploring laser self-injection locking enabled by crystalline whispering gallery mode resonators

Farhan Azeem[1,2], Josh T. Christensen, F. Sedlmeir, Harald G. L. Schwefel[1,2]

[1]The Dodd-Walls Centre for Photonic and Quantum Technologies, New Zealand
Harald.schwefel@otago.ac.nz
[2]Department of Physics, University of Otago, Dunedin, 9016, New Zealand

Laser Injection locking is achieved by injecting a slave laser's resonator with a master laser matching its operating frequency [1]. A variant of this process known as self-injection locking (SIL) can be realised by introducing external feedback in the shape of a cavity, eliminating the need for a master laser. Although most of the laser light passes through the cavity, if some light is back-scattered into the laser from the cavity, the SIL effect can occur. However, the cavity used for SIL must be of much narrower linewidth, i.e., higher quality factor (Q-factor) than the laser itself [2]. Whispering gallery mode resonators (WGMRs) serve as an excellent example of such a high Q-factor cavity and offer several advantages, i.e., compact sizes, high Q-factors that can exceed a billion and high coupling efficiencies [3]. WGMRs were first used to demonstrate SIL over two decades ago by using a Fabry–Pérot diode laser to couple light into a silica sphere [4]. This introduced the typical WGMR SIL configuration which involves coupling the diode laser to a WGMR mainly via prism coupling, as depicted in Figure 1(a). The Rayleigh backscattering from the WGMR helps in forming a feedback loop and SIL is achieved when the frequency of the excited WGM and the laser are similar. This can clearly be observed in the laser diode current (LI) curves recorded via a photodiode. One such example of LI curve is shown in Figure 1(b). SIL results in stabilisation of the laser, which consequently results in decreased phase noise and a reduced linewidth. SIL is particularly useful in applications requiring precise frequency control, such as in optical communication, spectroscopy, or high-resolution measurements and has previously shown sub-Hertz output linewidths [5].

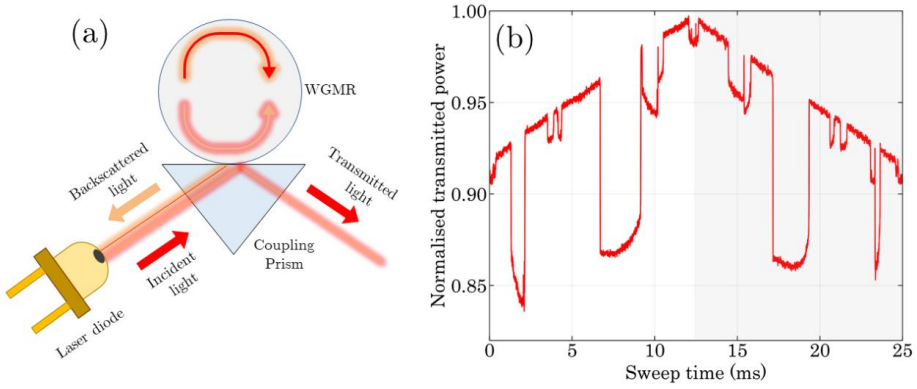

Figure 1: *(a) Depiction of SIL performed via a prism coupled WGMR. SIL is achieved when a laser is coupled to a WGMR and the resonant backscattered light helps form a feedback loop between the diode and WGMR. (b) The LI curve of a distributed feedback (DFB) laser diode operating at 1550nm observed via a photodiode. This curve illustrates the SIL effect in shape of a drop in the output power, which is observed when the laser locks to WGMs excited by it [6]. The white half of the plot shows the increase in frequency or forward sweep, ana the grey half shows the decrease in frequency or backward sweep.*

In this work, we explore SIL by utilising disc-shaped WGMRs fabricated using single-point diamond turning [7] from crystalline materials such as the previously extensively explored magnesium fluoride [5] and unexplored materials such as yttrium lithium fluoride (YLF) and yttrium orthosilicate (YSO). We use a 1550nm DFB laser diode to confine light inside these WGMRs via prism coupling technique. SIL is observed in the LI curves when optimal conditions are reached, i.e., efficient coupling resulting in sufficient backscattering and adequate optical path length between the laser and the WGMR [4,8]. The performance of the SIL is quantified by using heterodyning to determine the linewidth of the laser before and after successful implementation of SIL.

References

[1] C. J. Buczek, R. J. Freiberg, and M. L. Skolnick, 'Laser injection locking', Proc. IEEE, vol. 61, no. 10, pp. 1411–1431, 1973.
[2] B. Dahmani, L. Hollberg, and R. Drullinger, 'Frequency stabilization of semiconductor lasers by resonant optical feedback', Opt. Lett., vol. 12, no. 11, p. 876, 1987.
[3] S. Yang, Y. Wang, and H. Sun, 'Advances and Prospects for Whispering Gallery Mode Microcavities', Advanced Optical Materials, vol. 3, no. 9, pp. 1136–1162, 2015.
[4] V. V. Vassiliev, V. L. Velichansky, V. S. Ilchenko, M. L. Gorodetsky, L. Hollberg, and A. V. Yarovitsky, 'Narrow-line-width diode laser with a high-Q microsphere resonator', Optics Communications, vol. 158, no. 1–6, pp. 305–312, 1998.
[5] N. M. Kondratiev et al., 'Recent advances in laser self-injection locking to high-Q microresonators', Front. Phys., vol. 18, no. 2, p. 21305, 2023.
[6] A. Savchenkov, S. Williams, and A. Matsko, 'On Stiffness of Optical Self-Injection Locking', Photonics, vol. 5, no. 4, p. 43, 2018.
[7] F. Azeem, "Active and passive crystalline whispering gallery mode resonators," Thesis, University of Otago, 2022.
[8] R. R. Galiev, N. M. Kondratiev, V. E. Lobanov, A. B. Matsko, and I. A. Bilenko, 'Optimization of Laser Stabilization via Self-Injection Locking to a Whispering-Gallery-Mode Microresonator', Phys. Rev. Applied, vol. 14, no. 1, p. 014036, 2020.

Sounds waves and fluctuations in one-dimensional supersolids

L. M. Platt[1,2], D. Baillie[1,2], and P. B. Blakie[1,2]

[1]Dodd-Walls Centre for Photonic and Quantum Technologies, Dunedin 9054, New Zealand
[2]Department of Physics, University of Otago, Dunedin 9016, New Zealand

The experimental production of supersolid states in atomic gases [1, 2, 3, 4, 5] has generated interest in their properties, including their excitation spectra. In this presentation we discuss the low-energy excitations of a dilute supersolid state of matter with a one-dimensional crystal structure. A hydrodynamic description is developed based on a Lagrangian [6, 7], incorporating generalized elastic parameters derived from ground state calculations. The predictions of the hydrodynamic theory are validated against solutions of the Bogoliubov-de Gennes equations, by comparing the speeds of sound, density fluctuations, and phase fluctuations of the two gapless bands. Our results are presented for two distinct supersolid models: a dipolar Bose-Einstein condensate in an infinite tube and a dilute Bose-Einstein condensate of atoms with soft-core interactions. Characteristic energy scales are identified, highlighting that these two models approximately realize the bulk incompressible and rigid lattice supersolid limits. This work has been submitted for publication [8].

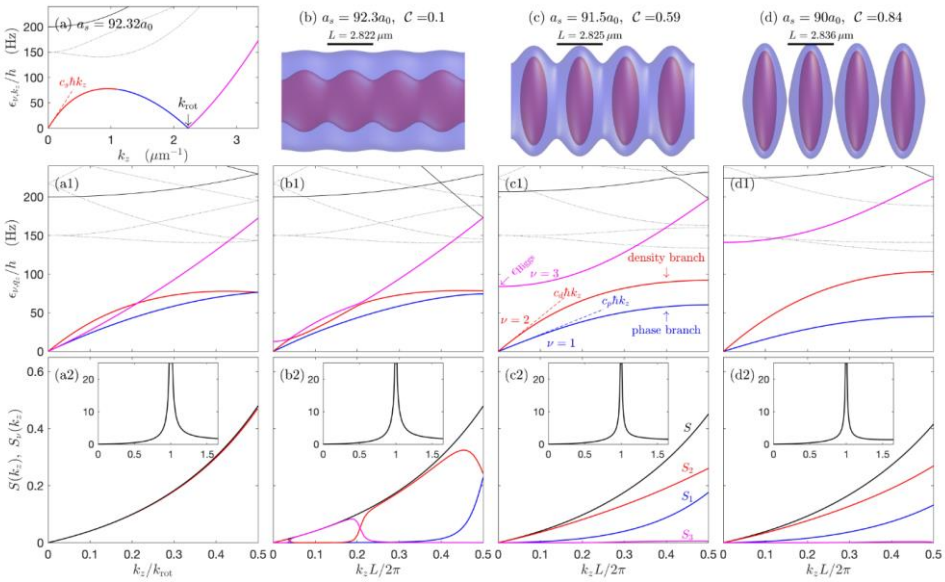

Figure 1: Density profiles, excitation spectra and structure factors of an infinite tube dipolar BEC. (a) Excitation spectrum for a uniform system at as = arot where the roton softens. (a1) The results from (a) reduced to the first Brillouin zone. (a2) The static structure factor $S(k_z)$. Inset shows S(kz) over a wider momentum range. (b)-(d) Density isosurfaces of crystalline ground states for $a_s < a_{rot}$. Red (blue) isosurface at $4 \times 10^{20} m^{-3}$ ($10^{20} m^{-3}$). Unit cell size L and density contrast C are also indicated. Corresponding excitation spectra (b1)-(d1) and static structure factors (b2)-(d2). The static structure factor (black line) and contributions of the lowest 3 bands. Results for ^{164}Dy with a linear density of $n = 2500\ \mu m^{-1}$ and confinement $\omega_p = 2\pi \times 150$Hz. [Figure from Ref. [9]].

References

[1] Julian Léonard, Andrea Morales, Philip Zupancic, Tilman Esslinger, and Tobias Donner. Supersolid formation in a quantum gas breaking a continuous translational symmetry. Nature, 543:87, 03 2017.

[2] Jun-Ru Li, Jeongwon Lee, Wujie Huang, Sean Burchesky, Boris Shteynas, F C ¸ Top, Alan O. Jamison, and Wolfgang Ketterle. A stripe phase with supersolid properties in spin–orbit-coupled Bose–Einstein condensates. Nature, 543:91, 03 2017.

[3] L. Tanzi, E. Lucioni, F. Fam ` a, J. Catani, A. Fioretti, C. Gabbanini, R. N. Bisset, L. Santos, and G. Modugno. Observation of a dipolar quantum gas with metastable supersolid properties. Phys. Rev. Lett., 122:130405, Apr 2019.

[4] Fabian Böttcher, Jan-Niklas Schmidt, Matthias Wenzel, Jens Hertkorn, Mingyang Guo, Tim Langen, and Tilman Pfau. Transient supersolid properties in an array of dipolar quantum droplets. Phys. Rev. X, 9:011051, Mar 2019.
[5] L. Chomaz, D. Petter, P. Ilzhöfer, G. Natale, A. Trautmann, C. Politi, G. Durastante, R. M. W. van Bijnen, A. Patscheider, M. Sohmen, M. J. Mark, and F. Ferlaino. Long-lived and transient supersolid behaviors in dipolar quantum gases. Phys. Rev. X, 9:021012, Apr 2019.
[6] D. T. Son. Effective lagrangian and topological interactions in supersolids. Phys. Rev. Lett., 94:175301, May 2005.
[7] C.-D. Yoo and Alan T. Dorsey. Hydrodynamic theory of supersolids: variational principle, effective lagrangian, and density-density correlation function. Phys. Rev. B, 81:134518, Apr 2010.
[8] L. M. Platt, D. Baillie, and P. B. Blakie. Sounds waves and fluctuations in one-dimensional supersolids (preprint: arxiv.org/abs/2403.19151), 2024.
[9] P. B. Blakie, L. Chomaz, D. Baillie, and F. Ferlaino. Compressibility and speeds of sound across the superfluidto-supersolid phase transition of an elongated dipolar gas. Phys. Rev. Res., 5:033161, Sep 2023.

Photophysics of Diphenylacene Metal Organic Frameworks

Sanutep V. Chan*[1,2,3], Lujia Liu[1,3], Nathaniel J. L. K. Davis[1,2,3]

[1]School of Chemical and Physical Sciences, Victoria University of Wellington, Wellington
sanutep.chan@vuw.ac.nz
[2]The Dodd-Walls Centre for Photonic and Quantum Technologies, Dunedin
[3]The Alan MacDiarmid Institute for Advanced Materials and Nanotechnology, Wellington

Energy transfer between luminophores – fluorescent species – depends on the distance between them and their spatial alignment. The commonly accepted exchange pathways are: Resonance interactions of molecular dipoles – Fluorescence Resonance Energy Transfer[1] – and electron transfers – Dexter Electron Transfer[2].

Metal organic frameworks are polycrystalline materials composed of metal ion clusters and organic molecule linkers[3]. The high degree of order gives directed arrangements of the monomers in space (Figure 1).

A series of diphenylacene monomers (Figure 2) were synthesised and subsequent metal organic frameworks constructed from them. The photophysical characteristics of the resulting materials were investigated.

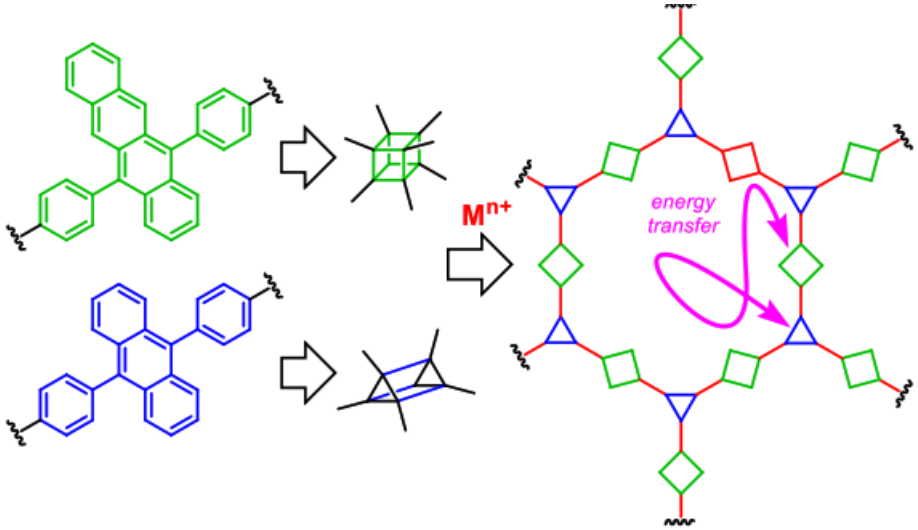

Figure 1 – Illustration of Metal Organic Framework design and monomer unit ordering.

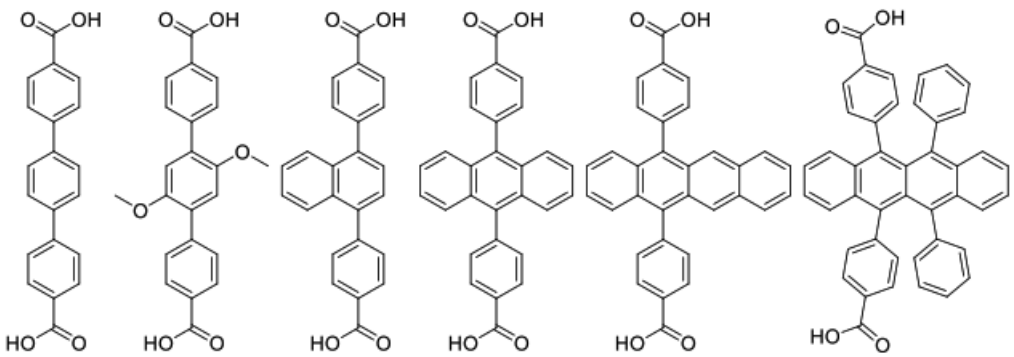

Figure 2 – Diphenlacene monomer units synthesized and used.

References

[1] Förster, T. Zwischenmolekulare Energiewanderung Und Fluoreszenz. Ann. Phys. 1948, 437 (1–2), 55–75. https://doi.org/10.1002/andp.19484370105.
[2] Dexter, D. L. A Theory of Sensitized Luminescence in Solids. J. Chem. Phys. 1953, 21 (5), 836–850. https://doi.org/10.1063/1.1699044.
[3] Kirlikovali, K. O.; Hanna, S. L.; Son, F. A.; Farha, O. K. ACS Nanosci. Au 2023, 3 (1), 37–45. DOI: 10.1021/acsnanoscienceau.2c00046.

Newton's Rings interferometry for distance calibration in whispering-gallery mode resonators.

Josh T. Christensen[1,2], Farhan Azeem[1,2], Luke S. Trainor[1,2], Dmitry V. Strekalov[3], and Harald G. L. Schwefel[1,2]

[1]Department of Physics, University of Otago, 730 Cumberland Street, Dunedin, New Zealand
chrjo748@student.otago.ac.nz
[2]The Dodd-Walls Centre for Photonic and Quantum Technologies, New Zealand
[3]Jet Propulsion Laboratory, California Institute of Technology, Pasadena, CA, USA

We present an application of Newton's rings used to measure the distance between a coupling prism and a whispering gallery mode resonator (WGMR)[1]. Three narrowband colour channels were used to illuminate these rings, which provided an absolute distance scale without the need for the resonator and coupling prism to come into contact. We demonstrate this method to be effective at measuring coupler separation distances to sub-nanometer precision, that further allow us to study the profile of modes coupled to the WGMR. Furthermore, this method is shown to provide an excellent beam alignment technique for coupling WGMR and prisms.

We follow up from our previous work[2] to demonstrate contact-free determination of the absolute distance between a WGMR and a prism by photographing the Newton's rings with illumination from an RGB diode, as seen in Figure 1. The captured image is decomposed into its R, G and B colour channels, Newton's rings phases of each channel are extracted and the differences between the respective colour channels' phases are studied to provide an absolute distance scale.

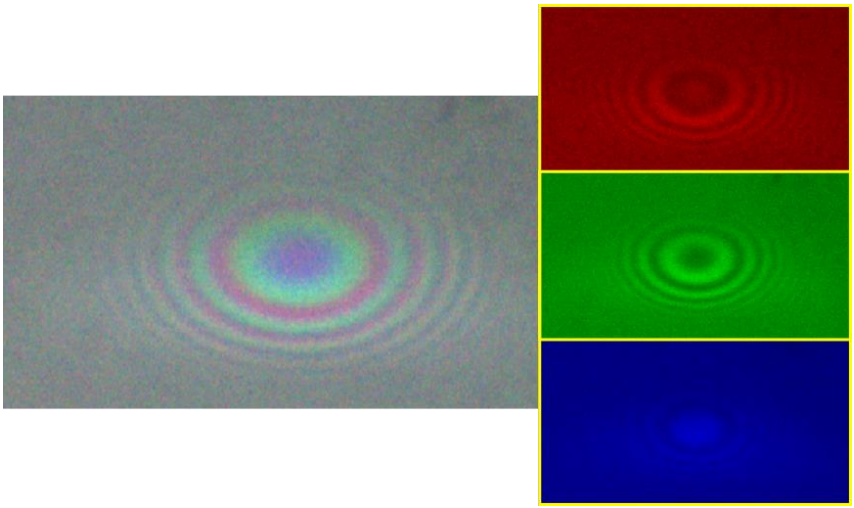

Figure 1: Newton's rings are observed at the interface between a coupling prism and WGMR when illuminated by an RGB diode. The R, G, and B colour channels are then digitally extracted, shown as the right insets, and the respective phase of the Newton's rings are used to determine the absolute distance between coupler and resonator.

This work aims to further investigations into the mode profiles of whispering gallery modes that require accurate distance measurements, as well as to provide a method of beam alignment in prism-WGMR systems.

[1] Luke S. Trainor, Florian Sedlmeir, Christian Peuntinger, and Harald G. L. Schwefel, “Selective Coupling Enhances Harmonic Generation of Whispering-Gallery Modes”, Phys. Rev. Applied 9, 024007 (2018)
[2] Josh T. Christensen, Farhan Azeem, Luke S. Trainor, Dmitry V. Strekalov, and Harald G. L. Schwefel, "Distance calibration via Newton’s rings in yttrium lithium fluoride whispering gallery mode resonators," Opt. Lett. 47, 6053-6056 (2022)

Experimental steps towards the creation of multiphoton states in a fiber cavity

W.P. Crump, M. Sadeghi and M.D. Hoogerland

Dodd-Walls Centre for Quantum and Photonic Technologies and Physics Department, The University of Auckland, Private Bag 92019, Auckland 1142, New Zealand.

In the expanding field of quantum technologies, the use and manipulation of non-classical states can in theory lead to great improvements in fields such as computing, sensing and communication. An example of one such technology is a source of single optical photons. These have been in use for some time and are important in photonic quantum computing, but as of this moment there is no such source of multiphoton states which could allow for more efficient quantum computing architectures. In this work we will show our progress towards an experimental implementation of a multiphoton source of optical photons.

The proposed scheme [1] to generate the multiphoton states uses a system comprised of a cavity coupled to an atom where the Zeeman substructure determines the multiphoton state. A circularly polarized laser drives the atom between Zeeman sublevels through a controlled cascade of Raman transitions, where a photon is emitted into the cavity for each transition. This produces 2F photons in the cavity, the desired multiphoton state, and the process can be repeated by driving with the opposite polarization.

In our system an optical nanofiber (ONF) provides the coupling between fiber photons and an atom. A Magneto Optical Trap provides a source of Caesium atoms to interact with the nanofiber. We have implemented a 2 colour dipole trap along the ONF using magic wavelengths to reduce light shifts between atom states. We show absorption measurements of the trap which indicate an optical depth as high as 15.5 ± 0.4 and a trap decay time of 28.2 ± 1.4 ms. Machine learning was used to optimise the trapping parameters.

We will show progress towards state preparation of the trapped atoms, where all atoms will be pumped into the F = 3 dark state and one atom will be excited to the F = 4 state. Finally, the cavity which is defined by using Fiber Bragg gratings is sensitive to environmental drifts and we will show our progress towards the stabilization of the cavity.

References

[1] A. Gogyan, S. Guerin, C. Leroy and Yu. Malakyan. ”Deterministic production of N -photon states from a single atom-cavity system” PHYSICAL REVIEW A 86, 063801 (2012).

$Yb3^{+}/Er3^{+}$ doped K2YF5 particles upconversion thermometry

Rezvan Anvari[a,b], Pratik S.Solanki[a,b], Benjamin Haenraets[a], Mike F.Reid[a,b], Jon-Paul Wells[a,b1]

[a]School of Physical and Chemical Sciences, University of Canterbury, Christchurch 8140, New Zealand
[b]Dodd_Walls Center for Photonic and Quantum Technologies, Dunedin 9056, New Zealand

In this work, we study the effect of the size of the host for K_2YF_5: Yb/Er nano and microparticles on their optical thermometric sensing capability[1,2]. We study the laser power-dependent upconversion fluorescence spectra, the fluorescence intensity ratio, the absolute temperature sensitivity, the relative temperature sensitivity, and thermal uncertainty using 980 nm laser excitation[3].

The absolute temperature sensitivity of the sample with microparticle host increased from 0.0018 to 0.0032 when the temperature changed from room temperature to 400K. Similarly, the absolute temperature sensitivity of the nanorod host increased from 0.0019 to 0.035. The highest values of maximum relative thermal sensitivity are 11.93%·K^{-1} (298 K) and 12.7%·K^{-1} (316 K) for the micro and nanorods host, respectively. The calculated temperature uncertainty for excitation at 977nm is 0.085-0.127 K for temperatures between 298 and 400 K for microparticles and is 0.075−0.122 K for nanorods host. Compared to the previous study utilizing KY_3F_{10}:Er/Yb, this research reveals an approximately 1.5 times lower thermal uncertainty[4]. On the other hand, the nanorods host exhibited better temperature uncertainty, compared to microparticles in above the ambient temperature.

References

[1] X. Wang, G. De, and Y. Liu, Mater. Res. Bull., vol. 110, 2019.
[2] X. Bian et al., Mater. Res. Bull., vol. 110, no. August 2018, pp. 102–106, 2019.
[3] A. Ćirić and M. D. Dramićanin, Journal of Luminescence, vol. 252. 2022.
[4] P. S. Solanki, S. Balabhadra, M. F. Reid, V. B. Golovko, and J. P. R. Wells, ACS Appl. Nano Mater., vol. 4, no. 6, pp. 5696–5706, 2021.

Mechanistic studies on the photodecomposition of photocaged (6-methoxynaphthalen-2-yl)methyl *N*-hydroxysulfonamides

Nimra A. Haleem[1], Michelle L. Lofink[2], Paul Sampson[2,] Alexander J. Seed[2], Nicola E. Brasch[1]

[1]School of Science, Auckland University of Technology
nimra.abdul.haleem@aut.ac.nz
[2]Department of Chemistry & Biochemistry, Kent State University, OH 44242, USA

Nitroxyl (HNO) is a simple triatomic molecule which shows promise in medical treatments like heart failure, cancer, and alcoholism.(1, 2) Its reactivity with biological molecules and instability complicates mechanistic studies of key biological reactions. There is, therefore, considerable interest in developing HNO donors – molecules which decompose to release HNO. Traditional HNO donors release HNO via spontaneous reactions with other species including solvent, whereas photoactive donors offer precise temporal and spatial control of HNO generation. Among these, (6-hydroxynaphthalen-2-yl)methyl (6,2-HNM) photocaged *N*-hydroxysulfonamides discovered by our research team are notable for rapid HNO generation via concerted C-O/N-S bond cleavage.(3) In addition to the desired HNO generating pathway, undesired O-N bond cleavage occurs. Substituting the 6-hydroxy substituent of the chromophore by a 6-methoxy (6-MeO) substituent reduces the amount of undesired O-N bond cleavage occurring (results unpublished), resulting in higher amounts of (H)NO generation via C-O/N-S bond cleavage. However, the newly released NO^- can rapidly react with the carbocation intermediate to form an E-oxime. We hypothesize that stabilising the carbocation intermediate by adding electron donating substituents at the benzylic carbon could reduce the amount of oxime formation. We present the results obtained for (6-methoxynaphthalen-2yl)methyl (6,2-HNM) photocaged N-hydroxysulfonamides with methyl and phenyl substituents on the benzylic carbon.

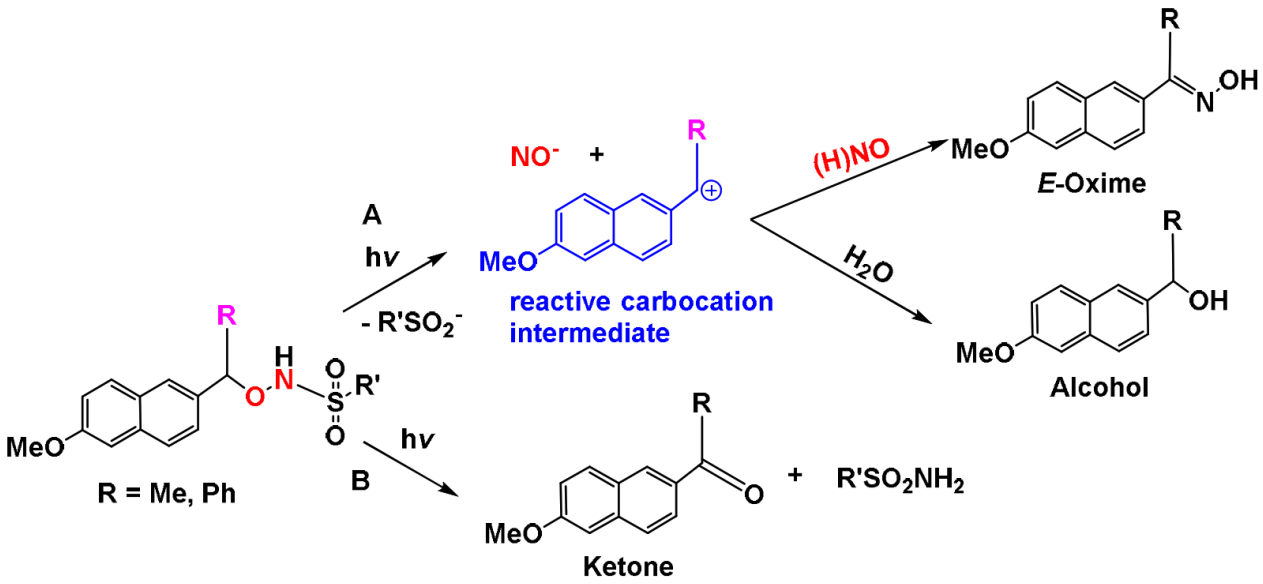

Pathways for photodecomposition of (6,2-MNM) photocaged N-hydroxysulfonamides. Pathway A releases NO^- via desired concerted C-O/N-S bond cleavage; however (H)NO may react rapidly

with the carbocation intermediate to generate an E-oxime. Pathway B is the undesired O-N bond cleavage pathway.

References

[1] Sabbah HN, Tocchetti CG, Wang M, Daya S, Gupta RC, Tunin RS, et al. Nitroxyl (HNO): A novel approach for the acute treatment of heart failure. Circ. Heart. Fail. 2013;6(6):1250-8.
[2] DeMaster EG, Redfern B, Nagasawa HT. Mechanisms of Inhibition of Aldehyde Dehydrogenase by Nitroxyl, the Active Metabolite of the Alcohol Deterrent Agent Cyanamide. Biochem. Pharmacol. 1998;55(12):2007-15.
[3] Cink RB, Zhou Y, Du L, Rahman MS, Phillips DL, Simpson MC, et al. Mechanistic Insights into Rapid Generation of Nitroxyl from a Photocaged N-Hydroxysulfonamide Incorporating the (6-Hydroxynaphthalen-2-yl)methyl Chromophore. J. Org. Chem. 2021;86(12):8056-68.

Coherent coupling of dopants to magnons in a rare earth antiferromagnet

Masaya Hiraishi, Gavin, G. G. King, Zach H. Roberts, Luke S. Trainor, Jevon J. Longdell*

Department of Physics, University of Otago, Dunedin New Zealand
Dodd-Walls Centre for Photonic and Quantum Technologies, New Zealand
*jevon.longdell@otago.ac.nz

Rare earth (RE) ions doped in solid state crystals have been a promising candidate for quantum applications such as quantum memories and transducers. These applications are building blocks for absolutely secure communication and computation beyond conventional computers. The RE ions can play an important role for them, owing to their long optical and spin coherence times. Host crystals are generally selected to have as few electron and nuclear spins as possible and even still magnetic dephasing is generally what limits coherence times. Finding a spin-free host (like isotopically pure Si) where RE dopants can substitute without causing lots of strain has not yet proved possible.

Here, we look at a host $GdVO_4$, which is fully concentrated with Gd^{3+} , an ion with large electron spin. We show at low temperatures where the Gd^{3+} spins magnetically order RE ion dopants see a magnetically quiet environment in spite of the Gd^{3+} spins. Optical coherence times we see for erbium dopants (Er^{3+}) in $GdVO_4$ are similar to those in the nonmagnetic crystal YVO_4. We also observed microwave to optical upconversion using these Er^{3+} dopants.

We observe a rich optical spectra for the Er^{3+} dopants which we can explain with a crystal field model for the Er^{3+} that is strongly coupled to the host Gd^{3+} magnons. This leads to the exciting possibility of high bandwidth microwave-to-optical transduction by the route: microwave cavity mode → magnons → Er^{3+} dopants → optical cavity mode.

Figure 1 shows experimentally observed and numerically simulated optical absorption spectra of the doped Er^{3+} ions in a magnetic field ranging from 0 to 3 T. It is clearly seen that there are avoided crossings at some absorptions. This occurs as a result of magnetic coupling of the doped Er^{3+} ions to the magnon formed by the host RE ions (here Gd^{3+} ions). We discuss the potential of the magnon-coupled RE transitions for quantum applications.

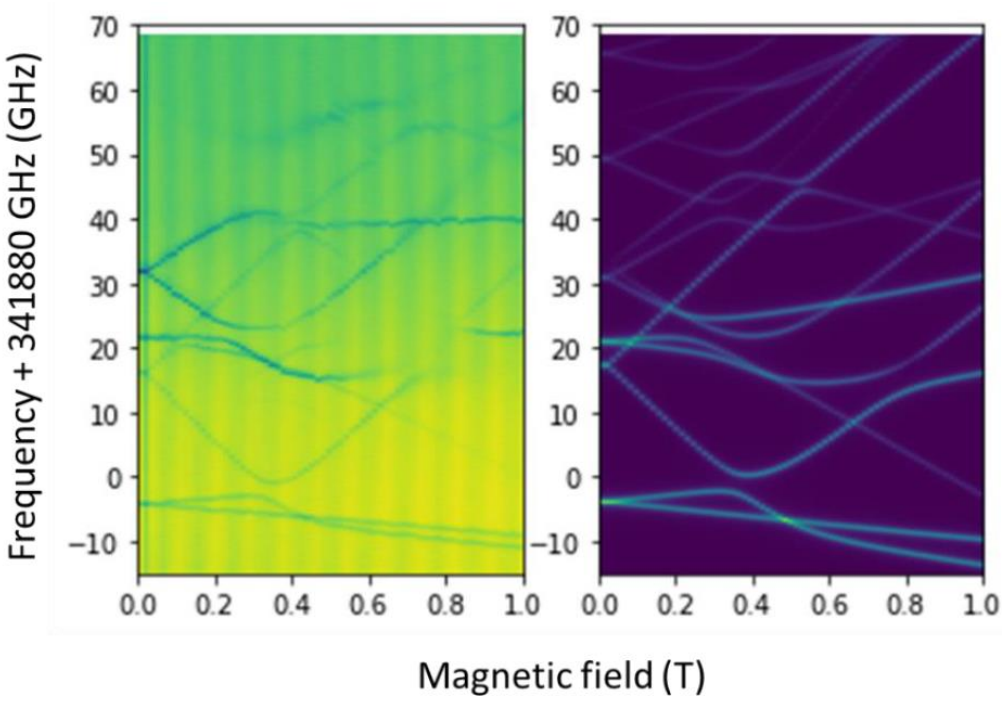

Figure 1. The experimentally observed optical spectra (left) and numerically simulated spectra (right) versus applied magnetic field. The numerical calculation is on the doped Er^{3+} ions coupled to the host Gd^{3+} ions in an antiferromagnetically ordered $GdVO_4$.

RAFT Hydrogel Photopolymerisation with NIR Light

Patrick Imrie[1,2], Max Neradt[1,2], Jianyong Jin[1,2]

[1]School of Chemical Sciences, The University of Auckland
pimr761@aucklanduni.ac.nz
[2]Dodd-Walls Centre for Photonic and Quantum Technologies

Reversible addition-fragmentation chain transfer (RAFT) polymer hydrogels have several superiorities over conventional free-radical polymerised hydrogels. These include greater network uniformity, higher swelling ratio, and “living” characteristics. Qualities such as these make RAFT hydrogels attractive smart materials for biomedical applications. However, RAFT hydrogel photopolymerisation is typically performed with harmful metal-containing photocatalysts at wavelengths with shallow penetration depth or low cytocompatibility.

Recently, Qiao et al. presented a novel metal-free photocatalyst with near-infrared (NIR) absorption which could be used for aqueous RAFT polymerisation. The group demonstrated NIR RAFT photopolymerization through 2.5 mm-thick pig skin and in the presence of living fibroblast cells, which highlights the potential for biomedical application. However, only linear polymer chains suspended in solution were produced, rather than solid crosslinked material.

In this work, we build upon the work of Qiao et al. to photopolymerise crosslinked RAFT hydrogels with NIR light. The network constituents and co-catalyst are selected for improved compatibility with the photocatalyst and faster polymerisation kinetics.

Quantum Chaos in Few-Body Systems

Alex Kerin and Joachim Brand

Dodd-Walls Centre for Photonic and Quantum Technologies, New Zealand Institute for Advanced Study and Centre for Theoretical Chemistry and Physics, Massey University, Auckland 0632, New Zealand
A.Kerin1@massey.ac.nz

The question of how quantum systems reach equilibrium is a fundamental and open one which is deeply tied to quantum chaos. The chaotic nature of a system will affect the path it takes towards equilibrium [1]. In particular, the far-from-equilibrium evolution of interacting many-body systems underpins a wide range of phenomena [2]; from the onset of superconductivity to the formation of molecules. The chaotic character of a system is important to these phenomena.

It is intuitive that systems of very many interacting bodies are typically chaotic and systems of one or two interacting bodies typically are not. It is natural to ask how large does a system have to be/how many bodies are needed before it becomes chaotic? Additionally, some subspaces of the total Hilbert space may display signatures of chaos but others don't [3]. It is worth asking how does chaos (if present) manifest in the system? To complicate this further some signatures of chaos may be present while others are not [3].

There are many signatures of quantum chaos such as level repulsion, correlation-holes, inverse participation rate and time evolution of the Shannon entropy and entanglement entropy [4]. These all relate to the correlations between eigenenergies. Namely that the eigenenergies tend to repel one another leading to anticrossings/avoided crossings. However, in general the total spectra may be made up of two (or more) subspectra one of which has the repulsive correlations of chaos and one which is non-chaotic and does not. This can make the signatures of chaos harder to observe and weaken its effects on the system.

In this work we consider a contact interacting three-body system in an three-dimensional isotropic harmonic trap. Such a system can be reliably realised and manipulated with modern experimental techniques [5]. We take advantage of existing tools to obtain the energy spectrum and wavefunctions analytically or semi-analytically [6, 7] which we then use to interrogate the static and dynamic properties of the system to search for signatures of quantum chaos.

We primarily investigate level repulsion and correlation-holes. In a non-chaotic system the energy level spacing distribution tend to be Poissonian, and in a chaotic system very small spacings between levels tend to be disfavoured. A correlation hole is a characteristic feature in the time evolution of the survival probability of chaotic systems. The survival probability is the probability of recovering the initial state of the system. For non-chaotic systems it tends to approach the longtime average from above. In chaotic systems it tends to dip below the long time average before rising up to it from below.

References

[1] Mauro Schiulaz, E Jonathan Torres-Herrera, and Lea F Santos. Thouless and relaxation time scales in many-body quantum systems. Physical Review B, 99(17):174313, 2019.

[2] EJ Torres-Herrera, Antonio M García-García, and Lea F Santos. Generic dynamical features of quenched interacting quantum systems: Survival probability, density imbalance, and out-of time-ordered correlator. Physical Review B, 97(6):060303, 2018.

[3] Javier de la Cruz, Sergio Lerma-Hernández, and Jorge G Hirsch. Quantum chaos in a system with high degree of symmetries. Physical Review E, 102(3):032208, 2020.

[4] E Jonathan Torres-Herrera and Lea F Santos. Extended nonergodic states in disordered many-body quantum systems. Annalen der Physik, 529(7):1600284, 2017.

[5] Qingze Guan, V Klinkhamer, Ralf Klemt, Jan Hendrik Becher, A Bergschneider, Philipp M Preiss, Selim Jochim, and Dörte Blume. Density oscillations induced by individual ultracold two-body collisions. Physical Review Letters, 122(8):083401, 2019.

[6] Félix Werner and Yvan Castin. Unitary quantum three-body problem in a harmonic trap. Physical Review Letters, 97(15):150401, 2006.

[7] Xia-Ji Liu, Hui Hu, and Peter D Drummond. Three attractively interacting fermions in a harmonic trap: Exact solution, ferromagnetism, and high-temperature thermodynamics. Physical Review A, 82(2):023619, 2010.

Topological Superfluidity in the Extended Hubbard Model

Satyanand Kuwar[1], Matija Čufar[1], Alex Kerin[1], Joachim Brand[1]

[1]Centre for Theoretical Chemistry and Physics, New Zealand Institute for Advanced Study, Massey University, Private Bag 102904, North Shore, Auckland 0745, New Zealand
satyanandkuwar3004@gmail.com

Topology in superfluids is explored in a one-dimensional fermionic extended Hubbard model with various boundary conditions. The main objective of this research are to achieve Majorana zero modes while maintaining particle number conservation and parallelly understanding superfluid behaviour. Majorana zero modes are unique spatially localized modes at the edges of a one-dimensional p-wave topological superfluid. We have analysed this system using a numerical approach using exact diagonalisation and projector Monte Carlo methods [1], focusing in the low-energy regime. This includes validating the ground state phase diagram [2] and examining various physical quantities such as the two-particle reduced density matrix and superfluid stiffness. The eigenvalues of the two-particle reduced density matrix play a crucial role in investigating this system's superfluid phase and directly correlate with the Cooper pair condensate that emerges in this system [3]. Moreover, the impact of the boundary conditions results in a modification of the energy gap (order-parameter).

References

[1] Rimu.jl software package, available online: https://github.com/joachimbrand/Rimu.jl
[2] L. Désoppi, N. Dupuis, C. Bourbonnais. “Functional renormalization group for fermions on a one-dimensional lattice at arbitrary fillings”. http://arxiv.org/abs/2309.16469.
[3] C. N. Yang. “Concept of Off-Diagonal Long-Range Order and the Quantum Phases of Liquid He and of Superconductors”. In: Reviews of Modern Physics 34 (1962), pp. 694–704. URL: https://api.semanticscholar.org/CorpusID:120918403.

Elucidating the structural features crucial for HNO generation for napthalenylmethyl-photocaged *N*-hydroxysulfonamides.

Anau Lautaha[1], Will Jencius[2], Michelle Lofink[2], Paul Sampson[2], Alexander J. Seed[2], Nicola E. Brasch[1]

[1]School of Science, Auckland University of Technology
anau.lautaha@aut.ac.nz
[2]Department of Chemistry & Biochemistry, Kent State University, OH 44242, USA

Nitroxyl (HNO is the reduction congener of nitric oxide (NO), a chemically reactive molecule with crucial roles in biology. HNO possesses unique chemical reactivity that has been shown to alleviate congestive heart failure[1], inhibit tumour growth and induce cancer cell death via apoptosis[1] among many other biological benefits.

Our research team is interested in developing molecules that spontaneously generate HNO at physiological pH. This will allow for controlled, fast releases of HNO so that a proper investigation into HNO's reactions with biologically important molecules can be done. We have so far observed that our photoactive *N*-hydroxysulfonamide caged with the (6hydroxynaphthalen-2-yl)methyl (6,2-HNM) chromophore generated HNO on a nanosecond timescale[2,3].

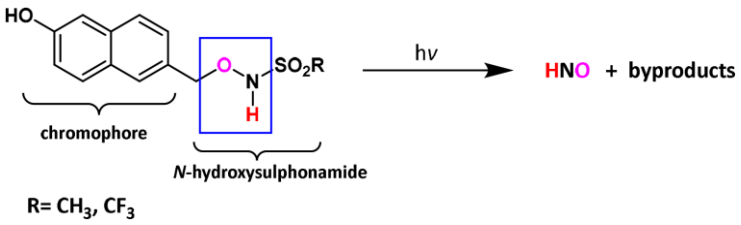

We have hypothesized that the protonation state of the nitrogen (N) atom of the photocaged N-hydroxysulfonamide plays a major role in determining whether or not HNO is generated upon exposure to light. To investigate this further, we have now synthesized and carried out studies on the decomposition of a novel series of *N*-hydroxysulfonamides where the proton on the O and N atoms has been substituted by a methyl group. Results from these studies have shown that deprotonation of the O(H) of *N*-hydroxysulfonamides leads to decomposition while deprotonation of the N(H) also generates up to 98% of HNO with R = CF3. Molecules with substituted methyl groups on both the O and N atoms do not lead to the production of HNO.

References

[1] Switzer CH, Flores-Santana W, Mancardi D, Donzelli S, Basudhar D, Ridnour LA, Miranda KM, Fukuto JM, Paolocci N, Wink DA. The Emergence of Nitroxyl (HNO) as Pharmacological Agent. Biochim. Biophys. Acta 2009; 1787(7):835-840. doi:10.1016/j.bbabio.2009.04.015

[2] Cink RB, Zhou Y, Du L, Rahman MS, Phillips DL, Simpson MC, Seed AJ, Sampson P, Brasch N. Mechanistic Insights into Rapid Generation of Nitroxyl from a Photocaged N Hydroxysulfonamide Incorporating the (6-Hydroxynaphthalen-2-yl)methyl Chromophore. J Org Chem. 2021; 86(12):8056-8068. doi:10.1021/acs.joc.1c00457

[3] Zhou Y, Cink RB, Seed AJ, Simpson MC, Sampson P, Brasch NE. Stoichiometric Nitroxyl Photorelease. Using the (6-Hydroxy-2-naphthalenyl)methyl Phototrigger. Org Lett. 2019; 21(4):1054-1057. doi:10.1021/acs.orglett.8b04099

Desynchronisation dynamics of ultrashort dissipative Raman solitons

Zongda Li[1,2], Yiqing Xu[1,2], Stéphane Coen[1,2], Stuart G. Murdoch[1,2] and Miro Erkintalo[1,2]

[1]Department of Physics, University of Auckland, Auckland 1010, New Zealand
[2]The Dodd-Walls Centre for Photonic and Quantum Technologies, New Zealand

The recently discovered ultrashort dissipative Raman soliton shows promising characteristics as a potential source of novel optical frequency combs [1,2]. Such Raman solitons arise when a passive Kerr resonator is desynchronously driven by a train of coherent pulses. While Ref. [1] demonstrated that the solitons' formation and characteristics are underpinned by the desynchronisation between the driving pulse periodicity and the cavity roundtrip time, the precise mechanism behind this dependence remains a mystery. In this work, we elucidate the role of desynchronisation through extensive numerical modelling.

We begin by numerically demonstrating that Raman solitons can exist even under conditions of continuous wave (CW) driving and that, as shown in Fig. 1(a) and (b), the soliton characteristics, including their group velocity, depend upon the intracavity background power that the soliton experiences. Similar dependency is also observed in pulse-driven scenarios. However, an additional constraint applies due to the presence of desynchronisation; specifically, the Raman soliton is attracted to, and trapped at, a background power that is associated with the group velocity that exactly cancels the desynchronisation [See Fig. 1(c)]. Furthermore, adjusting desynchronisation modifies the trapping power and thus influences the soliton characteristics. Understanding this mechanism allows us to qualitatively predict the trapping point of the Raman soliton [yellow marker in lower panel with Fig. 1(c)], as well as explain why soliton can only exist over a finite range of desynchronisation.

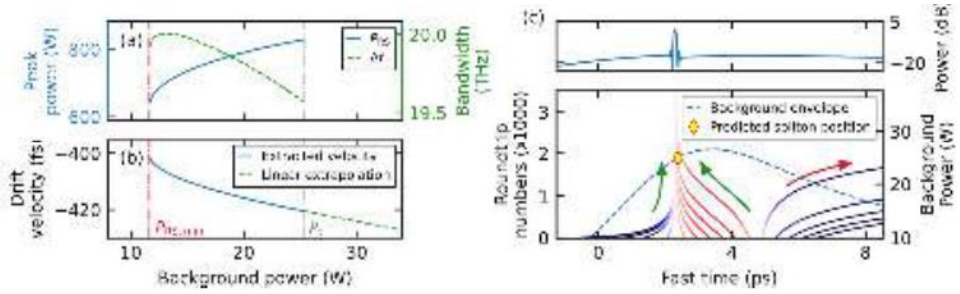

Fig. 1. (a) Solid blue and dashed green curves show Raman soliton peak power (left axis) and bandwidth (right axis) as a function of background power extracted from CW simulations. (b) Raman soliton temporal drift velocity as a function of background power. (c) Simulated response of Raman soliton in the upper panel when temporally displaced by various amounts. Solid lines in the lower panel indicate the evolution of the soliton's temporal position. The dashed curve shows the steady-state background envelope prior to the significant growth of the Raman signal. The yellow diamond indicates the predicted trapping position.

References

[1] Y. Xu, A. Sharples, J. Fatome, S. Coen, M. Erkintalo, and S. G. Murdoch, 'Frequency comb generation in a pulse-pumped normal dispersion Kerr mini-resonator', Opt. Lett., vol. 46, no. 3, p. 512, Feb. 2021.

[2] Z. Li et al., 'Ultrashort dissipative Raman solitons in Kerr resonators driven with phase-coherent optical pulses', Nat. Photon., vol. 18, no. 1, pp. 46–53, Jan. 2024.

Perturbation of whispering gallery modes using high-index substrates

Anna Petersen[1,2], Mallika Irene Suresh[1,2], Florian Sedlmeir[1,2], Harald G. L. Schwefel[1,2]

[1]The Dodd-Walls Centre for Photonic and Quantum Technologies, New Zealand,
[2]Department of Physics, University of Otago, Dunedin 9016, New Zealand
petan928@student.otago.ac.nz

We use coherent continuous wave THz spectroscopy and simulations to explore how nearby dielectric and metallic structures affect the spectrum of a disc-shaped silicon WGM resonator. Understanding the perturbing effects of such structures will enable further development in mode tuning techniques along the lines of that described in [1], as well as providing a better understanding of the actual field structure in resonators close to high-index materials.

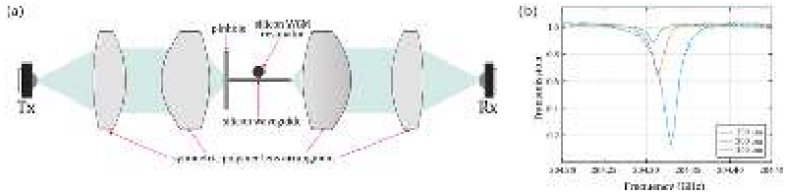

Figure 1: (a) Basic experimental setup, (b) Example of a mode shifting as the distance between the waveguide and resonator is increased.

Silicon can support high-Q resonances in the THz regime, and the refractive index is well known, making it a good candidate for characterising the effect of nearby high index structures. In our experiment [Fig. 1(a)] we use a cuboidal silicon waveguide to couple THz radiation into a silicon WGM resonator. The receiver RX measures the electric field, so both phase and amplitude information can be extracted and processed to identify and characterise the modes [2]. We have already seen shifts in the resonant frequencies caused by the nearby waveguide [Fig. 1 (b)]. As can be seen in the simulations in Fig. 2 (a) and (b), the nearby waveguide distorts the mode structure. Therefore, nearby high-index substrates perturb the electric field of the resonant mode. We plan to use a metal/high-index probe above the disc to map out the distribution of the electric field of the resonant mode along the circumference by measuring the shifts caused by the probe [Fig. 2 (c)].

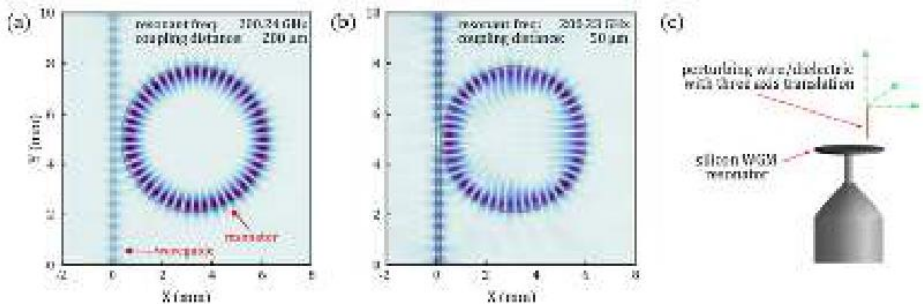

Figure 2: (a) and (b): Simulation of electric field norm when the distance between waveguide and resonator is (a) 200 µm and (b) 50 µm. In the latter case the mode structure is deformed, and the resonant frequency is redshifted by the waveguide. (c) Setup for mapping the electric field.

References

[1] D. W. Vogt, A. H. Jones, H. G. L. Schwefel, and R. Leonhardt, ‘Anomalous blue-shift of terahertz whispering-gallery modes via dielectric and metallic tuning’, Opt. Lett., vol. 44, no. 6, pp. 1319–1322, Mar. 2019, doi: 10.1364/OL.44.001319.

[2] D. W. Vogt, M. Erkintalo, and R. Leonhardt, ‘Coherent Continuous Wave Terahertz Spectroscopy Using Hilbert Transform’, J. Infrared Millim. Terahertz Waves, vol. 40, no. 5, pp. 524–534, May 2019, doi: 10.1007/s10762-019-00583-3.

Spectrally offset Kerr cavity soliton generation in a synchronously driven optical fibre resonator

Yiqing Xu,[1, 2, *] Xiaoyu Chen,[1,2,4] Matthew Macnaughtan,[1, 2] Zongda Li,[1, 2] Xiaoming Wei,[3] Zhongmin Yang,[3] Stéphane Coen,[1, 2] Miro Erkintalo, 1, 2 and Stuart G. Murdoch[1, 2]

[1]The Dodd-Walls Centre for Photonic and Quantum Technologies, Auckland, New Zealand
[2]Department of Physics, University of Auckland, Auckland, New Zealand
[3]School of Physics and Optoelectronics, South China University of Technology, Guangzhou, China
[4]College of Information Science and Engineering, Northeastern University, China
*yxu079@aucklanduni.ac.nz

The generation of stable Kerr frequency combs in optical resonators requires the formation of Kerr cavity solitons (CS) [1]. CS formation in turn relies on the generation of new frequency components initiated by modulation instability (MI). Specifically, the newly generated spectral components originate from phase-matched parametric gain. As a result, in a cavity with only second-order anomalous dispersion, the soliton spectrum is necessarily centred around the pump laser frequency, as this is the only spectral region that experiences phase-matched parametric gain. Recently, CSs with centre frequencies far from the driving pump(s) have been realised through the addition of second-harmonic generation, Raman nonlinearities, and parametric phase conjugation [2-5]. Here, we report the generation of spectrally offset Kerr CSs through the addition of desynchronisation when pulsed pumping. We consider a fibre Fabry-Pérot (FFP) resonator that is constructed by butt-coupling two highly reflective dielectric mirrors on the two ends of a piece of 1 m-long dispersion shifted fibre, giving a cavity finesse ~100. The resonator is (de)synchronously driven by a train of 1.5 ps-duration pulses centred in the anomalous dispersion regime at 1560 nm. Taking advantage of the resonator's broadband MI gain, the CS can be phase-matched over a large frequency shift range. Particularly, the phase-matched frequency of the generated CS can be selected by adjusting the pump-cavity desynchronisation $\Delta t = t_R - t_p$ where t_p is the period of the driving pulse train and t_R is the resonator round-trip time. We first numerically simulate the formation of the MI gain CS with the experimental resonator parameters and a desynchronisation of $\Delta t = -46$ fs, and plot in Fig. 1(a) the temporal evolution of the intracavity field, showing the spontaneous formation of the CS. The inset of Fig. 1(a) further displays the interference pattern between the MI CS and pump field due to their different carrier envelope offset frequencies. In Fig. 1(b), we plot the simulated existence range of these frequency-offset solitons as a function of detuning, showing they can be stably generated in a narrow region of drive powers. Finally, we experimentally generate the MI CS in our system, and plot in Fig. 1(c) both the simulated and experimentally measured output spectra, observing good agreement.

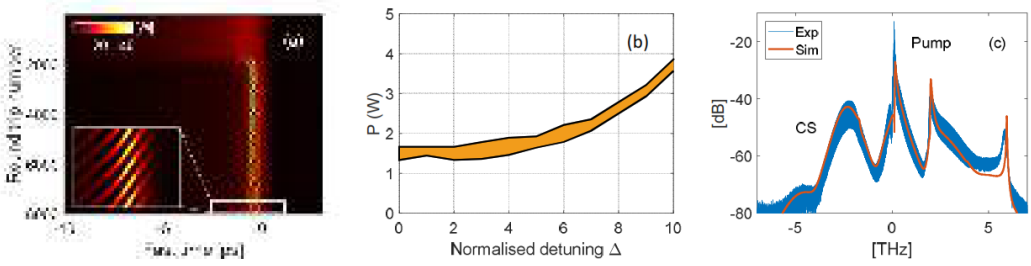

Fig.1 (a) Simulated temporal evolution of the intracavity field. Inset shows the temporal interference between the pump and the MI sidebands. (b) Simulated existence range of frequency-offset CSs plotted as a function

of normalised detuning for $\Delta t = -46$ fs. (c) Simulated and experimentally measured spectrum of the intracavity field.

Reference

[1] A. Pasquazi, et al., Physics Reports 729, 1 (2018).
[2] N. Englebert, et al., Nature Photonics 15, 857 (2021).
[3] Q. F. Yang, et al., Nature Physics 13, 53 (2017).
[4] Z. Li, et al., Nature Photonics 18, 46 (2024).
[5] G. Moille, et al., Nature Photonics 18, 617 (2024).

Modelling Transition Intensities of the $C_{3v}(O^{2-})$ Centre in Eu^{3+} Doped CaF_2 Crystals

Michael D. Moull[1,2], Jamin B. L. Martin[1,2], Michael F. Reid[1,2], Jon-Paul R. Wells[1,2]

[1]The School of Physical and Chemical Sciences, University of Canterbury
[2]The Dodd-Walls Centre for Photonic and Quantum Technologies, New Zealand
michael.moull@pg.canterbury.ac.nz

Rare-earth doped crystals are a strong candidate material for quantum information technologies that interface between light and matter, such as quantum memories, repeaters, and transducers [1]. In addition to high performance ensemble-based technologies, single rare-earth ions also show promise as spin-photon interfaces for entanglement distribution [2]. Transitions of interest, like most 4f-4f optical transitions of rare-earths in solid-state hosts, are weak. The weakly allowed electric dipole transitions are of similar strength to the magnetic dipole transitions, with dipole moments approximately 1000 times less than other solid-state emitters such as colour centres and quantum dots. Therefore, it is critical to gain understanding on the nature of the transitions that are of interest for quantum information applications.

We present a detailed crystal-field and transition intensity analysis of the trigonal (G1) site in Eu^{3+}:CaF_2 which arises from the substitutional charge compensation of an O^{2-} ion. The transition intensity analyses are based on a parametric model that retains explicit dependence on the SLJ and MJ compositions of the spectroscopic state vectors, allowing intensity distributions of transitions between the individual crystal-field levels to be addressed.

Twenty-eight excited state crystal-field levels were identified. A crystal-field fit resulted in extremely large axial crystal-field parameters that produce excellent agreement between the experimental and calculated crystal-field structure. This includes accounting for the overlap of the crystal-field levels of the $^7F_1$ and $^7F_2$ multiplets. Fitting the induced electric dipole intensity parameters to the relative intensities of the $^5D_0$ fluorescence reproduced the observed spectra impeccably well. The ability to reproduce the anomalously intense $^7F_0 \leftrightarrow {}^5D_0$ transitions showed the model's ability to account for higher order charge-transfer-state induced intensity contributions. The calculated radiative lifetime of the $^5D_0$ state of 2.1 ms was in good agreement with the observed 1.8 ms fluorescent lifetime.

References

[1] C.W. Thiel, T. Böttger, and R. L. Cone. Rare-earth-doped materials for applications in quantum information storage and signal processing. Journal of luminescence 131.3, pp. 353-361, 2011.
[2] A. Ruskuc, C.J. Wu, E. Green, S.L. Hermans, J. Choi, and A. Faraon. Scalable multipartite entanglement of remote rare-earth ion qubits. arXiv preprint arXiv:2402.16224, 2024.

Fourier-Domain Mode-Locked Laser-Based DepthResolved Vibrometry Indicates Involvement of Superficial Hair in the Sound Detection of Snapping Shrimp

Tillmann Spellauge[1,2], Frédérique Vanholsbeeck[1,2]

[1]The Dodd-Walls Centre for Photonic and Quantum Technologies, Auckland, New Zealand
[2]Department of Physics, The University of Auckland, Auckland, New Zealand
tillmann.spellauge@auckland.ac.nz

It is well established that crustaceans like the snapping shrimp and Aotearoa paddle crab utilize acoustic communication in several essential behaviors, such as feed and mating. While the sounds associated with these behaviors and the sound production mechanisms have been identified, the crustacean's sound-sensing apparatus is still poorly understood. While a number of organs sensitive to mechanical stimuli are suspected to also be sensitive to acoustic waves through mechanical interaction, this has not been shown to date. Thus, the involvement of the statocyst, chordotonal organ, and superficial hair in crustacean sound sensing remains speculative. [1,2]

To gain insight into the mechanical response of these organs to acoustic stimuli, we employ a Fourier-domain mode-locked laser (FDML) based OCT to gather depth profiles of the structures of interest. Since OCT is an interference-based imaging technique, it not only gives us access to the reflectivity of the sample in different depths but also to the interferometric phase. While the reflectivity gives structural information about the organs of interest, the interferometric phase contains information about the relative axial position of the reflections within the sample with precision in the single nanometer range. Taking multiple subsequent measurements of the interferometric phase in the same position makes it possible to analyze for periodic changes in the phase caused by an acoustic stimulus. Due to the high repletion rate of the FDML laser, it is possible to take up to 2000 depth profiles per second with a field of view of 2 mm by 4 mm (lateral, axial) and with a resolution of 21 µm by 7 µm (lateral, axial). The frame rate of 2000 depth profiles per second allows us to measure acoustic frequencies from 0 to 1000 Hz without aliasing. This frequency range is in excellent agreement with the known vocalization range of many crustaceans [1].

Using this system, we were able to show, for the first time, that superficial hair situated on the antennae of snapping shrimp exhibit a mechanical response to a 260 Hz sinusoidal particle wave. While the antennae oscillate with a low amplitude of 14 nm in response to the acoustic stimulus, the superficial hair oscillate with an amplitude of 130 nm. Additionally, there also appears to be a difference in the phase of the vibration between the superficial hair and antennae. These results, in combination with the known sensitivity of superficial hair to mechanical stimuli, indicate an involvement in the crustacean sound-sensing apparatus.

To further validate these preliminary findings, we plan to repeat the measurements in a range of acoustic frequencies within the crustacean vocalization range and at different acoustic amplitudes. We want to extract both the frequency and amplitude response functions of the superficial hair from these measurements, which we hope to match up with existing electrophysiological response curves. This procedure will be repeated for the statocyst and the

chordotonal organ to gain a better understanding of the complete crustacean hearing apparatus.

References

[1] C. A. Radford and J. A. Stanley, "Sound detection and production mechanisms in aquatic decapod and stomatopod crustaceans," Journal of Experimental Biology 226, jeb243537 (2023).

[2] T. Breithaupt and J. Tautz, "The Sensitivity of Crayfish Mechanoreceptors to Hydrodynamic and Acoustic Stimuli," in Frontiers in Crustacean Neurobiology, K. Wiese, W.-D. Krenz, J. Tautz, H. Reichert, and B. Mulloney, eds. (Birkhäuser Basel, 1990), pp. 114–120.

Photonic Belt Resonators for Broadband Frequency Combs

Vincent Ng[1], Luke S. Trainor[2], Harald G.L. Schwefel[2], Stéphane Coen[1], Miro Erkintalo[1]and Stuart G. Murdoch[1]

[1]The Dodd-Walls Centre for Photonic and Quantum Technologies, Department of Physics, University of Auckland, Auckland, New Zealand
[2]The Dodd-Walls Centre for Photonic and Quantum Technologies, Department of Physics, University of Otago, Dunedin, New Zealand
wng299@aucklanduni.ac.nz

Whispering-gallery mode (WGM) microresonators made from magnesium fluoride (MgF2) have been a useful platform for exploring the generation of optical frequency combs [1]. They support high-finesse whispering gallery modes which allow access to large intracavity powers, suitable for exciting optical nonlinearities, with only tens of milliwatts of optical power. These coherent frequency combs are known to coincide with the formation of localised structures known as temporal cavity solitons. WGM resonators typically support hundreds of spatial modes that interact in the form of avoided mode crossings. These mode crossings hinder the excitation of coherent soliton combs and introduce defects into the comb spectra. An additional constraint is the resonator's dispersion, which determines the existence criteria for the frequency comb, as well as its final properties—including its bandwidth and shape. So, while there have been many demonstrations of optical frequency combs in these devices, practical application of MgF2 microresonators have been limited.

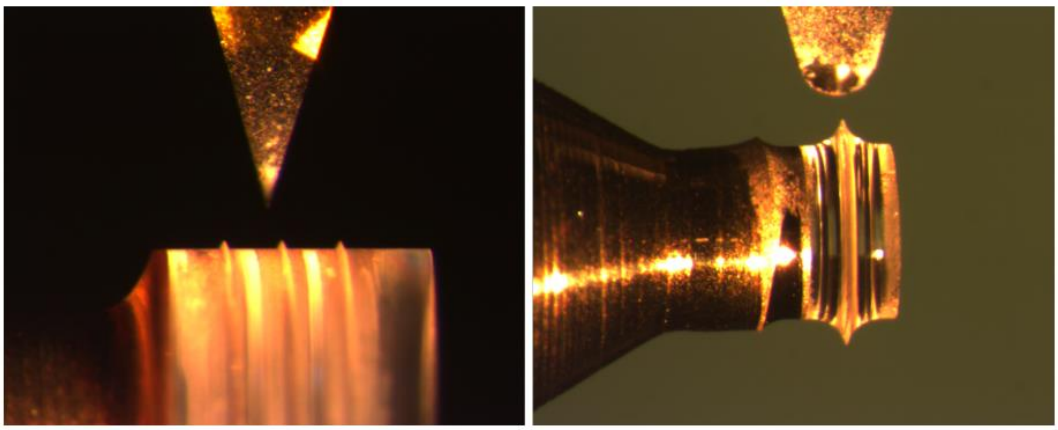

Figure 1: Microscope images of the microresonator devices just after diamond-turning (Left) A photonic-belt resonator device. (Right) Microresonator designed for dispersion engineering.

Here, we consider whispering-gallery mode resonators cut to an extremely fine point using diamond point turning techniques. The sharp tip of the resonator provides mode confinement, reducing the number of supported modes, and thus preventing the introduction of comb defects. One design presented is the so-called photonic-belt resonator [2]—a resonator where the optical mode is supported in a belt-like structure only several microns high and approximately ten microns across Fig. 1(Left). These photonic-belt resonators have been demonstrated to support broadband frequency comb structures. We also present resonator designs with a much larger protrusion Fig. 1(Right). Here, we hope to achieve much stronger optical mode confinement, which will allow strong modifications to be made to the resonator's

dispersion (dispersion engineering) and enable frequency comb optimisation at different center frequencies.

References

[1] A. Pasquazi et al., ”Micro-combs: A novel generation of optical sources,” Phys. Rep. 729, 1–81
[2] (2018).
[3] I. S. Grudinin and N. Yu, ”Dispersion engineering of crystalline resonators via microstructuring,”
[4] Optica 2, 221–224 (2015).

Monolithic Optical and Microwave Resonator-based Frequency Comb Generation

Pablo C. Paulsen[1,2], Mallika Irene Suresh[1,2], Nicholas J. Lambert[1,2], Harald G. L. Schwefel[1,2], Florian Sedlmeir[1,2]

[1]Department of Physics, University of Otago
[2]The Dodd-Walls Centre for Photonic and Quantum Technologies
paupa289@student.otago.ac.nz

Optical frequency combs have various applications in high-speed optical telecommunication, [1] spectroscopy[2] and other fields. One implementation of frequency comb generation is based on resonant electro-optics. This approach utilises an optical whispering gallery mode (WGM) resonator embedded into a microwave cavity, acting as a microwave resonator[3] (see Figure 1(a)). While this approach is highly efficient, it presents significant manufacturing and usability challenges due to the bulky and separate nature of the microwave cavity. the cavity must be engineered to physically fit and be phase-matched with the optical modes in the WGM resonator. This can limit the system's mechanical stability, reliability, and scalability.

To improve this design, we propose a new monolithic platform in which the metallic microwave resonator is directly coated onto the surface of the WGM resonator. We will use femtosecond laser micromachining to manufacture the lithium niobate ($LiNbO_3$) WGM resonator. This technique allows for more complex shapes than traditional diamond-cutting methods. The metallic microwave resonator will be coated using physical vapour deposition (PVD), electroplating and/or electroless deposition, with the desired pattern cut using femtosecond laser ablation.

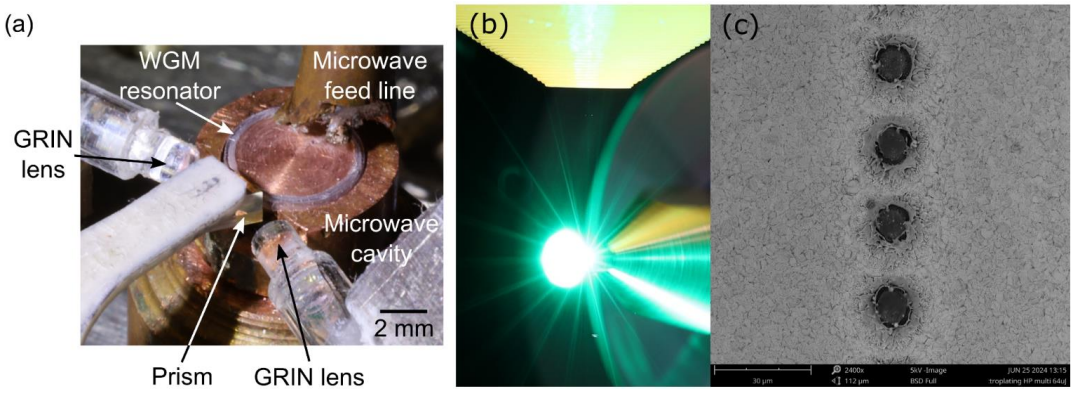

Figure 1: (a) Optical whispering gallery mode (WGM) resonator embedded into a microwave cavity acting as a microwave resonator (taken from ref[3]), (b) Femtosecond micromachining of lithium niobate WGM, (c) Single femtosecond laser pulses on electroplated copper.

We have developed and refined the process of manufacturing lithium niobate WGM resonators using femtosecond laser micromachining. Additionally, we have combined PVD and electroplating to create a metal coating that adheres sufficiently to the lithium niobate, allowing us to ablate patterns using the femtosecond laser. We expect these techniques to enable the design and manufacture of a monolithic WGM resonator with a coated microwave resonator, facilitating efficient and reliable frequency comb generation.

Reference

[1] Alfredo Rueda et al., “Resonant Electro-Optic Frequency Comb,” Nature 568, no. 7752 (April 2019): 378–81, https://doi.org/10.1038/s41586-019-1110-x.
[2] Tara Fortier and Esther Baumann, “20 Years of Developments in Optical Frequency Comb Technology and Applications,” Communications Physics 2, no. 1 (December 6, 2019): 1–16, https://doi.org/10.1038/s42005-019-0249-y.
[3] Nicholas J. Lambert, Luke S. Trainor, and Harald G. L. Schwefel, “Microresonator-Based Electro-Optic Dual Frequency Comb,” Communications Physics 6, no. 1 (May 3, 2023): 1–8, https://doi.org/10.1038/s42005-023-01197-x.

Upconversion of multiple non-resonant THz channels in an optical microresonator

Mallika Irene Suresh[1,2], Florian Sedlmeir[1,2], Dominik Walter Vogt[1,3], Harald G. L. Schwefel[1,2]

[1]The Dodd-Walls Centre for Photonic and Quantum Technologies, New Zealand,
[2]Department of Physics, University of Otago, Dunedin 9016, New Zealand,
[3]Department of Physics, University of Auckland, Auckland 1010, New Zealand
mallika.suresh@otago.ac.nz

We present multichannel nonlinear optical upconversion of THz signals at 0.137 THz, 0.147 THz, 0.157 THz, 0.167 THz, 0.177 THz, and 0.186 THz in a lithium niobate disk resonator. This scheme demonstrates the upconversion of multiple non-resonant THz signals using a resonantly enhanced continuous-wave optical pump.

Nonlinear frequency mixing in electro-optic crystalline whispering gallery mode resonators (WGMR) has been explored and discussed for a couple of decades now [1]. Such platforms have been used to shift signals from the microwave (e.g. 10 GHz [2] and 80 GHz [3]) up to the optical domain, i.e., "upconversion" via sum-frequency generation (SFG) and difference-frequency generation (DFG). Here, we demonstrate the multichannel upconversion of signals that are an octave higher than previously demonstrated [3].

The WGMR used here is a LiNbO3 disk with the crystal optic axis along the rotational axis, with a thickness of 163.6 μm and radius of 2.23 mm. The experimental setup [Fig. 1 (a)] for the upconversion has two parts for each frequency domain involved. In the optical domain, a continuous-wave tunable diode laser (~192 THz) from Toptica Photonics is used. The laser light is coupled in and out of the WGMR via two graded-index (GRIN) lenses and a diamond prism. The light emerging from the outcoupling GRIN lens is split with 10% of the signal being sent to a photodiode (PD) and the remaining 90% being sent via a filter to an optical spectrum analyser (OSA). The filter is used to decrease the outcoupled pump power being sent to the high-sensitivity OSA. A frequency-domain TeraScan system with photoconductive antennae (PCA) from Toptica Photonics was used as the source of THz radiation for upconversion. Ultrahigh-molecular-weight polyethylene (UHMWPE) lenses are used to couple the radiation to and from a silicon rod waveguide.

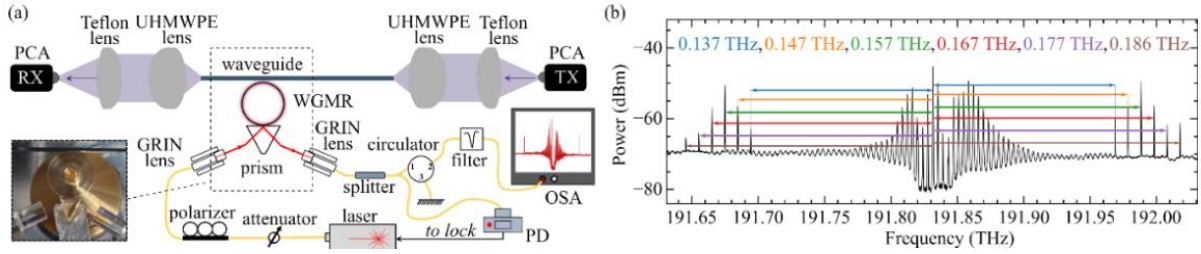

Figure 1: (a) Sketch of experimental set-up, (b) Optical spectrum showing upconverted peaks.

The spectrum shown in Fig. 1(b) depicts 6 channels of upconversion as can be seen by the SFG and DFG of frequencies from 0.137 THz to 0.186 THz observed as the sidebands on either side of the pump. These spectra are captured by the "Maximum Hold" function of the Finisar 1500S OSA as the TeraScan system is scanned and each pair of peaks appears when the system

reaches the respective THz frequency. The resolution of the OSA is 150 MHz, which is much larger than the expected bandwidth of the upconverted signal mode (approx. 1.4 MHz). These optical signals are integer multiples of the free spectral range of the optical mode. This indicates that the upconverted signal in each case is generated in an optical WGMR mode – so both the pump and upconverted signal are resonant in the WGMR. The THz radiation being upconverted overlaps with the optical mode but is not resonant in the disk, like that proposed in [4]. This broadens the range of frequencies being upconverted as the phase-matching requirements for all-resonant upconversion would allow only one frequency to be upconverted. However, an all-resonant scheme would provide upconversion efficiency and therefore, THz detection sensitivity that is far better than observed here.

References

[1] V. S. Ilchenko, A. A. Savchenkov, A. B. Matsko, and L. Maleki, “Whispering-gallery-mode electro-optic modulator and photonic microwave receiver,” J. Opt. Soc. Am. B, vol. 20, pp. 333–342, Feb. 2003.

[2] A. Rueda et al., “Efficient microwave to optical photon conversion: an electro-optical realization,” Optica, vol. 3, pp. 597–604, Jun. 2016.

[3] G. S. Botello et al., “Sensitivity limits of millimeter-wave photonic radiometers based on efficient electro-optic upconverters,” Optica, vol. 5, pp. 1210–1219, Oct. 2018.

[4] D. Strekalov et al., “W-Band Photonic Receiver for Compact Cloud Radars,” Sensors, vol. 22, pp. 804, Jan. 2022.

Characterisation and preservation of plastics in GLAM institutions.

Carlie Watt[1 2 3], Cushla McGoverin[1 2]

[1]The University of Auckland, Auckland 1010, New Zealand;
[2]Te Whai Ao — Dodd-Walls Centre for Photonic and Quantum Technologies, Department of Physics, The University of Auckland;
[3]Te Mana Tangata Whakawhanake — MacDiarmid Institute for Advanced Materials and Nanotechnology, Department of Physics, The University of Auckland
carlie.watt@auckland.ac.nz

Since invention, plastics have become increasingly significant in gallery, library, archive, and museum (GLAM) collections, encompassing various objects from wartime memorabilia to everyday items, polymeric-based painting material to 3D printed sculptures.

While there are many different plastic objects in collections, there are equally many different plastic materials used to make them. Scott Williams' work at the Canadian Conservation Institute on plastics lead to the identification of five polymers prone to degradation and the release of corrosive or toxic volatile compounds that affect the degrading object and other surrounding materials in GLAM collections. These five materials – termed "malignant polymers" by Williams back in 2002 – are cellulose nitrate, cellulose acetate, polyvinyl acetate, polyurethane, and rubber, and are the most common polymeric compounds used in early plastic materials. Beyond, the polymeric material used, the identification, understanding, and preservation of plastics is further complicated by the addition of adjuvants like fillers, plasticisers, colorants, stabilisers, anti-oxidants, and UV absorbers. Additionally, unknown origins of the object, which may have included poor storage before acquisition or experimental practices used by artists in the making of the object or artwork, again add variability. This research aims to address these challenges through a comprehensive interdisciplinary approach, applying photonics to investigate plastics within the context of museum collections and enable the development of preservation strategies.

Collaborating with conservators at the Auckland War Memorial Museum, we will conducting a thorough survey of a collection using non-destructive analysis techniques. Scientific analysis is a valuable tool for informing conservation and cultural heritage studies. These spectroscopic methods are information-rich, providing more information than the more easily administered burn or Oody tests that are commonly used to identify plastics. Additionally, given the fragility, historical and cultural significance of many objects, non-invasive or minimally invasive analytical techniques such as Raman and infrared spectroscopy provide another benefit and have been increasingly applied to the study of GLAM objects because of this reason. The survey focuses on identifying plastics using these scientific techniques to gain a deeper understanding of the associated problems and challenges of plastic item conservation.

Odd-frequency superfluidity from a particle-number-conserving perspective

K. Thompson,[1, 2] U. Zülicke,[1, 3] J. Schmalian,[4, 5] M. Governale,[1] and J. Brand[6]

[1]MacDiarmid Institute, School of Chemical and Physical Sciences, Victoria University of Wellington, PO Box 600, Wellington 6140, New Zealand
[2]Cavendish Laboratory, JJ Thomson Avenue, Cambridge CB3 0HE, United Kingdom
[3]Dodd-Walls Centre for Photonic and Quantum Technologies, School of Chemical and Physical Sciences, Victoria University of Wellington, PO Box 600, Wellington 6140, New Zealand
[4]Institute for Theory of Condensed Matter, Karlsruhe Institute of Technology, 76131 Karlsruhe, Germany
[5]Institute for Quantum Materials and Technologies, Karlsruhe Institute of Technology, 76126 Karlsruhe, Germany
[6]Dodd-Walls Centre for Photonic and Quantum Technologies, Centre for Theoretical Chemistry and Physics, New Zealand Institute for Advanced Study, Massey University, Private Bag 102904, North Shore, Auckland 0745, New Zealand

We investigate odd-in-time — or odd-frequency — pairing of fermions in equilibrium systems within the particle-number-conserving framework of Penrose, Onsager and Yang, where superfluid order is defined by macroscopic eigenvalues of reduced density matrices. We show that odd-frequency pair correlations are synonymous with even fermion-exchange symmetry in a time-dependent correlation function that generalises the two-body reduced density matrix. Macroscopic even-under fermion-exchange pairing is found to emerge from conventional Penrose-Onsager-Yang condensation in two-body or higher-order reduced density matrices through the symmetry-mixing properties of the Hamiltonian. We identify and characterise a transformer matrix responsible for producing macroscopic even fermion-exchange correlations that coexist with a conventional Cooper-pair condensate, while a generator matrix is shown to be responsible for creating macroscopic even fermion-exchange correlations from hidden orders such as a multi-particle condensate. The transformer scenario is illustrated using the spin-balanced s-wave superfluid with Zeeman splitting as an example. The generator scenario is demonstrated by the composite-boson condensate arising for itinerant electrons coupled to magnetic excitations. Structural analysis of the transformer and generator matrices is shown to provide general conditions for odd-frequency pairing order to arise in a given system. Our formalism facilitates a fully general derivation of the Meissner effect for odd-frequency superconductors that holds also beyond the regime of validity for mean-field theory.

References

[1] K. Thompson, U. Zülicke, J. Schmalian, M. Governale, and J. Brand, “Odd-frequency superfluidity from a particle-number-conserving perspective,” to appear in Phys. Rev. Research (2024), arXiv: arXiv:2403.06325. doi: 10.48550/arXiv.2403.06325.

Monitoring Buildings, Volcanoes and Seismic Activity Using Large Ring Laser Gyroscopes.

Roberta Parlavecchia[1,2], Robert J. Thirkettle[2], Jon-Paul R. Wells[1,2], Kasper van Wijk[1,3], Laura Cobus[1,2] and K. Ulrich Schreiber[4]

[1]Dodd-Walls Centre for Photonic and Quantum Technologies, New Zealand.
[2]School of Physical and Chemical Sciences, University of Canterbury, PB4800, Christchurch 8140, New Zealand.
[3]Department of Physics, University of Auckland, PB92019, Auckland 1142, New Zealand.
[4]Technische Universitaet Muenechen, Forschungseinrichtung Satellitengeodaesie Geodaetisches Observatorium Wettzell, 93444 Bad Koetzting, Germany.

A ring laser technology offers the ability to consistently and accurately monitor rotational ground motions induced by a wide range of earthquakes in both the near and the far field by exploiting the Sagnac effect inside a ring-cavity configuration. This project aims to utilise the unparalleled rotational sensitivity of a He-Ne based ring laser gyroscope (supported by conventional seismometers, tiltmeters and fibre optic gyroscopes) to provide long term monitoring of seismically induced ground rotations and associated building dynamics.

For this purpose, we are using the recently developed Ernest Rutherford 2 (ER-2) ring laser, which has a 17 meter perimeter. This device has been constructed and is located on the ground floor of the Ernest Rutherford building at the Ilam campus of the University of Canterbury. However, the operational parameters have not yet been optimised and characterized; this is our first objective.

The Er-2 laser operates using state-of-the-art intra-cavity supermirrors (mirrors having total optical losses in the single parts per million range) purchased in late 2023. Our initial measurements of the cold cavity ring-down time τ (and by inference the cavity quality factor Q) indicate a cavity photon lifetime of 1.4 milliseconds and an associated Q factor of 4.2x1012. This yields a raw sensitivity to rotation of 2.12x10-13 a sensitivity greater than that of the German Gross-ring and higher than any ring laser previously constructed in New Zealand.

Our next steps are going to optimise the gas composition and total pressure and investigate operation on both single and multiple longitudinal laser modes in a phase locked configuration.